GABAergic mechanisms in epilepsy and
contribution of the ClC-2 chloride channel to neuronal excitability

Dissertation

zur Erlangung des Grades eines
Doktors der Naturwissenschaften

der Mathematisch-Naturwissenschaftlichen Fakultät
und
der Medizinischen Fakultät
der Eberhard-Karls-Universität Tübingen

vorgelegt
von

Cristina Elena Niturad
aus Fagaras, Romania

Februar - 2016

Tag der mündlichen Prüfung: 25.04.2016

Dekan der Math.-Nat. Fakultät: Prof. Dr. W. Rosenstiel
Dekan der Medizinischen Fakultät: Prof. Dr. I. B. Autenrieth

1. Berichterstatter: Prof. Dr. Holger Lerche
2. Berichterstatter: Dr. Maria Kukley

Prüfungskommission: Prof. Dr. Holger Lerche

                              Dr. Maria Kukley

                              Prof. Dr. Rejko Krüger

                              Prof. Dr. Elke Guenther

Erklärung / Declaration:

Ich erkläre, dass ich die zur Promotion eingereichte Arbeit mit dem Titel:

„GABAergic mechanisms in epilepsy and contribution of the ClC-2 chloride channel to neuronal excitability"

selbständig verfasst, nur die angegebenen Quellen und Hilfsmittel benutzt und wörtlich oder inhaltlich übernommene Stellen als solche gekennzeichnet habe. Ich versichere an Eides statt, dass diese Angaben wahr sind und dass ich nichts verschwiegen habe. Mir ist bekannt, dass die falsche Abgabe einer Versicherung an Eides statt mit Freiheitsstrafe bis zu drei Jahren oder mit Geldstrafe bestraft wird.

I hereby declare that I have produced the work entitled "GABAergic mechanisms in epilepsy and contribution of the ClC-2 chloride channel to neuronal excitability", submitted for the award of a doctorate, on my own (without external help), have used only the sources and aids indicated and have marked passages included from other works, whether verbatim or in content, as such. I swear upon oath that these statements are true and that I have not concealed anything. I am aware that making a false declaration under oath is punishable by a term of imprisonment of up to three years or by a fine.

Tübingen, den ....
                          Datum / Date   Unterschrift /Signature

Table of Contents

List of abbreviations

aCSF	Artificial cerebro-spinal fluid
AP	Action potential
cAMP	Cyclic adenosine monophosphate
$Ca_v2.1$-2.2	Voltage gated calcium channels 2.1 or 2.2
CBS	Cystathionine-β-synthase
cDNA	Complementary deoxyribonucleic acid
ClC	Chloride channel
CMV	Cytomegalovirus
CNV	Copy number variant
CNS	Central nervous system
cRNA	Complementary ribonucleic acid
DEPC	Diethylpyrocarbonate
DMEM	Dulbecco's Modified Eagle Medium
dNTP	Deoxyribose nucleotide triphosphates
EC_{50}	Half maximal effective concentration
EDTA	Ethylenediaminetetraacetic acid
EGTA	Ethylene glycol tetraacetic acid
EE	Epileptic encephalopathy
EEIE	Early Infantile EE
ER	Endoplasmic reticulum
FDS	Focal dyscognitive seizures
GABA	γ-aminobutyric acid
$GABA_{A-B-C}R$	γ-aminobutyric acid receptor A, B or C subtype
$GABA_{B1-B2}$	γ-aminobutyric acid receptor B subunit 1 or 2
GIRK	G-protein inward rectifying potassium channel
GlialCAM	Glial cell adhesion molecule
GTCS	Generalized tonic-clonic seizure
HBSS	Hank's Balanced Salt Solution
HET	Heterozygous
IBI	Inter-burst interval
ID	Intellectual disability
IGE	Idiopathic generalized epilepsy
ILAE	International League Against Epilepsy

IS	Infantile spasm
ISI	Inter-spike interval
KCC2	Potassium-chloride cotransporter 2
KCTD	Potassium-channel tetramerization domain
Kir	Inward rectifying potassium channel
KO	Knockout
MEA	Microelectrode array
MFR	Mean firing rate
NB	Neurobasal
NCBI	National Center for Biotechnology Information
$Na_v1.1$	Voltage gated sodium channel 1.1
NMDA-R	N-Methyl-D-aspartic acid receptor
NRT	Nucleus reticularis of the thalamus
PB	Population burst
PCR	Polymerase chain reaction
PFR	Peak firing rate
p/s	Penicillin streptomycin
REM	Rapid eyes movement
SEM	Standard error of the mean
SD	Standard deviation
TEVC	Two-electrode voltage-clamp
TiN	Titanium nitride
TM	Transmembrane domain
VB	Ventrobasal
WS	West syndrome
WT	Wildtype

1 Summary

In this thesis, I aimed to investigate the role of anion conductances for neuronal hyperexcitability and inherited epilepsy. I examined the functional consequences of novel epilepsy-causing mutations identified in $GABA_A$ or $GABA_B$ receptors. Additionally, a ClC-2 knockout (KO) mouse model was used to investigate the ClC-2 channel contribution to neuronal excitability in the thalamus and hippocampus.

In the first part, four novel mutations, identified by our collaborators in the $\alpha3$ subunit of the $GABA_A$ receptor (gene *GABRA3* on the X chromosome), were functionally characterized. Two mutations, Q242L and T166M, were found in two families with epileptic encephalopathy (EE), intellectual disability (ID), and other symptoms, as nystagmus, cleft palate and micrognathia. The EE phenotype followed an X-chromosomal inheritance pattern, affecting more severely the males, whereas females were mildly affected. Furthermore, two non-co-segregating mutations were detected, T336M in one of two sisters affected with idiopathic/genetic generalized epilepsy (IGE/GGE), and G47R in one of two brothers with autism spectrum disorder, both inherited by their unaffected mothers. To assess the pathogenicity of these variants, we introduced them into the cDNA of the human *GABRA3* gene and compared their properties to the wildtype (WT) using a *Xenopus laevis* expression system. The cRNAs coding for $\alpha3$ WT or mutant $GABA_A$ receptor subunits were co-injected with β2 and γ2 subunits and recordings were performed using automated two-electrode voltage-clamp recordings. A strong loss-of-function with >75% reduction in GABA-induced current amplitudes in comparison to the WT was found for both mutations associated with EE (Q242L and T166M), and the one associated with IGE (T336M). The reduction in GABA-induced current was much less pronounced (46.04 ± 9.46%) for G47R. The obtained results suggest that *GABRA3* mutations with a severe loss-of-function can cause X-linked EE with dysmorphic features. The missing co-segregation and genotype-phenotype correlation for the IGE- and autism-associated mutations imply that further genetic factors are involved to cause the disease in these families.

In the second part of my thesis, I have analyzed two *de novo* mutations found in *GABBR2,* encoding subunit 2 of the metabotropic $GABA_B$ receptor, in two unrelated patients with severe EE. Both patients present with profound ID and severe seizures. Functional analysis was also performed in *Xenopus laevis* oocytes. cRNAs of $GABA_B$ receptor subunits 1

and 2 were co-injected to form functional GABA$_B$ receptor, and Kir3.1/3.2 K$^+$ channels were co-expressed as a reporter. Both mutations caused a gain of channel function manifesting at lower GABA concentrations. A significant increase in GABA sensitivity was found for I705N (EC$_{50}$ of 0.48 ± 0.16 μM vs. 3.98 ± 0.68 μM for the WT) and S695I (EC$_{50}$ of 0.31 ± 0.2 μM vs. 3.96 ± 0.85 μM for the WT). Additionally, a significantly slower deactivation time constant in comparison with the WT, indicating a gain of function effect was observed for the S695I mutation. The increased sensitivity of both mutations at nanomolar GABA concentration, suggest a common pathomechanism based on increased activity of GABA$_B$Rs at extrasynaptic sites. Nevertheless, for a deeper understanding of how gain of function of the GABA$_B$ receptor could mediate the epileptic phenotype, further functional investigations using neuronal cells are necessary.

In the third part of my thesis, I worked on the contribution of ClC-2 channels to neuronal excitability. To this end, I analyzed neuronal activity in thalamo-cortical brain slices and hippocampal primary cultures obtained from WT and ClC-2 KO mice. Recordings from brain slices revealed that the action potential firing rate was significantly reduced in inhibitory neurons of the *nucleus reticularis thalami* (NRT) in ClC-2 KO mice in comparison with those from WT animals, suggesting less inhibition in the thalamocortical system and possibly increased excitability of the whole network. To verify this hypothesis, I recorded network activity using extracellular synchronous recordings in NRT, ventrobasal nucleus (VB) and cortex. An increase in synchronized activity in the three areas was observed in ClC-2 KO mice when GABA$_A$ receptors were blocked by picrotoxin, suggesting that the lack of ClC-2 may present a susceptibility factor for increased neuronal excitability. In addition, microelectrode array (MEA) recordings of hippocampal primary cultured neurons derived from KO and WT mice revealed that the lack of ClC-2 increases neuronal excitability by increasing the duration of spontaneous burst activity. Furthermore, the network properties of neurons derived from ClC-2 KO mice were not further altered by the GABA$_A$ receptor antagonist bicuculline in contrast to those of WT mice, suggesting that the loss of ClC-2 alone modulates the action of GABA$_A$ receptors. These results suggest that the ClC-2 channel has complex and important physiological functions and does play a role in the regulation of neuronal excitability.

Altogether, my thesis shows the importance of three players of neuronal excitability and inhibitory function of the nervous system, revealing different roles for epileptogenic mutations in GABA$_A$ and GABA$_B$ receptor subunits, and loss of the ClC-2 Cl$^-$ channel.

2 Introduction

2.1 Epilepsy

Epilepsy (from ancient Greek: to seize) is a common brain disorder characterized by an alteration of the normal brain excitability. Approximately 50 million people worldwide are affected by this disease. The International League Against Epilepsy (ILAE) defined epilepsy in relation to the incurrence of one (or more) of the following clinical conditions: The patient has (1) at least two unprovoked seizures occurring >24h apart or (2) one unprovoked seizure and at least 60% probability of further seizures, or (3) a previous diagnosis of an epileptic syndrome (Fisher *et al.*, 2014).

Epilepsy can be defined as "symptomatic" when it manifests as a consequence of metabolic or structural brain defects. In some cases, such a disorder can originate from a focal region, meaning that the seizure starts from a point around the lesion and may spread and involve the whole brain. Conversely, in other situations, the seizure may be generalized and begin simultaneously in both brain hemispheres. Typical brain lesions that may provoke epilepsy include tumors, stroke or hippocampal sclerosis. They may cause one of the most frequent and often pharmacoresistant epilepsy type, namely mesial temporal lobe epilepsy (Lerche *et al.*, 2013).

A second group of epileptic disorders has a genetic origin. These epileptic disorders are called "idiopathic" (Epilepsy, 1989), but use of the term "genetic" has been recently proposed (Berg *et al.*, 2010). They are a consequence of genetic defects, without any structural lesions and with a resulting phenotype that can vary from mild for the "idiopathic/genetic generalized epilepsies" (IGE/GGE) to severe, for the "epileptic encephalopathies" (EEs) (Lerche *et al.*, 2013). A majority of the mutations causing epilepsy affects voltage- or ligand-gated ion channels, but mutations in non-ion channels genes were identified as well as genetic cause of epilepsy. Interestingly, many of these genes mainly encode for proteins, which interact with ion channels or present a part of the synaptic complex (Weber & Lerche, 2008; Carvill *et al.*, 2014; Schubert *et al.*, 2014). A variation of ion charges due to mutations affecting ion channels could produce an imbalance between glutamate-mediated excitation and GABA-mediated inhibition, thus leading to a condition of neuronal hyperexcitability and epileptic seizures.

2.1.1 Idiopathic epilepsies

As mentioned before, idiopathic epilepsies are a consequence of genetic mutations. In the last twenty years a number genes from all major ion channel categories have been linked to different types of epilepsy. Especially the development of new DNA sequencing techniques, including whole exome and whole genome sequencing, contributed to the detection of rare and common variants affecting known or novel disease genes (Weber & Lerche, 2008; Myers & Mefford, 2015). It is believed that only a small percentage of the idiopathic epilepsies are due to single genes mutations and, therefore, monogenic, whereas most of them are caused by mutations in more than one gene and thus are polygenic (Dibbens *et al.*, 2007). In particular, the monogenic forms include rare focal epilepsy disorders, whereas the more common idiopathic generalized epilepsies (IGEs) belong to the latter category.

The first ion channel mutation identified in an inherited form of epilepsy was found in the gene *CHRNA4*, encoding the alpha 4 subunit of the neuronal nicotinic acetylcholine receptor (Steinlein, 1995) and causing *autosomal dominant nocturnal frontal lobe epilepsy* (ADFNLE)*.* Soon after, mutations in potassium channels *KCNQ2* and *KCNQ3* were identified as responsible for the benign familial neonatal seizures (BFNS) (Biervert *et al.*, 1998). Beside BFNS, other forms of benign seizures include the benign familial neonatal-infantile seizures (BFNIS), caused by *SCN2A* mutations and benign familial infantile seizures (BFIS) linked to the presynaptic protein encoding gene *PRRT2* (Herlenius *et al.*, 2007; Schubert *et al.*, 2012).

The IGE forms include (i) absence epilepsies, characterized by a brief loss of consciousness, or (ii) generalized epilepsy including childhood absence epilepsy (CAE), juvenile absence epilepsy (JAE), juvenile myoclonic epilepsy (JME) and epilepsy with generalized tonic-clonic seizures on awakening (EGTCA) (Crunelli & Leresche, 2002). Several mutations causing IGE were identified in γ-aminobutyric acid receptor A (GABA$_A$R) and associated with childhood absence epilepsy (*GABRG2*, (Wallace *et al.*, 2001)) or juvenile myoclonic epilepsy (*GABRA1*, (Cossette *et al.*, 2002)). Mutations in sodium channels (Na$_v$1.1, (Escayg *et al.*, 2000)) are responsible for genetic epilepsy with febrile seizures plus, in which the seizures occur in conjunction with fever. Moreover, during the last decades the number of IGE-related variants has been continuously increasing (Steinlein, 1995; De Fusco *et al.*, 2000; Jouvenceau *et al.*, 2001; Aridon *et al.*, 2006). Interestingly, it is a deletion on Chromosome 16 that has the highest frequency in IGE patients (de Kovel *et al.*, 2010).

2.1.2 Epileptic encephalopathies

Epileptic encephalopathies (EEs) are severe types of epilepsies which occur early in life and are characterized by pharmacoresistant epilepsy, electroencephalographic abnormalities, and intellectual disability, due to progressive cerebral dysfunction. For this reason, this subgroup of epilepsies encompasses complex and heterogeneous genetically inherited disorders, difficult to diagnose and to treat. Estimated 40% of seizures occurring during first three years of life are due to epileptic encephalopathies (Nieh & Sherr, 2014).

Recently, exome sequencing and whole genome copy number variant (CNV) analysis has suggested that mutations causing EEs often represent sporadic cases, occurring "*de novo*", or for the first time in a family. *De novo* mutations in the voltage-gated sodium channel $Na_v1.1$ (*SCN1A* gene) are the most common variants associated with a severe childhood epileptic encephalopathy, namely Dravet syndrome. Nevertheless, inherited autosomal dominant and recessive mutations or X-linked mutations were also identified (Allen *et al.*, 2013; Duszyc *et al.*, 2015).

The most common early and mild childhood onset EE are Ohtahara Syndrome, Dravet syndrome, West Syndrome and Lennox-Gastaut Syndrome. The seizure onset may occur in the first months of age, but also in the first years of life (3 to 7 years) as for the Lennox-Gastaut Syndrome (Nieh & Sherr, 2014).

2.2 GABA$_A$ Receptors structure and function

Synaptic inhibition in the central nervous system (CNS) is a result of γ-aminobutyric acid (GABA) signaling. The fast inhibition mediated by GABA takes place through the ligand-gated GABA$_A$ receptors (GABA$_A$Rs) in the brain and GABA$_C$R in the retina. Once GABA binds to GABA$_A$R, the channel opens, and the permeability to chloride and bicarbonate ions increases. This process leads to a hyperpolarized post-synaptic response in neurons, which decreases the probability of an action potential to occur. Besides binding to GABA$_A$R or GABA$_C$R, the GABA transmitter can also mediate a slower and more sustained inhibition by binding to the metabotropic GABA$_B$R (Farrant & Nusser, 2005; Jacob *et al.*, 2008).

GABA$_A$Rs are pentameric assemblies of different subunits that form the pore of the channel. 19 subunits have been identified so far: α (1-6), β (1-3), γ (1-3), δ, ε, θ, π, ρ (1-3). Furthermore, the composition of the receptor can also vary due to alternative splicing of some

subunits. Each subunit shares a common structure and is formed by four transmembrane domains (TMs), a long N-terminal domain on the extracellular side, and a large intracellular loop between TM3 and TM4. The N-terminal domain mediates the ligand binding, and the TM3-TM4 loop is responsible for the interaction with scaffolding proteins like gephyrin (Alldred *et al.*, 2005). The TM2 domains of the five subunits form the pore of the channel (Fig. 1 A, B). The most common composition of the receptor in the mammalian brain is made by two α subunits, two β subunits and one γ subunit, $\alpha1\beta2\gamma2$ representing ca. 60% of the whole GABA$_A$R population in brain (Mohler, 2006).

Receptors composed by $\alpha1$, $\alpha2$, $\alpha3$, or $\alpha5$ subunits, coupled with β and γ subunits, are sensitive to benzodiazepines and are localized at the post-synaptic site. The only exceptions to this rule are $\alpha5$-containing GABA$_A$ receptors, localized extrasynaptically, where they mediate tonic inhibition, a more sustained form of inhibition mediated by ambient concentrations of GABA. Other receptors with extrasynaptic localization are those containing $\alpha4$ or $\alpha6$ subunits. Furthermore, these receptors are insensitive to benzodiazepines. Thorough analysis of the GABA$_A$R expression in the mouse brain revealed high levels of $\alpha1$, $\alpha2$, $\alpha3$, $\alpha4$, $\beta1$, $\beta2$, $\beta3$ subunits and moderate presence of $\alpha5$, $\gamma1$ and $\gamma2$ in the cortex. In hippocampus, the most abundant are $\alpha1$, $\alpha2$, $\alpha4$, $\alpha5$, $\beta1$, $\beta2$, $\beta3$, $\gamma2$. The thalamus shows higher expression of $\alpha1$, $\alpha4$, $\beta1$, $\beta2$, and a milder expression of $\alpha2$, $\alpha3$, $\beta3$, $\gamma1$ and $\gamma2$. $\alpha6$ is found
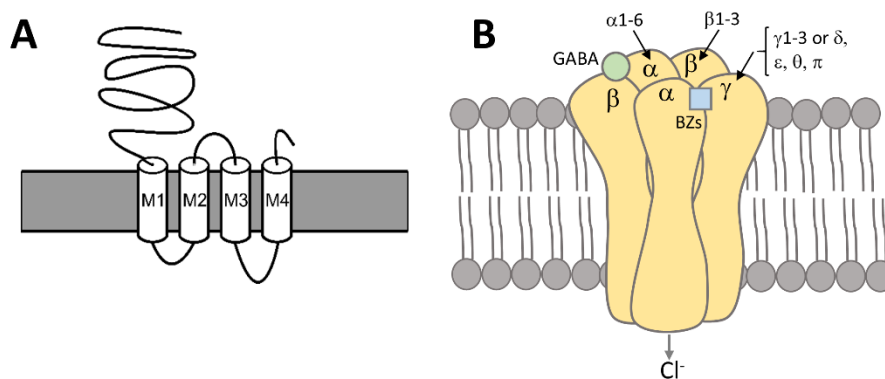

Figure 1. GABA$_A$R structure. (A) Each GABA$_A$R subunit consists of four transmembrane domains (TMs), a big extracellular N-terminal and a big intracellular loop between TM3 and TM4. (B) pentameric assembly of GABA$_A$R showing the binding sites of GABA (between α and β subunits) and of benzodiazepines (between α and γ subunits).

only in the cerebellum. Interestingly, the $\alpha3$ subunit is the only α subunit expressed in the nucleus reticularis of the thalamus (NRT, Hortnagl *et al.,* 2013).

2.2.1 Dysregulation of GABA$_A$Rs in epilepsy

Mutations causing epilepsy have been identified in different subunits of the GABA$_A$R, including $\alpha1$ (Cossette *et al.*, 2002; Maljevic *et al.*, 2006), $\beta2$, $\beta3$ (Allen *et al.*, 2013), $\gamma2$ (Harkin *et al.*, 2002; Ishii *et al.*, 2014) and δ subunits (Dibbens *et al.*, 2004). These mutations were identified in patients with different epilepsy syndromes, ranging from the less severe IGE to the more severe EE. Mutations in $\alpha1$ and $\gamma2$ subunits were found in families with Dravet Syndrome (Ishii *et al.*, 2014; Carvill *et al.*, 2015) and Infantile Spasms (Allen *et al.*, 2013), and $\beta3$ mutations were associated with Lennox-Gastaut syndrome (Allen *et al.*, 2013). Functional assays revealed that these mutations cause a loss of channel function. The mechanisms leading to reduced GABA-induced currents include a lower surface expression, reduced protein stability, reduced GABA-sensitivity and altered gating kinetics (Kananura *et al.*, 2002; Krampfl *et al.*, 2005; Maljevic *et al.*, 2006; Hirose, 2014). Decreased GABA-induced currents will have a dramatic repercussion on the physiological balance between inhibition/excitation in the brain, and may be the reason for increased seizure activity in patients (Benarroch, 2007). Proconvulsive activity of GABA$_A$R antagonists, such as bicuculline or picrotoxin, shown in different *in vitro* and *in vivo* assays supports this hypothesis (Cortez *et al.*, 2010; Hedrich *et al.*, 2014).

Trafficking mechanisms have been suggested as one of the reasons for the disruption of normal GABAergic activity. GABA$_A$Rs undergo complex trafficking processes, and mutations in the GABA subunits might contribute to the loss of the expression of these receptors at the synapses. Moreover, scaffold proteins, such as gephyrin, bind intracellularly to the GABA$_A$R receptors, clustering them at the synapses and loss of interaction with these proteins disorganize the complex synaptic localization of the GABA$_A$Rs (Studer *et al.*, 2006). The processes described above decrease the number of GABA$_A$Rs expressed at the synapses, thus leading to reduced synaptic inhibition, lower seizure threshold and a decreased sensitivity to anti-epileptic drugs binding to GABA$_A$Rs.

Mouse studies are important for the understanding of the complex genetic heterogeneity of epileptic disorders seen in patients. In the last twenty years, several knockout (KO) mouse models of different GABA$_A$R subunits were developed (DeLorey *et al.*,

1998; Mihalek *et al.*, 2001; Kralic *et al.*, 2002; Rudolph & Mohler, 2004), but so far only one knock-in mouse model of epilepsy, carrying the R43Q mutation in the $\gamma 2$ subunit, was produced and analyzed. This mouse model displays spike-wave discharges and absence-like seizures similar to those detected in patients (Reid *et al.*, 2013).

2.3 GABA$_B$ receptors

GABA$_B$ receptors are seven transmembrane domain guanine nucleotide-binding (G) protein-coupled receptors. After binding of their endogenous agonist GABA, they mediate slow and sustained inhibitory responses through the modulation of K^+ and Ca^{2+} channels. Perturbation of GABA$_B$R responses during development may alter the inhibitory/excitatory processes in the brain, resulting in several neurological disorders, including absence seizures.
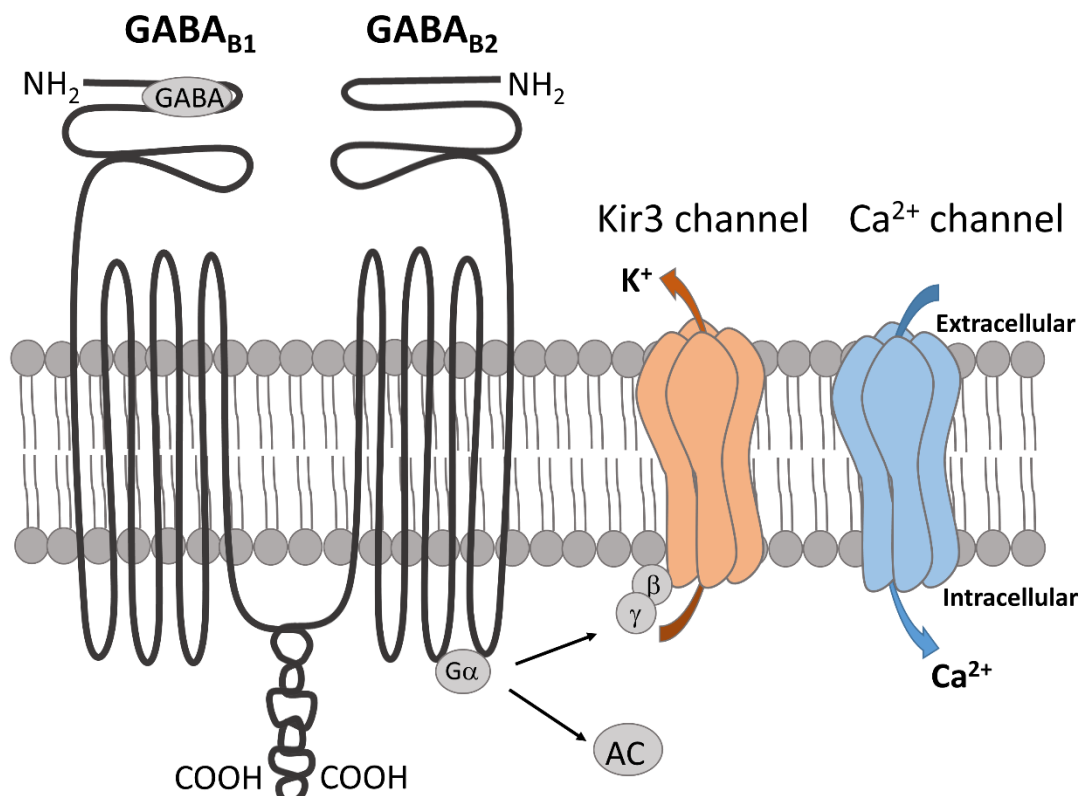
Figure 2. GABA$_B$R structure. The GABA$_B$R is formed by two subunits, GABA$_{B1}$ and GABA$_{B2}$. Each subunit is formed by seven transmembrane domains, a big extracellular N-terminus and an intracellular C-terminus. The N-terminal domain of the GABA$_{B1}$ subunit is responsible for binding the ligand, while the C-terminal one of GABA$_{B2}$ interacts with the G-protein to activate the K^+ channels Kir3 at postsynaptic sites or to inhibit the Ca^{2+} channels presynaptically.

Rodents treated with baclofen, the GABA$_B$R agonist, show an absence seizure phenotype, which in contrast can be suppressed by the treatment with the GABA$_B$R antagonist CPG35348 (Cortez & Snead, 2006; Wu *et al.*, 2007).

The cloning of GABA$_B$R has identified two GABA$_B$ genes, GABA$_{B1}$ and GABA$_{B2}$. Each gene encodes for a different subunit comprising a long N-terminal domain, a heptahelical transmembrane domain and a C-terminal intracellular tail (Lujan & Ciruela, 2012). To be functional, GABA$_B$Rs require heterodimerization of the two subunits (Pin, 2007). The N-terminus of the GABA$_{B1}$ binds ligands, whereas the C-terminal domain of the GABA$_{B2}$ subunit facilitates the G-protein activation. The C-terminal domains of both subunits interact with each other and are the target of several associated proteins, including transcription factors, scaffolding and adaptor proteins (Pin *et al.*, 2004).

GABA$_B$R signaling occurs through activation of G$_{i/o}$ proteins. Their primary action is the inhibition of presynaptic voltage-gated Ca^{2+} channels (N type, Ca$_v$2.2, or P/Q type, Ca$_v$2.1), which results in inhibition of neurotransmitter release. They also activate postsynaptic K$^+$ currents (the G-protein-coupled inward rectifying potassium channels, GIRK or Kir3) that results in hyperpolarization and late inhibitory postsynaptic potentials (Fig. 2). In addition, through G$_{i/o}$ α subunit, they inhibit the adenylyl cyclase, and therefore the cyclic adenosine monophosphate (cAMP)-protein kinase A pathway, which stands as necessary for the phosphorylation and upregulation of NMDA receptors (Ulrich & Bettler, 2007).

GABA$_B$Rs have a broad distribution in the brain. High expression of these receptors was found in the olfactory bulb, neocortex, hippocampus, thalamus and cerebellum (Fritschy *et al.*, 1999). Moreover, mice lacking GABA$_B$R have spontaneous epileptiform activity (Schuler *et al.*, 2001).

No epilepsy-causing mutations have been identified in the GABA$_B$Rs genes until recently, when two *de novo* mutations in the GABA$_{B2}$ subunit were found in patients with severe epilepsy. Both mutations are located on the sixth transmembrane domain. The first mutation was found at the amino acid position 695 wherein a serine was exchanged by an isoleucine (S695I) and the second mutation at the amino acid position 705 wherein an isoleucine was exchanged by an asparagine (I705N). The functional consequences of these mutations are investigated in the current thesis (Appenzeller *et al.*, 2014).

2.4 ClC-2 channels

The first ClC channel was cloned from *Torpedo marmorada* 25 years ago by Jentsch *et al.* (1990). This channel was called ClC-0 and used to define the ClC family. ClCs are anion channels and transporters that include nine human members. Four of them are ClC channels, ClC-1, ClC-2, ClC-Ka and ClC-Kb, while the other five are anion-proton transporters, ClC-3 through ClC-7 (Scheel *et al.*, 2005). The ClC channels and transporters have different physiological roles. The ClC transporters are mainly expressed intracellularly, in cellular compartments such as lysosomes and endosomes, where they contribute to the regulation of these organelles. In contrast, the ClC channels are mainly expressed on the surface membranes of excitable and epithelial cells, where they regulate either membrane excitability or they participate to the transport of water and electrolytes (Stölting *et al.*, 2014). Analysis of the crystal structure in prokaryotic cells has revealed that ClC channels and transporters share a similar structure (Dutzler *et al.*, 2002). The ClC proteins were identified as dimers, and each monomer is composed of 18 transmembrane helices. Intracellularly, each monomer ends with a long C-terminal domain containing two conserved cystathionine-β-synthase (CBS)
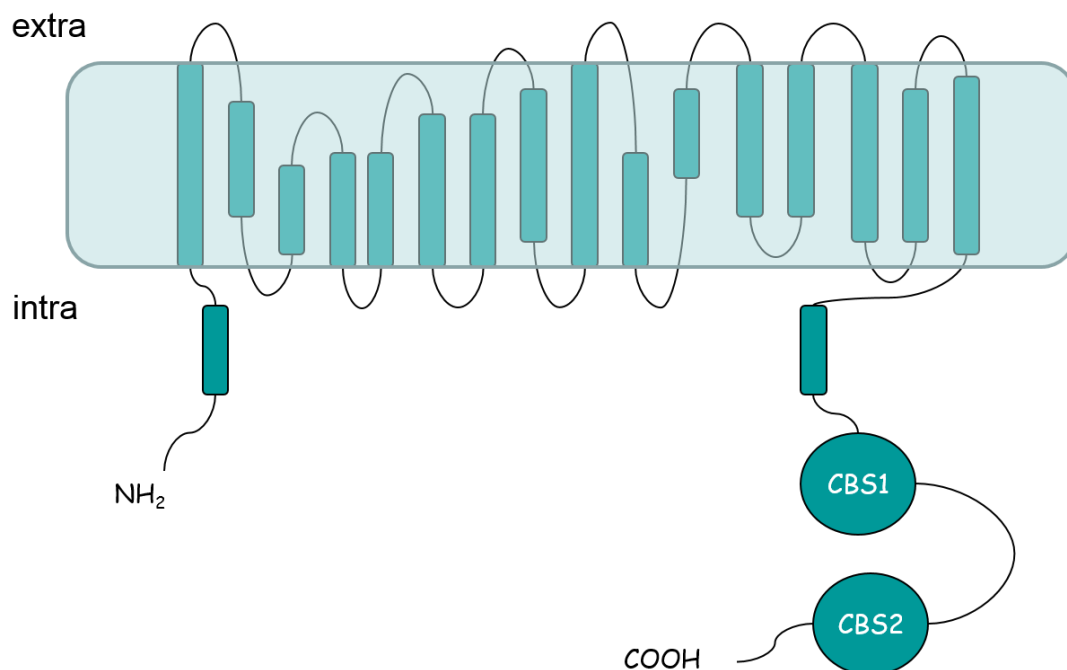

Figure 3. ClC structure. Each channel is a dimer and each monomer is formed by 18 transmembrane domain helices. The C-terminus contains two CBS domains responsible for the gating properties of the channels.

domains (Fig. 3). The CBS domains are important for channel gating, and their removal can cause loss of channel function (Garcia-Olivares *et al.*, 2008).

ClC-2 channel was cloned shortly after ClC-1 (Thiemann *et al.*, 1992). This channel is broadly expressed in excitable and not excitable cells. In the brain, it is highly expressed in pyramidal cells of the hippocampus, in Purkinje cells of the cerebellum, but also in the cortex, thalamus and other regions of the brain (Smith *et al.*, 1995; Sık *et al.*, 2000). Besides neurons, a high expression was observed in glial cells. Outside the CNS it is found in epithelia and the hearth (Thiemann *et al.*, 1992). ClC-2 channel activates slowly upon hyperpolarization, but it may also be activated by cell swelling and mild acidic extracellular pH, and it shows inward rectification (Staley, 1994). The opening probability of the channel depends on the concentration of intracellular chloride. More precisely, the channels open at membrane potentials more negative than the chloride equilibrium potential of the cell. Under these circumstances, ClC-2 channels allow chloride ions to exit the cell until the chloride equilibrium potential equals with the membrane potential, contributing to the stabilization of intracellular anion concentration in the cells in which the channel is expressed (Stölting *et al.*, 2014).

ClC-2 also has a role in glial cells, where it associates with an accessory subunit and cell adhesion molecule, GlialCAM. In heterologous systems, it was shown that this association is responsible for keeping the channel in a constant open state (Jeworutzki *et al.*, 2012). However, recordings from brain slices derived from GlialCAM KO mice showed that ClC-2 currents were not significantly different from the wildtype (WT), indicating that the effect is less pronounced *in vivo* than in heterologous systems (Hoegg-Beiler *et al.*, 2014).

ClC-2 variants were reported in patients with idiopathic generalized epilepsy (D'Agostino *et al.*, 2004; Saint-Martin *et al.*, 2009), but additional mutations, which disrupt channel function, have been reported in patients with leukoencephalopathy and brain matter oedema (Depienne *et al.*, 2013). These patients did not present any epileptic phenotype, suggesting that ClC-2 alone cannot be a major cause of epilepsy. Similar with the patients` phenotype, the ClC-2 KO mice show vacuolization of the white matter. Additionally, these mice have retinal and testicular degeneration (Bösl *et al.*, 2001; Blanz *et al.*, 2007). Eventhough they show abnormal cortical activity with an increased susceptibility to induced seizures (Cortez *et al.*, 2010), no spontaneous seizures have been detected (Bösl *et al.*, 2001; Blanz *et al.*, 2007).

The physiological role of these channels is not fully understood. It is believed that ClC-2 acts as an exit valve for chloride, therefore reducing the intracellular chloride concentration, which is normally increased by $GABA_AR$ (Rinke *et al.*, 2010). Thus, ClC-2 would help to keep the hyperpolarizing effect of $GABA_AR$ (Staley *et al.*, 1996). This is a similar role to the potassium-chloride cotransporter 2 (KCC2), which is the major chloride extruder in neurons (Kaila *et al.*, 2014). Oppositely, a modeling study suggested that in physiological conditions ClC-2 channels are open at positive potentials, leading Cl^- into the cells and therefore directly contributing to the increased intracellular Cl^- and neuronal excitability (Ratté & Prescott, 2011).

2.4.1 The thalamo-cortical system

The thalamus is a subcortical region responsible for the generation of synchronized oscillatory activity in the cortex, in normal and pathological conditions (Steriade *et al.*, 1993). In physiological conditions, thalamocortical oscillations are responsible for generating the sleep spindles during non-rapid eyes movement (REM) sleep. In pathological conditions, the thalamocortical system can generate spike and wave discharges occurring at 2.5-4 Hz in patients with idiopathic generalized epilepsy and more specifically with absence seizures (D'Arcangelo *et al.*, 2002).
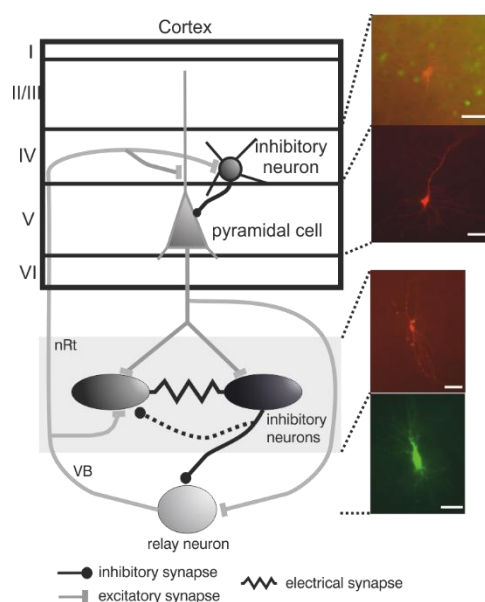
Figure 4. Thalamocortical system. The relay neurons receive inhibitory connections from the nucleus reticularis thalami (NRT) and excitatory connections from pyramidal cells of the cortex. In turn they send their excitatory connections to the NRT and back to the cortex. The cortex activates relay neurons in the ventrobasal complex (VB) and the inhibitory neurons in the NRT, which inhibit each other through electric synapses and inhibit the relay neurons, activating low threshold Ca^{2+} channels in these neurons, which give rise to bursting activity. Adapted from Hedrich *et al.* (2014).

Three neuronal populations are involved in this circuit: (i) the thalamic relay neurons in the ventrobasal complex (VB), (ii) the inhibitory neurons of the nucleus reticulari thalami (NRT), formed by a thin layer of GABAergic neurons surrounding the thalamus, and (iii) the pyramidal neurons in the fifth cortical layer (Fig. 4). The thalamic relay neurons can activate the cortical pyramidal neurons in two ways: in a tonic mode, which in normal conditions occurs during REM sleep, or in a burst mode, which occurs during non-REM sleep. The burst mode is mediated by T-type Ca^{2+} channels that are activated by hyperpolarization and mediate low-threshold depolarization with bursts of action potentials (Lee *et al.*, 2014). The rhythmic oscillatory activity is generated by the inhibitory neurons of the NRT. These neurons send their inputs to the relay neurons of the VB, hyperpolarizing them and activating the T-type Ca^{2+} channels and the burst activity. The relay neurons, in turn, send their projection to the inhibitory neurons in the NRT and to cortical pyramidal neurons starting another cycle of the oscillation. The pyramidal cells of the cortex, in turn, activate the inhibitory neurons in the NRT and the relay neurons in the VB (Chang & Lowenstein, 2003). A characteristic feature of inhibitory neurons of the NRT is that they are reciprocally connected through electrical synapses and can inhibit each other (Landisman *et al.*, 2002). In pathological conditions, such as absence epilepsy, the intra-NRT synaptic inhibition is reduced, transforming the normal synchronous activity into a hypersynchronous state, which leads to seizure-like activity (Huntsman *et al.*, 1999).

Interestingly, the KCC2 transporter has an extremely low expression in the inhibitory neurons of the NRT, which makes the GABAergic synapses in these cells to act through depolarization (Sun *et al.*, 2012). Furthermore, the absence of KCC2 in the inhibitory neurons of the NRT makes it easier to isolate the ClC-2 contribution to the thalamocortical circuit, which is one of the focuses of this study.

2.5 Aims

Within this thesis, three projects were developed with an overall aim to better understand the role of the GABAergic system in the generation of seizures and epilepsy. For this purpose, newly detected mutations affecting one GABA$_A$ and one GABA$_B$ encoding gene have been studied using a heterologous expression system. Moreover, the potential physiological role of the ClC-2 channel, related to the function of the GABAergic system has been investigated using a ClC-2 KO mouse model.

Specific aims were as follows:

1) To assess the functional defects of four novel mutations in the *GABRA3* gene, encoding the α3 subunit of the GABA$_A$R. The *GABRA3* mutations have been detected by our collaborators for the first time in patients affected with different forms of epilepsy, from mild idiopathic generalized epilepsy to severe epileptic encephalopathy with intellectual disability and dysmorphic features. Functional consequences of these mutations were analyzed using the two-microelectrode voltage-clamp technique in *Xenopus laevis* oocytes as a heterologous expression system.

2) To functionally analyze the first two epilepsy-causing mutations associated with the metabotropic GABA$_B$ receptors. These *de novo* mutations, found in the GABA$_{B2}$R subunit encoded by the *GABBR2* gene, were identified in patients affected by severe epileptic encephalopathies. The mutations were characterized by the two-microelectrode voltage-clamp technique and *Xenopus laevis* oocytes as a heterologous expression system.

3) To analyze the role of ClC-2 channels in neurons, more specifically its contribution to the neuronal excitability. For this purpose, a ClC-2 channel KO mouse model was used and patch-clamp and extracellular recordings experiments were performed in thalamocortical brain slices of ClC-2 KO, heterozygous (HET) and WT littermates. Additionally, network activities of primary hippocampal neuronal networks were compared for the three phenotypes using microelectrode array (MEA) analysis.

3   Materials and Methods

3.1   Molecular biology

3.1.1 Vector constructs

For oocytes measurements, the human cDNA of *GABRA3* was inserted in the pcDNA 3.1- vector. The WT construct was provided by Prof. Steven Petrou (Florey Institute of Neuroscience and Mental Health, Melbourne, Australia). cDNA encoding the human isoform of *GABBR2* and the two constructs containing missense mutations (I705N and S695I) were synthesized and cloned into the pcDNA 3.1+ vector by Gene-Script. *GIRK1* and *GIRK2* clones were synthesized and cloned into pCMV-XL5 and pCMV-XL4 respectively, by Origene. The expression of all clones is guided by a Cytomegalovirus (CMV) promoter in mammalian cells. The T7 promoter sequence existed as a template for T7 RNA polymerase, which is catalyzing DNA-dependent RNA synthesis.

3.1.2 Mutagenesis

In this study, our collaborators (Dorit Lev, Tally Lerman-Sagie (Metabolic-Neurogenetic Clinic, Wolfson Medical Center, Holon, Israel), Esther Leshinsky-Silver (Institute of Medical Genetics, Wolfson Medical Center, Holon, Israel), Vera M. Kalscheuer (Department of Human Molecular Genetics, Max Planck Institute for Molecular Genetics, Berlin, Germany), Agnieszka Charzewska (Institute of Mother and Child, Department of Medical Genetics, Warsaw, Poland), Nicola Specchio (Neurology Unit, Bambino Gesù Children's Hospital, IRCCS, Rome, Italy), Giuseppe Capovilla (Department of Child Neuropsychiatry, Epilepsy Center, C. Poma Hospital, Mantova, Italy), Pasquale Striano (Pediatric Neurology and Muscular Diseases Unit, Department of Neurosciences, Rehabilitation, Ophtalmology, Genetics, Maternal and Child Health, Institute "G. Gaslini", Genova, Italy), Federico Zara (Laboratory of Neurogenetics and Neuroscience, Institute "G. Gaslini", Genova, Italy)), identified four novel mutations in the *GABRA3* gene (p.Q242L, p.T336M, p.T166M, p.G47R). Two *de novo* mutations in the *GABBR2* gene (p.I705N and p.S695I) were identified by the EuroEPINOMICS Consortium (Appenzeller *et al.*, 2014). The *GABBR2* variants were delivered by Gene-Script (see 3.1.1). Properties of each plasmid construct (regarding the inserted DNA, length and position of the insertion) are shown in Table 1. Site-directed mutagenesis was performed for the *GABRA3* variants into the

Table 1. Properties of the inserted mutations

Gene	Vector	Mutation	Size of the insert
hGABRA3	pcDNA 3.1-	c.A725T/ p.Q242L	1478 bp
	pcDNA 3.1-	c.C497T/ p.T166M	1478 bp
	pcDNA 3.1-	c.C1007T/ p.T336M	1478 bp
	pcDNA 3.1-	c.G139A/ p.G47R	1478 bp
hGABBR2	pcDNA 3.1+	c.T2114A/ p.I705N	2825 bp
	pcDNA 3.1+	c.G2084T/ p.S695I	2825 bp

Table 2. Primers sequences

Primer name	Sequence	Used for
GABRA3 Q242L F	5´- GTTCTCGCTTGAACCTGTATGACCTTTTGGG - 3´	Mutagenesis
GABRA3 Q242L R	5´ - CCCAAAAGGTCATACAGGTTCAAGCGAGAAC - 3´	Mutagenesis
GABRA3 T166M-F	5´- CATAACATGACCATGCCCAACAAGCTG-3´	Mutagenesis
GABRA3 T166M-R	5´- CAGCTTGTTGGGCATGGTCATGTTATG-3´	Mutagenesis
GABRA3 T336M F	5´- GTGGCATATGCGATGGCCATGGACTGG - 3´	Mutagenesis
GABRA3 T336M R	5´- CCAGTCCATGGCATCGCATATGCCAC - 3´	Mutagenesis
GABRA3 G47R-F	5´- GGACATTGGCAGGCTGTCTCC- 3´	Mutagenesis
GABRA3 G47R-R	5´- GGAGACAGCCTGCCAATGTCC- 3´	Mutagenesis
GABRA3 seq-R	5´- CACAGTCGAGGCTGATCAGCG- 3´	Sequencing
T7 - F	5´- TAATACGACTCACTATAGGG- 3´	Sequencing

human cDNA using the QuickChange kit (Stragene, Agilent Technologies), *GABRA3* WT as a template and mutagenesis primers shown in Table 2.

The PCR conditions were as follows: 50 ng DNA template, 10x reaction buffer, 0.5 µl 10 pmol/µl of each primer, 0.5 µl dNTPs, 0.5 µl PfuUltra Turbo polymerase, up to 25µl with Ampuwa water. Products were confirmed by agarose gel electrophoresis (1% agarose

dissolved in Tris/Borate/EDTA; the solution was supplemented with 20,000x Red safe dye). Gel image was obtained by fluorescence illumination. The correct PCR product was first treated with the restriction enzyme DPN1 for an hour at 37°C to allow the digestion of the template.

3.1.3 Transformation

5 µl of the PCR product were transformed in 50 µl Top 10 *E. coli* strain. After 30 minutes of incubation on ice, cells were heat shocked for 30 s at 42°C. 250 µl of pre-warmed SOC medium was added for recovery and cells were incubated at 37°C, shaking at 300 rpm for 60 min. After recovery, cells were spread onto Ampicillin containing Agar plates (100 µg/ml Ampicillin; 10x Agar plates: 20 ml LB medium including 1.5% Agar).

3.1.4 DNA purification

Following overnight incubation at 37°C, resistant colonies that emerged on the LB plates were picked and inoculated in LB medium (10 g/l B-trypton, 5 g/l Bactoyeast, 10 g/l NaCl with pH 7.0 and autoclaved) containing Ampicillin (100 µg/ml) and cultured overnight at 37°C. On the next day, mini-prep was performed to obtain plasmid-DNA from the bacterial cultures by using Illustra plasmid Prep Mini Spin kit (GE Healthcare). For larger plasmid DNA amounts maxi-prep was performed using Genopure plasmid Maxi prep kit (Roche). Concentration of the plasmid DNA was measured using the Nanodrop spectrophotometer.

3.1.5 Sequencing

The correct insertion of the mutations was confirmed and additional mutations excluded by Sanger sequencing, performed by GATC Biotech Company. The used primers are shown in Table 2. Reference sequences for *GABRA3,* obtained from the National Center for Biotechnology Information (NCBI) nucleotide database, has Accession number: NM_000808. Sequences obtained from GATC were analyzed by CLC Sequence Viewer software (CLC Bio, QIAGEN).

3.1.6 DNA linearization

After obtaining the plasmid DNA in large quantities, the next step was to linearize the circular plasmid DNA to ensure the production of defined length RNA transcripts during the *in*

vitro RNA synthesis. For linearization, 10 μg of plasmid DNA, 2 μl restriction enzyme (that cuts downstream of the insert), 5 μl of respective enzyme buffer (10x) and up to 50 μl distilled water were mixed and incubated at 37°C for 2 h. For *GABRA3,* linearization was performed with HindIII, whereas for *GABRB2* and *GABRG2* with BamHI. Linearization for *GABBR1* and *GABBR2* was performed with XhoI and XbaI respectively, whereas *GIRK1* and *GIRK2* were linearized using SacII and SmaI respectively. DNA restriction was followed by a phenol/chloroform extraction to remove proteins from the nucleic acid samples. 100 μl DEPC-treated water and 150 μl phenol/chloroform were added to the DNA mixture, followed by a centrifugation step at 13,000 g for 2 min. The resulting upper phase (which includes the nucleic acids) was collected and 100 μl chloroform/isoamylalcohol added to the solution. After gently mixing and centrifuging (13,000 g, 2 min), the DNA was precipitated with 10 μl Ammonium-acetate and 300 μl 100% Ethanol, mixed gently and incubated at -80°C for 30-60 minutes. After this incubation, the mixture was centrifuged (12,000 g, 15 min, at 4°C), the supernatant discarded and the pellet was washed with 200 μl of 70% Ethanol and centrifuged (12,000 g, 15 min, 4°C). As the last step, the pellet was air-dried, dissolved in 10 μl DEPC-treated water and the linearized DNA was confirmed by Agarose gel electrophoresis.

3.1.7 RNA preparation

The linearized DNA-constructs were transcribed into capped RNAs using *in vitro* RNA synthesis. As the constructs in this study comprise T7 promoter, T7 polymerase was used to transcribe the corresponding RNA. Mixtures including 1 μg linearized DNA, 2.5 μl of T7 polymerase buffer (10x), 1 μl rNTPs, 2.5 μl cap analogue, 1 μl RNAse inhibitor, 2 μl T7 polymerase and up to 25 μl with DEPC-treated water were incubated at 37°C for 60 min. To degrade the DNA template, the products were further incubated with 1 μl of 10U DNase at 40°C for 15 min. Transcript mixture together with 100 μl DEPC-treated water and 125 μl Phenol/Chloroform was added in a phase-lock gel tube to perform phenol-chloroform extraction. After a centrifugation step (14,000 rpm, 5 min), 375 μl 100% Ethanol and 12.5 μl 3M Na$^+$ Acetate (pH 5.2) were added to the supernatant, mixed, and incubated for 30 min at -80°C. Incubation was followed by a further centrifugation step (14,000 rpm 15 min, at 4°C) and the pellet was washed with 500 μl 70% Ethanol. After a final centrifugation (14,000 rpm, 15 min at 4°C), the pellet was air dried and dissolved in DEPC-treated water. The RNA

transcripts were confirmed via Agarose gel electrophoresis and the concentrations were measured using the Nanodrop spectrophotometer.

3.1.8 Genotyping

ClC-2 mice used for MEA experiments or acute brain slices experiments were genotyped after each experiment. Tails or ear biopsies were digested over night at 55°C with proteinase K in lysis buffer (in mM: 50 Tris-HCl pH 7.5, 50 EDTA pH 8, 100 NaCl, 5 DTT, 0.5 Spermidine, 2 % SDS (v/v)). After the digestion, the DNA was precipitated in 100% of isopropanol, washed in 70% of ethanol and dissolved in Ampuwa water. PCR reaction was performed using primers listed in Table 3, and the obtained product visualized on the agarose gel. The expected size of the bands was 200 bp for the WT and 300 bp for the KO allele.

Table 3 Primers used for genotyping

Primer name	Sequence
ClC-2 KO - F	5´- ATGTATGGCCGGTACACTCAGGAACTC - 3´
ClC-2 NeoKO - F	5´- CCT GGA AGG TGCCACTCCCACTGTCC - 3´
ClC-2 KO - R	5´- ACACCCAGGTCCCTGCCCCAATCTGG - 3´

3.2 *Xenopus laevis* oocyte experiments

3.2.1 Oocyte preparation and RNA injection

Xenopus laevis oocytes are widely used as a heterologous expression system. The large size of the mature oocyte ($\approx$ 1.2 mm diameter) allows easy *in vitro* manipulation and injection of mRNAs or DNAs. Moreover, the oocytes express low levels of endogenous channels, making it easier to distinguish the heterologous ones. For ion channel expression, full mature oocytes in stage V-VI were used.

The use of animals and all experimental procedures were approved by local authorities (Regierungspraesidium Tuebingen, Tuebingen, Germany). Oocytes were obtained from the Institute of Physiology I, Tübingen, or purchased from EcoCyte Bioscience (Castrop-Rauxel, Germany). Preparation of oocytes for two-electrode voltage clamp (TEVC) recordings included treatment with collagenase (1mg/ml of type CLS II collagenase, Biochrom KG, Berlin, Germany) in OR-2 solution (mM: 82.5 NaCl, 2.5 KCl, 1 $MgCl_2$ and 5 Hepes, pH 7.6), to remove the external

layer containing the follicular cells, surrounding the oocytes. This process was necessary because the follicular layer expresses ion channels which could interfere with further electrophysiologically measurements and could additionally impair the RNA injection. Next, the oocytes were washed and stored at 16 °C in Barth solution (mM: 88 NaCl, 2.4 NaHCO$_3$, 1 KCl, 0.41 CaCl$_2$, 0.82 MgSO$_4$ and 5 Tris/HCl, pH 7.4 with NaOH) supplemented with 50 µg/ml gentamicin (Biochrom KG, Germany). To compare current amplitudes of WT and mutant channels, the same concentrations of cRNA were injected on the same day using the same batch of oocytes plated in 96 well-plates and measured 3 days after injection. To produce a functional GABA$_A$ receptor, the combination of subunits injected was $\alpha3\beta2\gamma2s$ in a 1:1:2 ratio. All cRNA concentrations were adjusted to 2 µg/µl and 70 nl of the corresponding cRNA were injected using Robooinject® (Multi Channel Systems, Reutlingen, Germany, Fig.5). For GABA$_B$ receptor expression, 50 or 70 nl of *GIRK1, GIRK2, GABBR1, GABBR2* (WT or mutation) were injected in a 1:1:2:2 ratio with a final RNA concentration of 1.5 µg/µl.
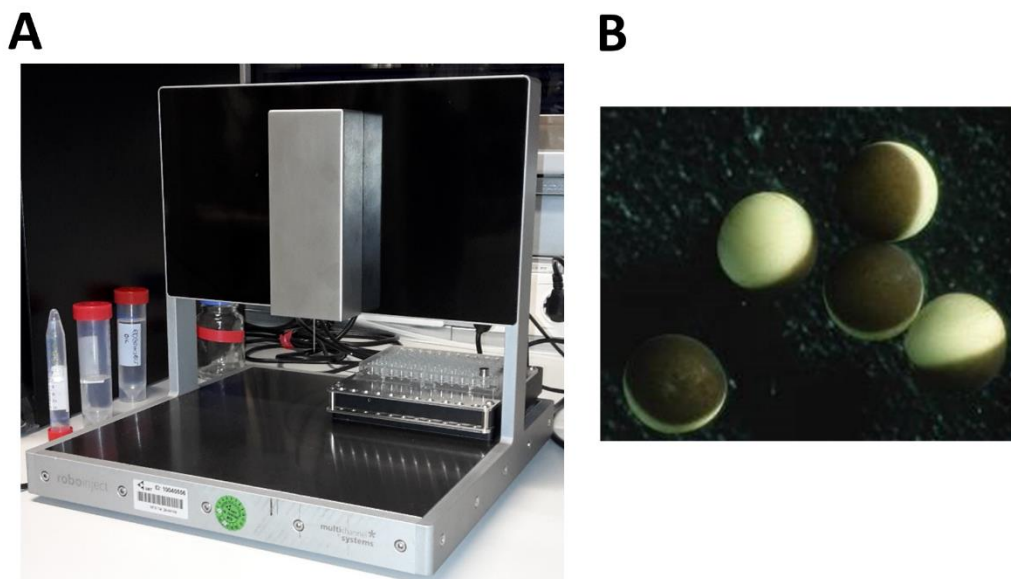

Figure 5. Automated Roboinject used for RNA injection into *Xenopus laevis* oocytes. (A) In the middle, the plate carrier can be observed, containing a 96 well plate, in which each well can potentially contain one oocyte. Additionally, the plate carrier contains spaces for eight different RNA tubes that could be used for injection. The injection needle is shown above the plate. (B) Stage V *Xenopus laevis* oocytes (≈ 1.2 mm diameter); the brown pigmented half, the so-called animal pole, is containing the nucleus, while the light half is the vegetal pole, which contains the primary energy source of the oocyte. The RNA was injected in the animal pole.

3.2.2 Automated oocyte two-electrode voltage clamp

GABA-evoked currents in oocytes were recorded at room temperature (20-22°C) using the fully automated Roboocyte2® (Multi Channel Systems, Reutlingen, Germany). Because of the large size of the oocytes, the two-electrode voltage clamp (TEVC) technique was applied (Fig. 6). TEVC is based on the use of two low resistance electrodes: one is measuring the voltage, and the other one is injecting the current. Prepulled and prepositioned intracellular glass microelectrodes had a resistance of 0.3–1 MΩ when filled with 1 M KCl/ 1.5 M KAc. The bath solution was ND96 (in mM: 93.5 NaCl, 2 KCl, 1.8 CaCl$_2$, 2 MgCl$_2$, 5 Hepes, pH 7.5). Currents were sampled at 1 kHz. The holding membrane potential was set at -70 mV. Different GABA concentrations (in µM: 1, 3, 10, 40, 100, 300, 1000) diluted in ND96 solution, were applied for 15 s to activate the GABA$_A$ channels. GABA$_B$ expressing oocytes were incubated with KD40 solution (in mM: 40 KCl, 52 NaCl, 5 Hepes, 1.8 CaCl2, 1 MgCl2, pH= 7.4) for 20 min to one hour before the recording. To activate GABA$_B$ channels, GABA was diluted in KD40 and different concentrations (in µM: 0.001, 0.1, 1, 3, 10, 100) were applied for 60s.
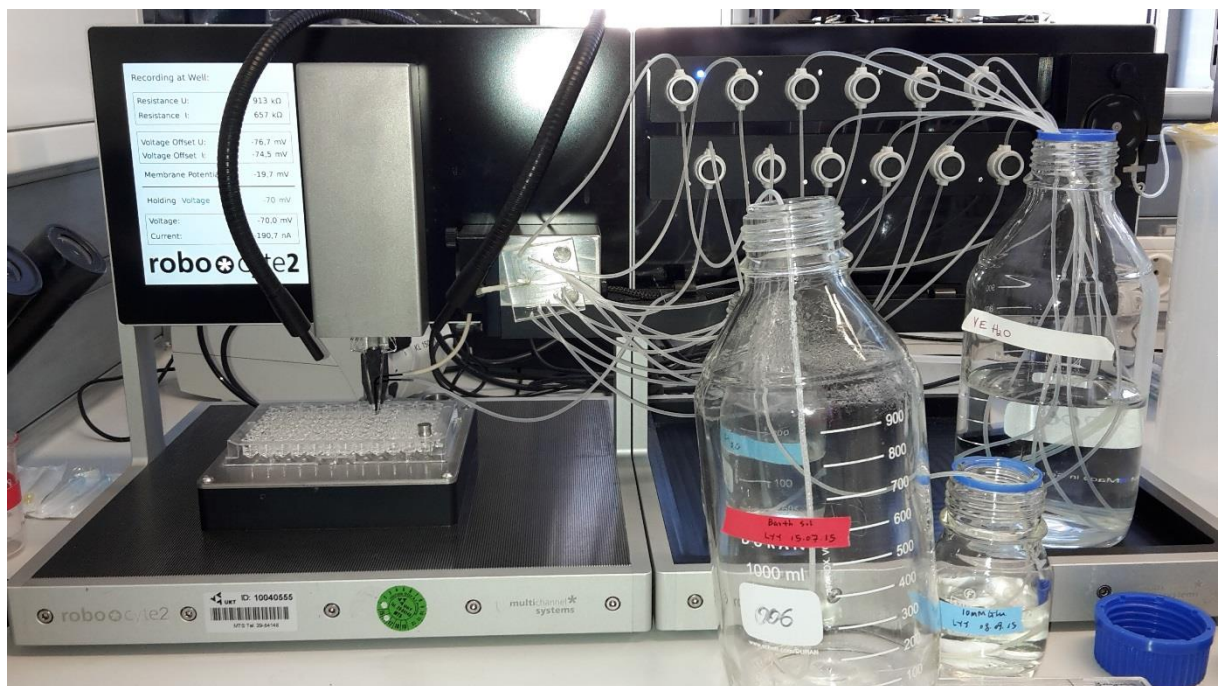

Figure 6. The fully automated Roboocyte 2. Left: plate carrier with the 96 well plate containing the oocytes and measuring head above the plate. Right: Perfusion system with 12 valves available for the agonist application.

3.3 Cell culture

3.3.1 Mouse hippocampi cell culture preparation

The hippocampi were collected from E17.5 pregnant *Clcn2* wildtype (WT), heterozygous (HET) and knockout (KO) mouse (BL.6-CLCN2<<tm1Mlv>>/Hlerc; Prof. James E. Melvin, University of Rochester). After suppressing the pregnant mice with CO_2, the embryos were removed from the uterus and decapitated. For genotyping, a piece of tail was collected for each embryo. The brain was removed, washed in HBSS and the hippocampi were isolated.

Table 4. Cell culture media, drugs and other materials

Media for primary hippocampal cell culture	Ingredients	Company
DMEM +	44.75 ml DMEM	Gibco
	5 ml FCS	PAN-Biotech, Aidenbach
	250 µl p/s (10 mg/ml)	Biochrom, Berlin
Neurobasal +	58.65 ml Neurobasal	Gibco
	1 ml B27	Gibco
	250 µl L-glutamine (200 mM)	Gibco
	p/s (10 mg/ml) 100 µl	Biochrom, Berlin
Other materials and drugs used for cell culture		
	PBS	Gibco
	HBSS	PAA Laboratories, Cölbe
	Poli-D-lysin (PDL) 0.1 mg/ml	Sigma-Aldrich
	1:200 in HBSS Laminin (1mg/ml)	Sigma-Aldrich
	0.05 % Trypsin	Gibco
	Bicuculline	Sigma-Aldrich

The dissociation of the hippocampi was performed under a sterile hood. After washing the hippocampi in HBSS, they were incubated in 0.05% of Trypsin at 37°C for 15 min. The reaction was stopped with DMEM supplemented with 10% FCS and penicillin/streptomycin.

Subsequently, the hippocampi were mechanically dissociated and the cell suspension filtered through a 40 µM cell strainer. 120.000 cells/100 µl DMEM, supplemented with 10% FCS and penicillin/streptomycin, were plated on each MEA dish. The MEA dishes were coated with poly-D-lysine (0.1 mg/ml) overnight at 4°C, followed by washing with water (2x) and PBS (1x). After washing, the dishes were dried and sterilized with the UV light (20 min) in the cell culture hood. Subsequently, 10-15 µl of laminin were placed in the middle of the dish and kept overnight at 4°C. Laminin was removed shortly before plating of cells. Four hours after plating, Neurobasal media supplemented with B27, penicillin/streptomycin and L-glutamine was added to each MEA (Table 4). Half of the media was exchanged every 3-4 days.

3.3.2 Network activity recordings using the microelectrode arrays (MEAs)

MEA dishes were bought from Multi Channel Systems (Reutlingen, Germany). A standard MEA dish has a square recording area of 700 µm to 5 mm of length. In this area, 60 planar titanium nitride (TiN) electrodes of 30 µm size are aligned in an 8x8 grid (Fig. 7).

To record spontaneous activity of primary *Clcn2* WT and KO, primary hippocampal neurons MEA dishes were prepared as described above (see section 3.3.1). The recordings were performed after 11, 18 and 25 days in vitro (DIV). According to the specification of the manufacturer, electrodes had an input impedance of 30-50 kΩ. Signals from all 60 electrodes were simultaneously sampled at 25 kHz, visualized and stored using the software MC_Rack provided by Multi Channel Systems. Extracellular recordings were performed at 37°C as follows: after two minutes of habituation, two minutes of recordings were done in the control condition (only media). Bicuculline (final concentration 10 µM) was added to the MEA dish and after two minutes of incubation time, two additional minutes were recorded. After the
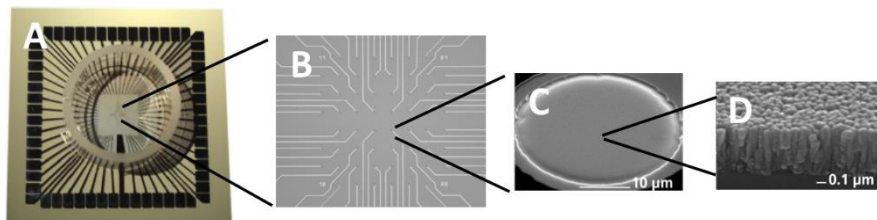

Figure 7. MEA chip. (A) Classical MEA chip with 60 extracellular electrodes**.** (B) The electrode spacing was 200 µm and the diameter of each electrode 30 µm. (C), (D), Magnification of one TiN microelectrode.

recording, each MEA dish was washed with the NB medium to remove any remains of the drug.

3.4 Acute thalamo-cortical brain slice preparation

For patch-clamp and extracellular experiments, acute brain slices preparation from *Clcn2* WT, HET or KO mice were prepared according to Agmon and Connors, 1991. Mice were analyzed between post-natal day (P) 10 and 18. To prepare the brain slices, the animals were anesthetized with Isoflurane (Cp-Pharma, Burgdorf, Germany) and quickly decapitated. The head was placed in the ice-cold cutting artificial cerebrospinal fluid (aCSF, Table 4), saturated with carbogen (95 % O_2, 5 % CO_2). Subsequently, the brain was carefully removed and placed on a glass ramp with a 10° slope. Using a sharp single edge blade, the brain was vertically cut at a 55° angle, about one-third from the anterior part (Fig. 8). Therefore, the special cut of the brain, using a 10° slope and a 55° angle, was made to allow the intact connectivity between
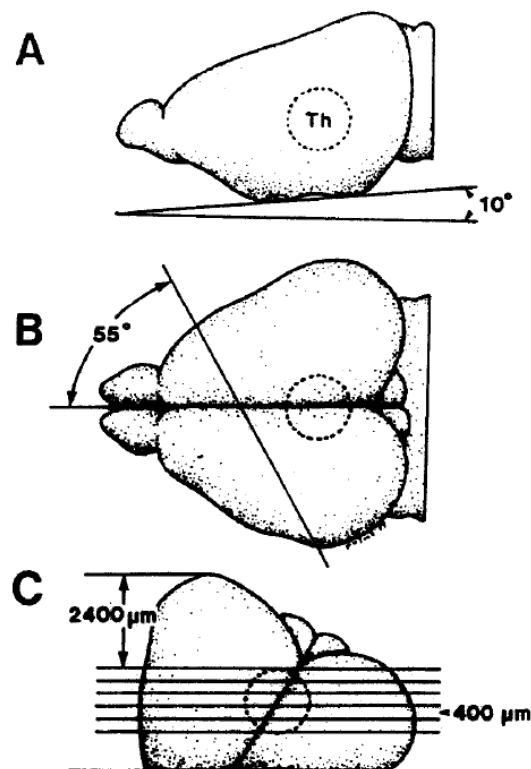

Figure 8. Preparation of acute thalamocortical brain slices. (A) The brain was laid on the 10° angle ramp. (B) The 55° angle used to cut vertically through the tissue. (C) The glued brain on the vibratome stage and the position of the slices containing the full connectivity between thalamus and cortex. Figure modified from Agmon and Connors (1991).

the cortex and the thalamic area, including the nucleus reticularis thalami (NRT) and the ventrobasal (VB) nucleus of the thalamus. The anterior part of the cut tissue was discarded while the posterior part was glued onto a Vibratome stage. The cut surface was glued down to the stage, with the dorsal part of the brain facing the blade. A small agar piece glued on the stage was used to hold the brain in this conformation. The tissue was completely immersed in cutting aCSF and three to four coronal 500 µM slices were cut and discarded. Once the thalamic area was reached, three to four 400 - 450 µM thalamocortical brain slices were cut. The slices were placed on a net in recording aCSF saturated with 95 % O2 and 5 % CO_2 and incubated for 40 min to one hour at 37°C. The incubation period increased the slices viability and was allowing the removal of dead cells on the tissue surface. Afterwards, the slices were transferred into the submerged recording chamber (Luigs & Neumann Feinmechanik und Elektrotechnik GmbH, Germany), continuously perfused with recording aCSF. All electrophysiological experiments were performed at 34°C.

3.5 Electrophysiological techniques

Neurons make use of the ion fluxes across their membrane to generate electrical signals. They evolved this mechanism to be able to transmit information. An approach to identify these electrical signals is to use electrophysiological techniques, which record ion fluxes across a cell membrane. They can include the use of extracellular electrodes or micropipettes to make a direct contact with the cell of interest. The latter technique can include the intracellular recording method, where sharp micropipettes penetrate the cell or the patch-clamp method, where the micropipette makes a tight contact with the cell, without entering inside the cell (Molleman, 2003).

3.5.1 Patch-clamp method

Over the past decades we have acquired plenty of new information due to the patch-clamp technique which was invented by Neher and Sakmann (1976). This finding made it possible to record currents from single ion channels and to understand their contribution to the transmission of electrical information in neurons. This method is based on the use of a glass pipette with a very small opening (some µm) to make a tight contact with tiny area or patch of cellular membrane. After applying negative pressure, the seal is produced by the very

high resistance contact between the pipette and the membrane. The resulting small current can be measured by an amplifier connected to the pipette. This first conformation is called *cell-attached patch-clamp recording method* (Fig. 9) and enables recordings of single channel currents. If the patch membrane is disrupted through suction, the intracellular solution
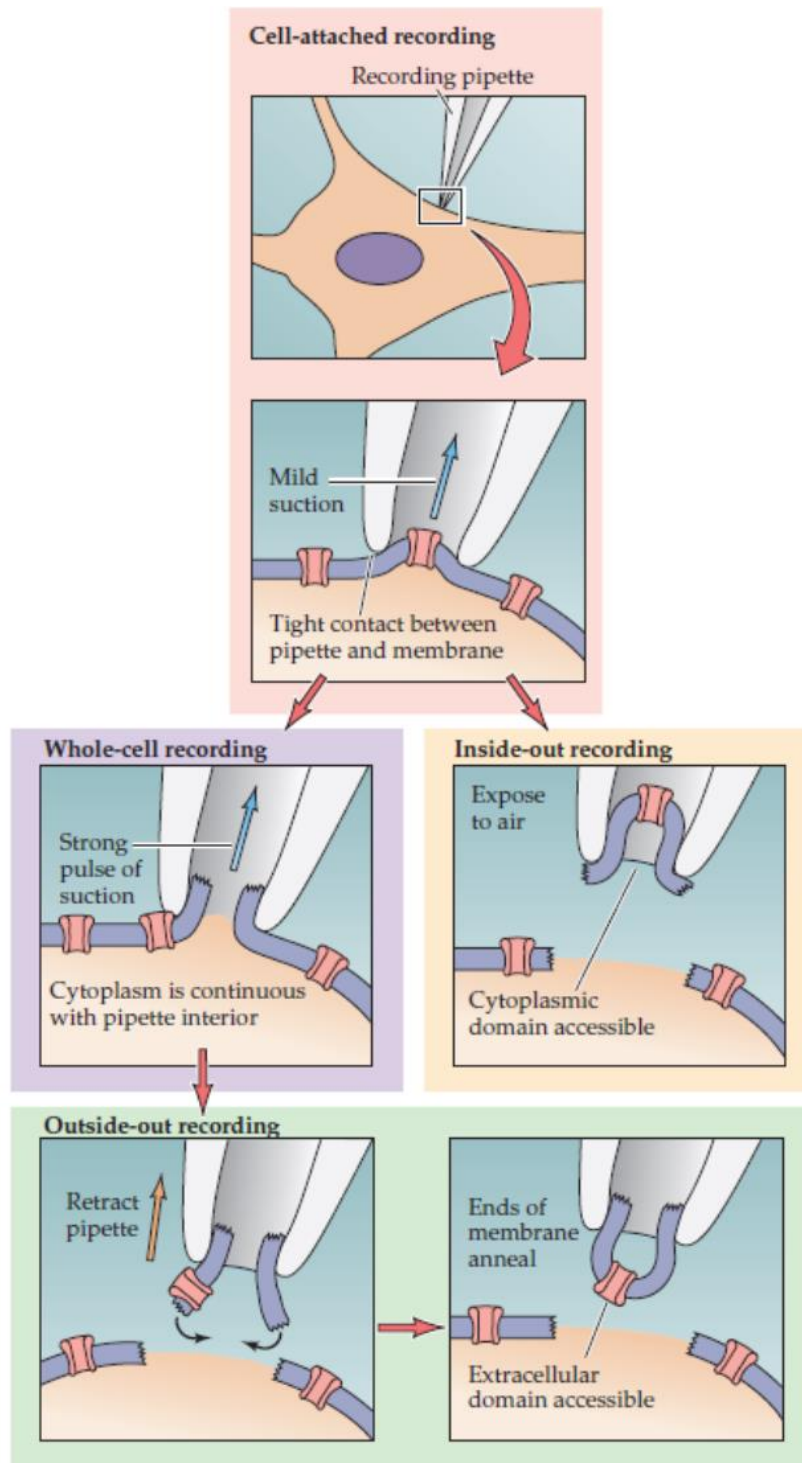

Figure 9. Four patch clamp configuration (picture from Purves *et al.* (2004)).

contained in the glass pipette is mixing with the cytoplasm of the cell, allowing measurements of electrical potentials and currents of the entire cell. This conformation is called *whole-cell patch-clamp* (Fig. 9). Another variant of the patch-clamp methods includes pulling the glass pipette away from the cell, keeping a small piece of membrane attached to the pipette without breaking the seal. Overall, these configurations, make the patch clamp technique an extremely flexible and resourceful method to study how ion channels function (reviewed by Purves *et al.,* 2004) .

All voltage clamp experiments performed in this study were done using an Axopatch 200B amplifier (Molecular Devices, Union City, CA, USA), while the current clamp experiments (paragraph 3.5.2 and 3.5.3) were performed using a BVC-700A Bridge and VC amplifier (Dagan Corporation, Minneapolis MN USA). The amplifier head-stage was mounted on a motorized manipulator (LN Unit Junior, Luigs & Neumann Feinmechanik und Elektrotechnik GmbH,

Table 5. Brain slices solutions

aCSF for ClC-2 currents recordings	Chemicals	Working solution (mM)
Cutting aCSF	NaCl	130.9
315-325 mOsm/l	KCl	2.75
pH = 7.4	$MgSO_4*7H_2O$	1.43
	$NaHCO_3$	28.82
	$NaH_2PO_4*H_2O$	1.1
	$CaCl_2$	2.5
	Glucose	11.1
Recording aCSF	NaCl	70
290 mOsm/l	KCl	2.5
pH = 7.4	$MgSO_4*7H_2O$	16
	$NaHCO_3$	26.2
	CsCl	10
	Glucose	11
	TEA	30
	TTX	$0.2*10^{-6}$
	ZD 7288	0.05
aCSF for APs and extracellular recordings		

Cutting aCSF	NaCl	125
305 mOsm/l	NaHCO$_3$	25
pH = 7.4	KCl	2.5
	MgCl$_2$ *6 H$_2$O	1
	NaH$_2$PO$_4$	1.25
	CaCl$_2$ * H$_2$O	1
	MgCl$_2$ *6 H$_2$O	7
	Glucose	10
Recording aCSF	NaCl	125
305 mOsm/l	NaHCO$_3$	25
	KCl	2.5
	MgCl$_2$ *6 H$_2$O	1
	NaH$_2$PO$_4$	1.25
	CaCl2 * H2O	2
	MgCl$_2$ *6 H$_2$O	1
	Glucose	10
Intracellular solution for ClC-2 currents recordings		
290 mOsm/l	CsCl	90
pH = 7.2	Cs-Gluconate	20
	NaCl	8
	MgCl$_2$	2
	HEPES	10
	EGTA	1
	QX-314 (Lidocaine)	2
Intracellular solution for APs measurements		
290 mOsm/l	KCl	5
pH = 7.2	ATP-Mg	4
	Phosphocreatine	10
	GTP-Na	0.3
	HEPES	10
	K-Gluconate	125
	MgCl2*6H$_2$O	2
	EGTA	10

Germany) and fixed next to a Axioskop 2 microscope (Zeiss, Germany), connected to an image acquisition B/W CCD-camera, which allowed brain slices visualization on a screen. The submerged recording chamber and the microscope were placed on an anti-vibration table for patch-clamp setups and a Faraday cage was built around the setup. All metal parts inside the cage were grounded using the ground input of the amplifier. The outputs signals of the amplifiers were digitalized by a Digidata 1440A digitizer (Axon Instruments, Union City, USA), connected to a personal computer, using Clampex 10.2 (Axon Instruments, Union City, USA) as acquisition system. Glass pipettes were pulled from borosilicate glass (Science Products GmbH) using a Sutter P97 puller (Sutter Instruments).

3.5.2 Voltage clamp experiments

Whole-cell voltage clamp technique is a patch-clamp method that controls or clamps the voltage (or membrane potential) at a value chosen by the experimenter. This method is using a microelectrode to measure the membrane potential and compares it to a set command voltage, which is the voltage the experimenter wants to maintain. The microelectrode is connected to an amplifier, which injects current into the cell when the membrane potential differs from the set command voltage. Therefore, this method is very useful to understand how the membrane potential can affect the current flow of different ion channels.

Whole-cell recordings were obtained from neurons of NRT, VB or cortex (layer IV- V) of analyzed brain slices. The solutions I have used to record the ClC-2 chloride currents are shown in Table 5 (after Rinke *et al.,* 2010). When filled with intracellular solution the borosilicate glass microelectrodes had a resistance of 3-5 MΩ. The signals were low-passed filtered at 5 kHz and sampled at 20 kHz. Because of the equimolar concentration of Cl$^-$ between extra- and intracellular solution, the holding voltage was set at 0 mV. ClC-2 chloride currents were evoked by stepping the membrane potential from +40 mV to -120 mV for 4 s with an additional 1 s step to +40 mV to record tail currents.

3.5.3 Current clamp experiments

The current clamp technique is a patch-clamp method that controls or clamps the current while measuring the resulting membrane potential. The whole cell current clamp recordings in this study were obtained from the NRT. Extracellular and intracellular solutions

that were used are summarized in Table 5. For these experiments, the data were low-pass filtered at 30 kHz and sampled at 100 kHz. When filled with an intracellular solution the glass electrodes had a resistance of 3-5 MΩ. The cells were held at -70 mV. Establishing of the whole cell configuration was done in voltage clamp mode. Once this configuration was reached the mode was changed into current clamp and the balance bridge compensated. After 5 min of incubation time, allowing the exchange of intracellular solution within the cell, hyperpolarizing (from -10 to -110 pA for 500 ms) or depolarizing current injections (from -50 to 300 pA for 800 ms) were applied to measure the input resistance or evoke action potential (AP) trains.

3.5.4 Extracellular field recordings

The extracellular field potential measures the extracellular electric potential produced by a group of neurons in the proximity of the pipette as a result of synaptic activity. As for the patch-clamp experiments, brain slices were positioned in a submerged chamber continuously perfused with aCSF and all recordings were performed at 32°C. For these recordings, a four channels differential AC amplifier model 1700 (A-M Systems, USA) was used. Extracellular signals were recorded simultaneously by three suction electrodes placed on the slice in three different areas (NRT, VB, Cortex; Fig. 10). The obtained signals were amplified 10.000 times
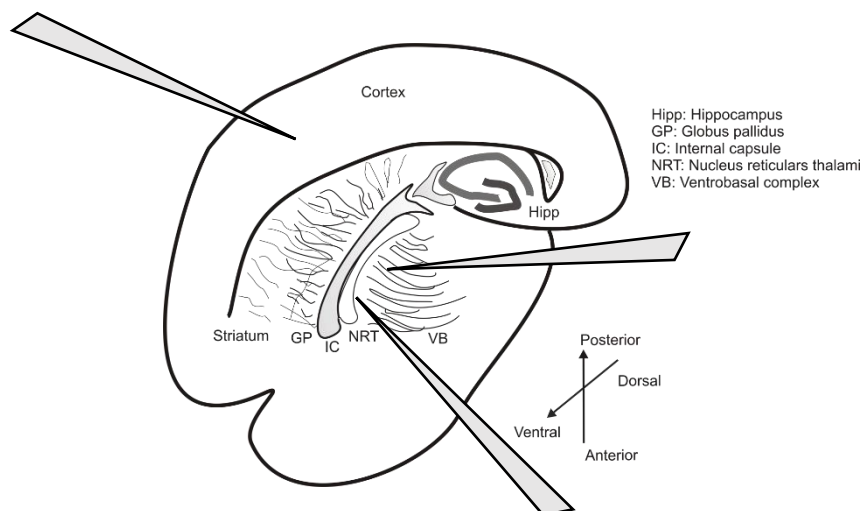

Figure 10. The thalamocortical brain slice showing the three recordings electrodes for the extracellular configuration. One electrode is placed in the cortex (layer IV-V), one in the NRT and one in the VB. Scheme from Nele Dammeier (Department of Neurology and Epileptology, Tübingen).

and filtered between 0.25 and 1.5 kHz and the resulting trace represented the multiunit AP activity.

3.6 Data analysis

3.6.1 GABA-induced currents

The amplitude of the GABA-induced currents was analyzed using Roboocyte2+ (Multi Channel Systems, Reutlingen, Germany), Clampfit (pClamp 8.2, Axon Instruments), Microsoft Excel (Microsoft, Redmond, WA) and Graphpad Prism software (GraphPad Software, La Jolla, CA, USA). The obtained currents were analyzed in two different ways. First, the current response of each GABA concentration was normalized to the maximum response evoked by the highest GABA concentration. The normalized GABA responses of each cell were fitted to the four parameter logistic equation:

$$\text{Y} = \min + \frac{(max - min)}{1 + 10^{((\text{LogEC50} - \text{X}) * \text{nH})}}$$

with max and min being the maximum and minimum evoked responses and X the corresponding GABA concentration. The EC_{50} value is the concentration of the agonist for which half of the maximum response is achieved, while nH is the Hill coefficient, which determines the steepness of the dose-response curve. EC_{50} values were determined for each oocyte and the averaged EC_{50} values for WT and each mutation are shown as mean ± SEM. To test the differences in current amplitudes generated in response to 1 mM or 100 µM GABA application (for activating $GABA_A$ or $GABA_B$ receptors, respectively), current responses of wildtype and mutant channels recorded on the same day were normalized to the mean value of the wild-type channel currents recorded on that day. The ratio between WT and mutation obtained in this way was used to calculate the reduction of GABA-induced currents for each GABA concentration in the dose-response curve for each mutation in comparison with the WT and to draw the predicted dose-response curve. For $GABA_B$Rs, deactivation time constants were derived from a single-exponential fit to the decay phase of Kir 3.1/3.2 GABA mediated currents after agonist application. Curve fitting was performed in Clampfit (pClamp 8.2, Axon Instruments) and further data analysis were performed with Graphpad Prism software (GraphPad Software, La Jolla, CA, USA).

3.6.2 GIRK current analysis

To verify that the oocytes were expressing the injected WT GIRK channels and that there was no change in the amplitude of the evoked currents between WT and mutated *GABBR2* channels in absence of GABA application, potassium currents were recorded either in ND96 or in KD40 solution. The latter bath solution was used because a higher potassium concentration is necessary to activate the GIRK channels (Ng *et al.*, 1999). The currents were induced by 500 ms voltage commands from a holding potential of -10 mV, delivered in 10 mV increments from -140 mV to +60 mV. The current amplitudes were measured when they reached the steady state and the resulting current-voltage curves were plotted.

3.6.3 MEA analysis

Spike and burst analysis were performed off-line by a custom build software, SPANNER (RESULT Medical, Düsseldorf, Germany). The analyzed parameters were: number of spike per minute, inter-spike interval (ISI), number of bursts per minute, burst duration, inter-burst interval (IBI), number of spikes per burst, and kappa (Fig. 11 A). Kappa is a parameter that measures the probability of spikes occurring on at least three electrodes at the same time in a 10 ms bin. Individually for each channel, the threshold for spike detection was set to 6.2 standard deviations (SDs) of the average noise amplitude during a 10% "learning phase" at the beginning of each measurement. An absolute refractory period of 4 ms and a maximum spike width of 2 ms were set on the spike detection algorithm. Burst detection was performed for each electrode and the temporal clustering of spikes was compared with a Poisson process of independently occurring spikes at the same mean firing rate (null hypothesis). Given the mean firing rate (MFR) of each electrode, the probability P (N, Δt|MFR) of finding at least N spikes within the time span Δt was calculated using the Poisson distribution. An observed cluster of N>3 spikes occurring within Δt was considered as burst, if its Poisson probability P (N, Δt|MFR) was below 0.005 (Illes *et al.*, 2009).

Synchronous network activity was analyzed by population burst (PB) detection using custom build Matlab software (RESULT Medical, Düsseldorf, Germany). Spikes from all electrodes were aggregated in nonoverlapping 5 ms bins and smoothed by a Gaussian kernel with a 100 ms SD to obtain the population firing rate (PFR and Fig. 11 B).
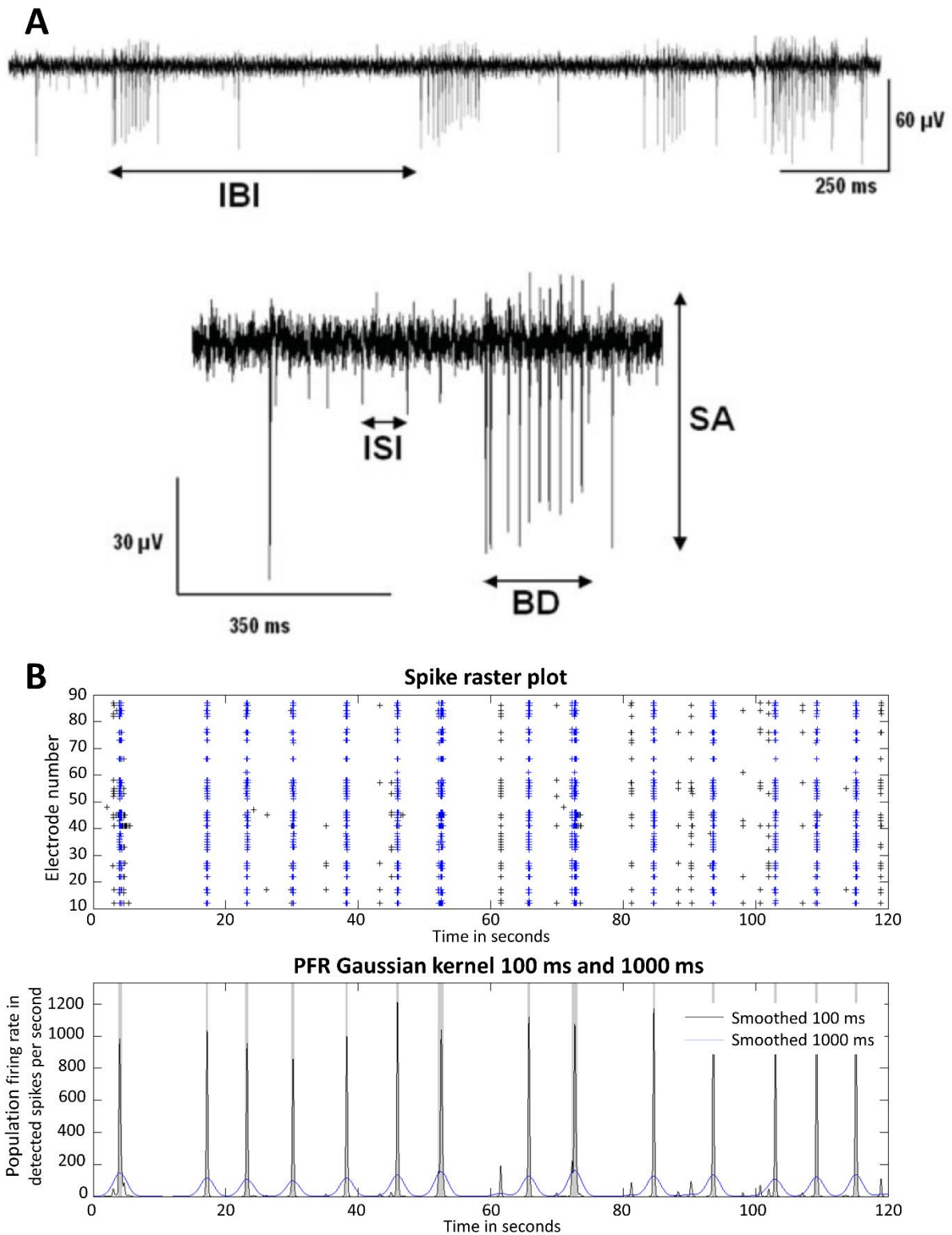
Figure 11. MEA Analysis. (A) Recording trace of one channel of a single MEA electrode; several electrophysiological parameters may be visualized and analyzed using SPANNER software: inter-burst interval (upper trace), inter-spike interval (ISI), burst duration (BD), and spike amplitude (SA) (lower trace). Figure adapted from Otto *et al.* (2009). (B) Representative spike raster plot illustrate spike activity on all 60 electrodes. The synchrony of neuronal networks is shown as the population burst (PB) shown in blue (upper panel). PFR is shown as the amplitude of total number of spikes in a PB in an interval of 100 ms.

PB detection was performed in a three-step procedure. First, PB candidate intervals were identified as the PFR exceeding the slowly varying 1 s firing rate average. In a second step, the PBs from previous described intervals were selected, if their peak firing rate exceeded 3 standard deviations (SDs) of the recording PFR and 10% of the average of the top five peaks, and at least three electrodes participated. Finally, if neighbouring PBs were <200 ms apart, they were merged together. The peak firing rate (i.e., the maximum PFR within a PB interval, reported in spikes per second) and the number of PBs per minute were analyzed. Additionally spikes were collected in 10-ms-wide bins and used for the quantification of firing synchrony across pairs of electrodes. Spikes were dichotomized to either zero spikes or at least one spike. For two electrodes, they were either active during a time bin or only one electrode active, or both were silent. The synchrony was tested by Cohen´s kappa (Woolson & Clarke, 2011).

3.6.4 Electrophysiological analysis

For the voltage clamp experiments, the amplitude of the ClC-2 chloride currents was calculated as the difference of the inward current at the beginning and the end of the voltage step when the steady state was reached. Current-voltage curves were plotted. In this study, I was interested in verifying if neurons from NRT, VB or cortex express the ClC-2 channel. Therefore the maximal current response was measured and plotted in a scatter dot plot graph.

For the current clamp experiments, several parameters were analyzed: the AP frequency per each current injection, the input resistance, the AP threshold and the AP width. An AP was considered for analysis when the overshoot was exceeding the 0 mV. The AP frequency was measured using the automatic event detection setting in Clampfit. A threshold was set between the membrane potential (-70 mV) and above 0 mV. All events above the set threshold were automatically counted for each current injection. Additionally, the inter-spike interval was determined for each AP train for five spikes within the burst and for the last five spikes within the tonic firing (Fig. 12). To calculate the input resistance the hyperpolarizing current injection steps were applied and potentials´ amplitudes determined for each current injection. These amplitudes were plotted against the current injection to obtain a scatter plot graph and a trend line was produced. The AP input was measured as the "x" coefficient of the trend line. To measure the AP threshold and the AP width, the first AP in the depolarizing current injection protocol was used. The AP threshold was defined as the membrane potential at which the rate of rise of voltage crossed 50 mV/ms in the first derivative, whereas the AP

width was the time occurring between the two peaks in the first derivative of the AP trace (Kole and Stuart, 2008 and Fig. 13).
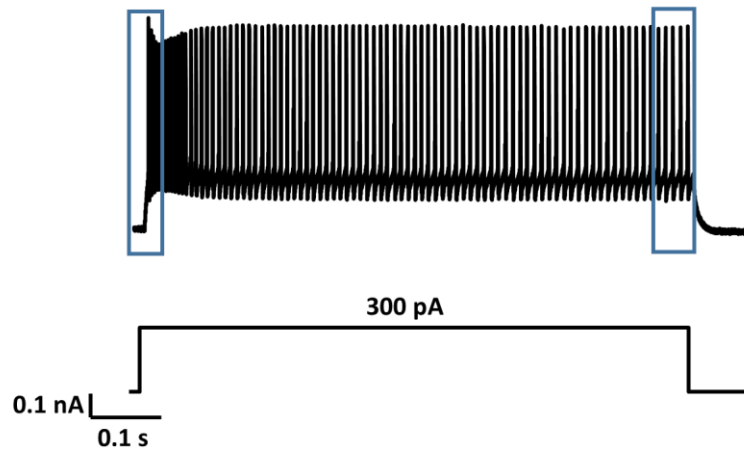

Figure 12. Interspike interval. The interspike interval was analyzed for the first five spikes within the burst and the last spikes within the tonic firing in the AP train induced by 300 pA of current injection.
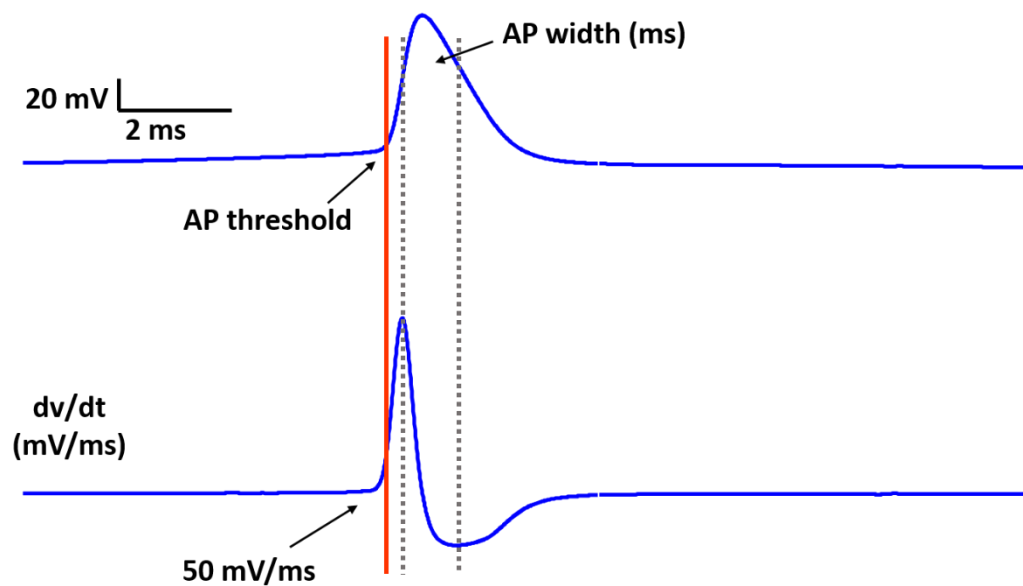

Figure 13. AP threshold and width. Upper graph: an example of a recorded AP. Lower graph: first derivative of the same AP. The AP threshold was calculated as the membrane potential at the 50 mV/ms of the first derivative, while the width was calculated as the time between the two peeks in the first derivative.

For the extracellular recordings, the synchrony of the occurring bursts across the three areas (NRT, VB and cortex) was calculated. Using Clampfit, the synchronous bursts were

automatically counted above a set threshold in all three areas before and after application of picrotoxin, which is a non-competitive blocker of GABA$_A$Rs.

3.6.5 Statistical analysis

Data distribution was tested for normally distribution using GraphPad Prism 6 (GraphPad Software). Groups were compared using one-way ANOVA with Dunnett´s *post-hoc* test for normally distributed data or one-way ANOVA on ranks with Dunn´s *post-hoc* test for not normally distributed data. For some data, two-way ANOVA and Sidak´s multiple comparison test was used. For unpaired or paired data sets and normally distributed data, Student´s t test was adopted. Mann-Whitney rank-sum test was used for the not normally distributed data. All data is presented as mean ± standard error of the mean (SEM). Statistical differences are indicated in the figures legend with the following symbols: $*p < 0.05$, $**p < 0.01$, $***p < 0.001$.

4 Results

4.1 *GABRA3* mutations as a cause of X-linked epileptic encephalopathy

In this study, four missense variants and a microduplication in the *GABRA3* gene were found in five different families by our collaborators (Fig. 14).

Genetic analysis and clinical evaluations were done in collaboration with Dorit Lev, Tally Lerman-Sagie, Esther Leshinsky-Silver from the Wolfson Medical Center (Holon, Israel), Vera M. Kalscheuer from the Max Planck Institute for Molecular Genetics (Berlin, Germany), Agnieszka Charzewska from the Department of Medical Genetics (Warsaw, Poland), Pasquale Striano and Federico Zara from Institute G. Gaslini (Genova, Italy), Nicola Specchio from IRCCS (Rome, Italy), Giuseppe Capovilla from Epilepsy Center, C. Poma Hospital (Mantova, Italy) and CeGaT GmbH (Tübingen, Germany).

In the first family, the affected individuals show a pattern of X-linked inheritance. As shown in the pedigree of the family, two males are severely affected with pharmacoresistant epileptic encephalopathy and early seizure onset (Fig. 15 A and Table 7). The type of seizures
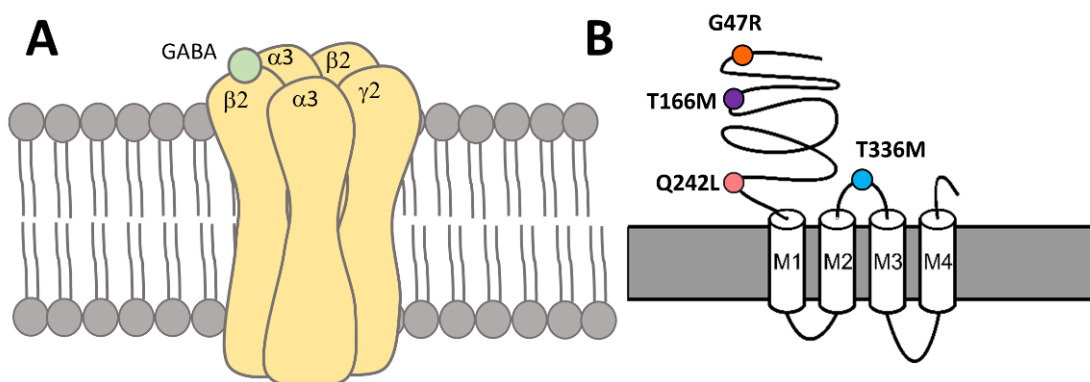

Figure 14. Localization of the four *GABRA3* identified missense variants. (A) GABA$_A$R structure with 2α3 2β2 1γ2 subunit. (B) α3 subunit representation with four transmembrane domains and localization of the four identified variants: three missense variants are localized in the N-terminal domain and one mutation is located on the extracellular loop between transmembrane domain two and three.
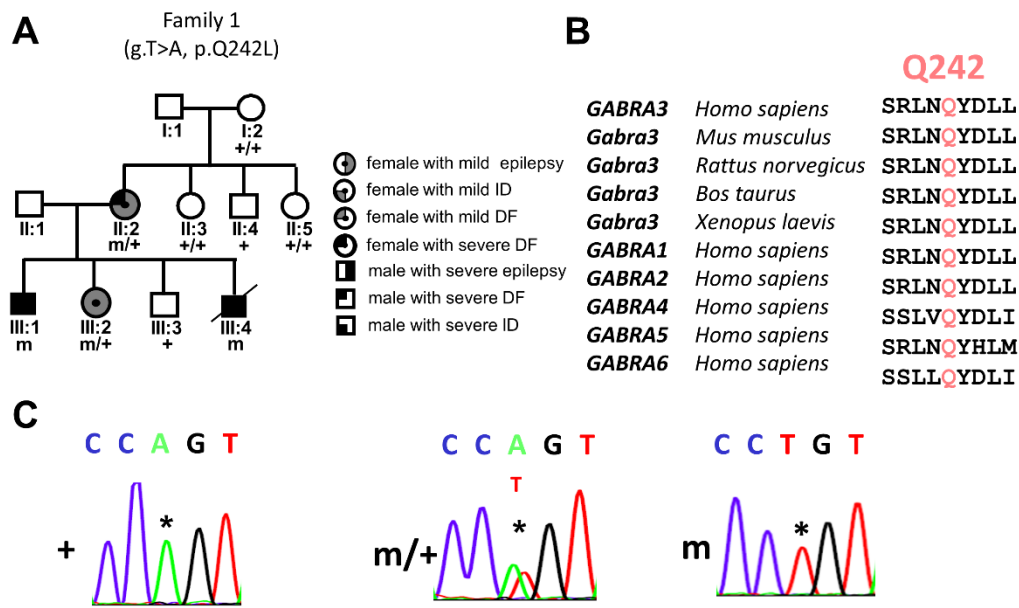
Figure 15. First identified missense variant p.Q242L in the *GABRA3* gene. (A) Family pedigree showing the p.Q242L co-segregation. (B) Evolutionary conservation of the amino acid. (C) Sequence reads showing the genomic nucleotide change from T (thymidine in red) to A (adenine in green); left: healthy individual, middle: female affected, right: male affected.

is very severe with infantile spasm Lennox-Gastaut syndrome for one male and epileptic spasm and tonic seizure for his brother. Additionally, they also show severe intellectual disability with global developmental delay and late speech development. The other two carriers of the mutation, the mother and the sister, show a less severe phenotype with a milder developmental delay and some learning disabilities. They have also experienced generalized tonic-clonic seizures. One feature of the patients is that they all show common dysmorphic features, such as micrognathia and nystagmus. Additionally, the mother and the two sons have a cleft palate.

Table 6. Scores from Prediction software

Family	Mutation	PolyPhen-2	SIFT	MutationTaster
1	p.Q242L	0.985 (probably damaging)	0.11 (tolerated)	0.999998345510216 (disease causing)
2	p.T166M	1.000 (probably damaging)	0.19 (tolerated)	0.999980339497156 (disease causing)
3	p.T336M	1.000 (probably damaging)	0.12 (tolerated)	0.999999448138709 (disease causing)
4	p.G47R	1.000 (probably damaging)	0.04 (damaging)	0.76938630907083 (disease causing)

Our collaborators performed whole exome sequencing of the proband (patient III-1), which revealed a mutation in *GABRA3* gene as the most plausible variant causing the disease (c.A725T, p.Q242L). Indeed, all affected individuals, the mother, the two affected sons, and daughter carry this mutation, while the healthy father and brother do not (Fig. 15, Table 7). The p.Q242 is an evolutionary highly conserved amino acid and the mutation is predicted to be deleterious according to prediction software analysis (Table 6). These programs are used to predict the possible impact of an amino acid substitution on the structure and function of a human protein. By whole exome sequencing of the patients and the healthy brother, our collaborators aimed to identify variants which could explain the complex phenotype in this family. Since they did not detect any relevant variants in the known genes associated with dysmorphic features, it was assumed the p.Q242L in *GABRA3* to be the only variant responsible for the observed clinical features. Later on, this variant was confirmed in the other patients by direct sequencing and excluded in the healthy father, brother, aunts and uncle of the proband.

As a next step, our collaborators wanted to identify if other variants in the *GABRA3* gene or other X-chromosome linked genes were associated with similar clinical features as the
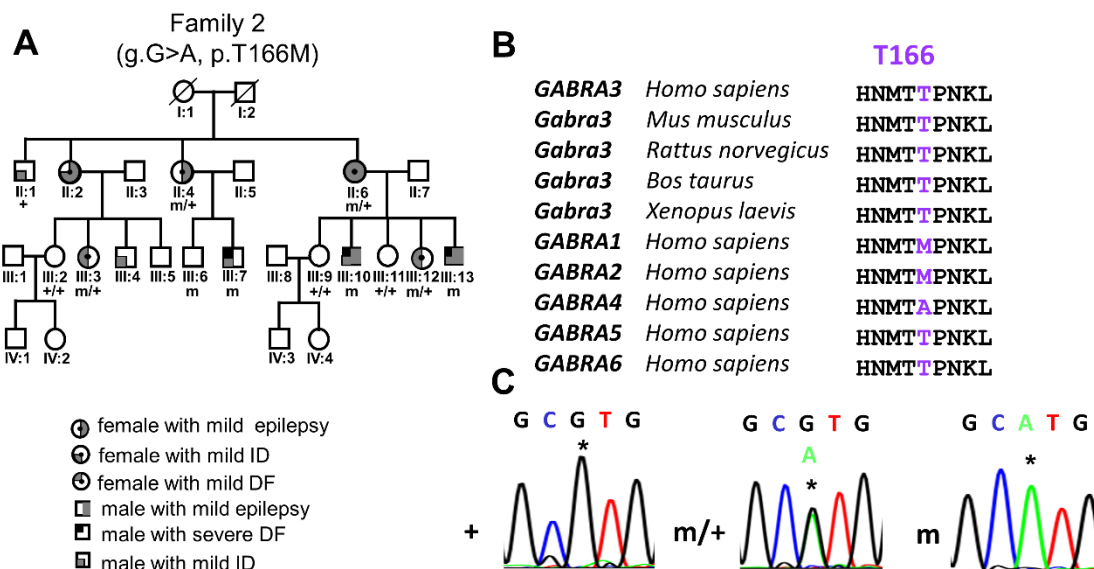

Figure 16. Second identified missense variant p.T166M in the *GABRA3* gene. (A) Family pedigree showing the T166M co-segregation. (B) Evolutionary conservation of the amino acid. (C) Sequence reads showing the genomic nucleotide change from G (guanine in black) to A (adenine in green); left: healthy individual; middle: female affected, right: male affected.

ones described in the first family. For that purpose a cohort of 480 individuals showing X-linked intellectual disability was analyzed by whole X chromosome sequencing. A second variant (c.C497T, p.T166M) in the *GABRA3* gene was identified in a large family, in which eight individuals, four females and four males, are carrying the mutation (Fig. 16 and Table 7). Interestingly, some affected individuals displayed similar dysmorphic features with the patients from family 1 (e.g. nystagmus, micrognathia, archate palate), but some differences as well, such as tall stature (Table 7). The female carriers have experienced incidents of loss of consciousness and present some of the dysmorphic features, while two of the males carrying the mutation have epilepsy with generalized tonic-clonic seizures. Patients III-6 and III-7, although mutation carriers, do not have epilepsy and only III-7 has mild intellectual disability. This may be explained by incomplete penetrance. The mutated amino acid, as in the previous case, is partially evolutionary conserved and the change in amino acid was found to be deleterious according to two prediction programs (Fig. 16 B; Table 6).

To investigate the functional effects of both *GABRA3* variants and their impact on the functionality of the alpha-3 subunit of the GABA$_A$ receptor, *Xenopus laevis* oocytes were used as a heterologous expression system and an automated two-microelectrode voltage clamp technique. The predicted positions of these mutations are shown in Figure 14 B. First, these mutations were introduced in the human isoform of the *GABRA3* cDNA. Secondly, to have a functional GABA$_A$ receptor, cRNAs coding for WT or mutant alpha-3 subunit together with β2 and γ2s subunits in an 1:1:2 ratio were transcribed and co-injected into the oocytes. After three days of incubation to allow optimal expression of the GABA$_A$ receptors, the GABA-induced currents were recorded. First, the response to a high GABA concentration of 1 mM was examined. This concentration is mimicking the physiological concentration of GABA in the synaptic cleft (Roth and Draguhn, 2012) (Fig. 17 C). This first experiment revealed a dramatic reduction in the GABA-evoked currents, showing 84 ± 3% less current response in comparison to the WT for the Q242L mutation, while the T166M mutation showed a reduction of 76 ± 3%. These results clearly indicate a loss of channel function for both variants (Fig. 17 B, C, D). Further investigation of GABA-induced currents in response to different GABA concentrations revealed a strong decrease in the whole concentration range.

Table 7. Main phenotypic characteristics of patients carrying GABRA3 mutations

Family/ mutation	Individual/ Gender	Seizure onset (Age)	Seizure type	Dysmorphyc features	Development
Family 1 c.A725T p.Q242L	**II-2/F**	**21**	generalized tonic-clonic	cleft palate, nystagmus, microretrognathia, synophiris	mild developmental delay
c.A725T p.Q242L	III-1/M	3	Infantile spasms Lennox-Gastaut	cleft palate, nystagmus, micrognathia, sloping shoulders, short neck	severe intellectual disability
c.A725T p.Q242L	III-2/F	7	generalized tonic-clonic	retrognathia, sloping shoulders, fine nystagmus	mild learning disabilities
c.A725T p.Q242L	III-4/M	3	Epileptic spasms and tonic seizures	cleft palate, micrognathia, short neck, nystagmus, sloping shoulders	global developmental delay, walking at age 3 y, speech starting at age 6 y. Moderate intellectual disability
Family 2 c.C497T p.T166M	II-4/F	In adulthood	Incident of loss of consciousness	ND	ND
c.C497T p.T166M	II-6/F	In childhood	Incident of loss of consciousness	micrognathia, long fingers, big low set ears, small mouth, high stature (172 cm)	learning difficulties
c.C497T p.T166M	III-3/F	absent	absent	Small mouth, micrognathia, height 160 cm	learning difficulties
c.C497T p.T166M	III-6/M	absent	absent	ND	unaffected
c.C497T p.T166M	III-7/M	absent	absent	elongated skull, long neck, narrow and narrowly spaced palpebral fissures, sharply ended and long nose, arched palate, large protruding ears,	mild intellectual disability, learning difficulties, hyperactivity, disturbances of visual-motor

|				sloping shoulders, long fingers, second and third toes – small syndactyly	integration, speech defect
c.C497T p.T166M	III-10/M	17	Attack of unconsciousness; generalized tonic-clonic seizures	horizontal nystagmus, micrognathia, elongated skull, arched palate, small mouth, long fingers, big low set ears, high stature (190 cm)	delayed speech; mild intellectual disability
c.C497T p.T166M	III-12/F	absent	absent	Small mouth, micrognathia, height 160 cm	Learning difficulties
c.C497T p.T166M	III-13/M	12	Attack of unconsciousness; generalized tonic-clonic seizures	horizontal nystagmus, micrognathia, elongated skull, arched palate, small mouth, long fingers, big low set ears, high stature (182 cm)	Mild intellectual disability; speech starting at age 3y
Family 3 Intragenic *GABRA3* duplication	I-2/F			no	normal
Intragenic *GABRA3* duplication	II-2/M	3	Generalized tonic-clonic seizures		Borderline intellectual disability
Family 4 c.C1007T p.T336M	I-2/F				
c.C1007T p.T336M	II-2/F	8	Generalized tonic-clonic seizures		
Family 5 c.G139A p.G47R	II-1/M				Speech starting at age 6y; autism spectrum disorders
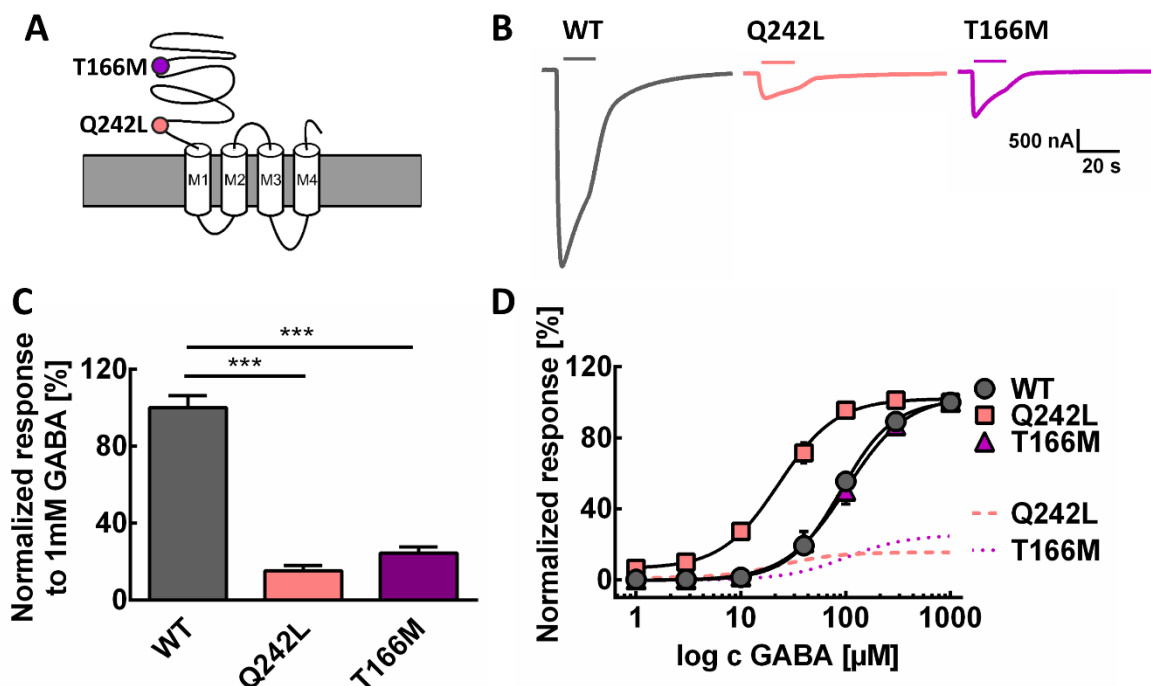
Figure 17. Functional analysis of GABRA3 mutations associated with severe EE, ID and DF. (A) Schematic representation of the $\alpha 3$ subunit and localization of the Q242L and T166M mutations at the N-terminal domain. (B) Example of a $\alpha 3\beta 2\gamma 2s$ induced current by 1 mM GABA application recorded in *Xenopus laevis* oocytes (left: WT, center: Q242L, right: T166M); 15 s of GABA application is indicated by the line above each current trace. (C) Normalized current response to 1 mM GABA application for WT (n = 63), Q242L mutation (n = 29) and T166M mutation (n = 37); ***p< 0.001; one-way ANOVA, Dunn´s multiple comparisons test. (D) Dose-response curve for $\alpha 3\beta 2\gamma 2s$ WT (n = 71), Q242L (n = 16) and T166M (n = 25) recorded upon application of different GABA concentrations (in µM: 1, 3, 10, 40, 100, 300 and 1000) and normalized to the maximal response (1000 µM) for each cell. EC_{50} values were: 93 ± 3, 25 ± 2 (***p< 0.001; one-way ANOVA, Dunn´s multiple comparisons test) and 104 ± 4 µM for the WT, Q242L and T166M, respectively. The predicted dose-response curves, calculated from the ratio of the mutant *vs.* WT response to the application of 1 mM GABA (C) are shown as dashed (Q242L) or dotted (T166M) lines.

The GABA sensitivity was increased only for the Q242L mutation (EC_{50} of 93 ± 3 and 25 ± 2 µM for WT and mutant, respectively), which could however not compensate for the severe loss of current amplitudes (see dotted line in Fig. 17 D).

In parallel to the exome sequencing studies, a diagnostic screening for copy number variations (CNV) in patients with severe epilepsy was performed by our collaborators in Italy. A new family was identified in which the proband carries a microduplication of the *GABRA3* gene. This duplication was inherited by the healthy mother (Fig. 18 A). The proband suffers from severe pharmacoresistant epilepsy with generalized seizures and unlike the previously described cases, does not present any dysmorphic features (Table 7, Family 3). Using cultured

fibroblasts derived from the patient, our collaborators confirmed by RT-PCR that the duplications completely disrupts the gene expression. For the proband, it was not possible to identify any transcript of the *GABRA3* gene after the RT-PCR (II-2, Fig. 18).
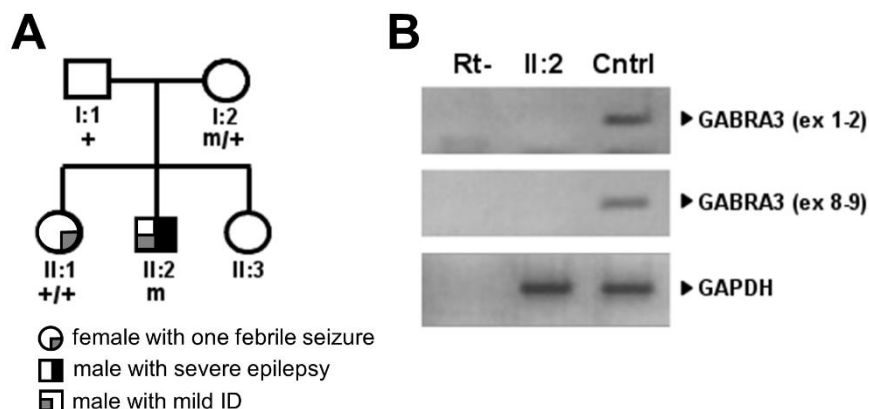

Figure 18. *GABRA3* microduplication. (A) Family pedigree revealing the co-segregation of the microduplication. (B) RT-PCR showing that reversely transcribed *GABRA3* RNA (exons 1-2 and exons 8-9) from cultured fibroblasts of the proband could not be detected; GAPDH was used as a housekeeping gene control. Analysis performed by Prof. Federico Zara (the Laboratory of Neurogenetics and Neuroscience, Institute G. Gaslini, Genova, Italy).

Furthermore, our collaborators searched for additional mutations in *GABRA3* gene in a cohort of 243 independent families with IGE/GGE syndromes, which were analyzed by whole exome sequencing. In one of these families, another mutation could be detected (c.C1007T, p.T336M) in a female suffering from IGE with generalized tonic-clonic seizures. Her unaffected mother carries the mutation as well, while her father and sister are affected, but they do not carry the T336M mutation (Fig. 19 B). Her father has experienced only few generalized tonic-clonic seizures, while the sister is suffering from childhood absence epilepsy. However, the patients do not present any dysmorphic features as the one described for the first two families.

The fourth identified missense variant (c.G139A, p.G47R) emerged from the same cohort of 480 patients with X-linked disability, in which the already described variant T166M was found. The proband carrying the mutation does not present any epileptic phenotype, but he is affected by an autism spectrum disorder and severe learning disabilities. The second affected patient in the family with similar phenotype is his brother, which on the contrary does not carry the mutation (Table 7, Family 5 and Fig. 20 B).

The last two described mutations, associated with a milder phenotype and no co-segregation with disease status in the respective pedigree, were also functionally analyzed using *Xenopus laevis* oocytes as a heterologous expression system. The T336M mutation revealed a strong loss of channel function when compared to the WT. GABA-evoked currents were reduced by 91 ± 2% after application of 1 mM of GABA. This was also confirmed for the
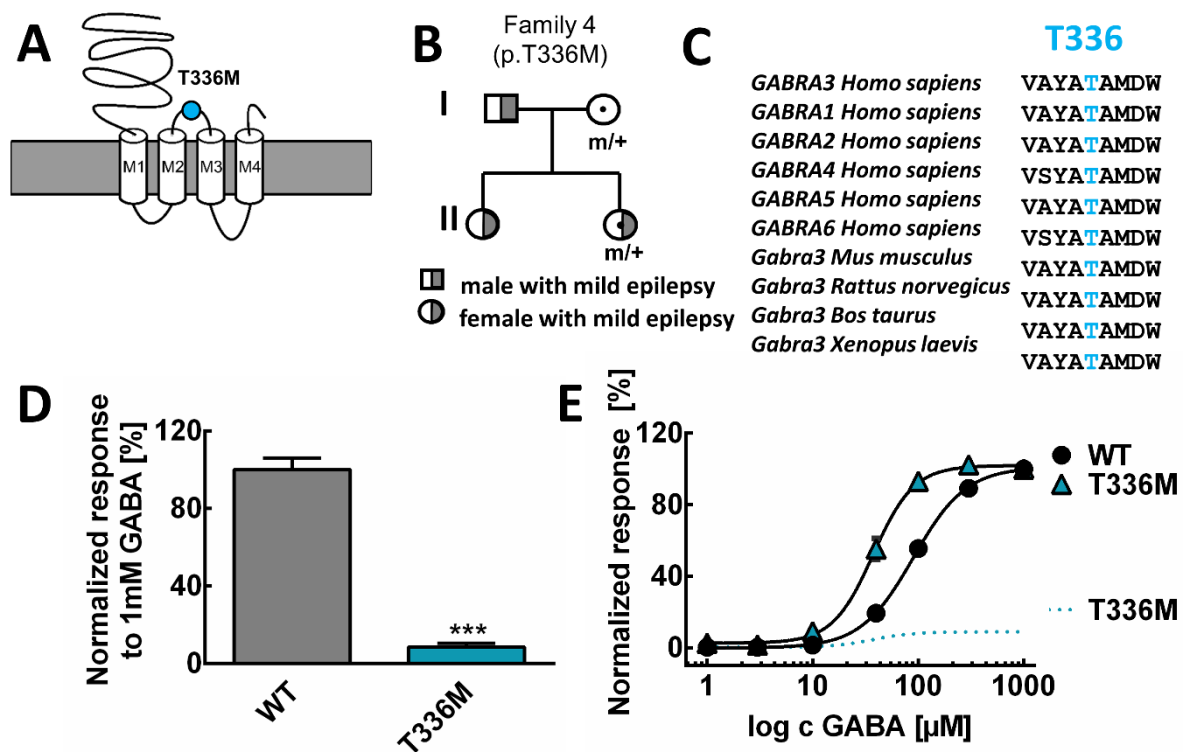

Figure 19. Functional analysis of the T336M mutation of the *GABRA3* gene found in a patient affected with IGE. (A) Schematic representation of the α3 subunit and localization of the T336M mutation in the extracellular loop between domain M2 and M3 of the α3 subunit. (B) Pedigree of the family revealing the co-segregation of the mutation. (C) Evolutionary conservation of the amino acid. (D) Normalized current response to 1 mM GABA application for WT (n = 47), T336M mutation (n = 28); ***p< 0.001; Mann-Whitney test. (E) Dose-response curves for α3β2γ2s WT (n = 71) and T336M (n = 14) recorded upon application of different GABA concentrations (in µM: 1, 3, 10, 40, 100, 300 and 1000) and normalized to the maximal response (1000 µM) for each cell. EC50 values were: 93 ± 3 µM for the WT and 38 ± 3 µM for the T336M, respectively; ***p<0.001; Mann-Whitney test. The predicted dose-response curves calculated from the ratio of the mutant *vs*. WT response to application of 1 mM GABA (D) are shown as dotted lines.
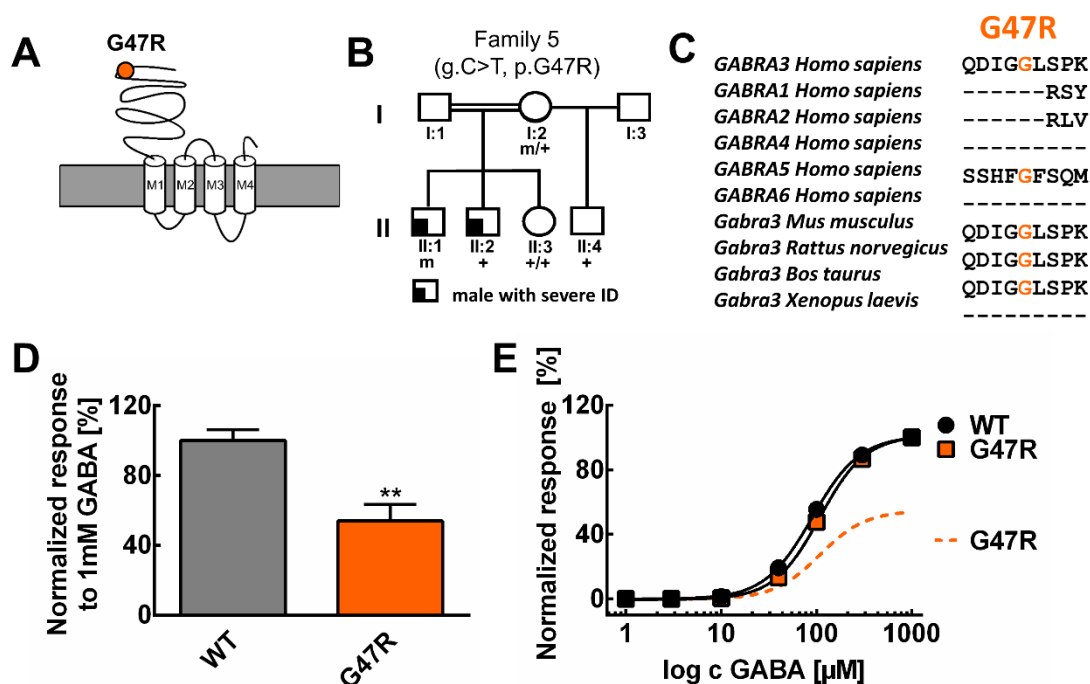
Figure 20. Functional analysis of the G47R mutation of the *GABRA3* gene found in a patient affected with autism spectrum syndrome. (A) Schematic representation of the α3 subunit of the GABA$_A$R and localization of the G47R mutation on the N-terminal domain. (B) Pedigree of the family revealing the co-segregation of the mutation. (C) Evolutionary conservation of the amino acid. (D) Normalized current response to 1 mM GABA application for WT (n = 47) and G47R mutation (n = 10); **p< 0.01; t-test. (E) Dose-response curve for α3β2γ2s WT (n = 71) and G47R (n = 19) recorded upon application of different GABA concentrations (in µM: 1, 3, 10, 40, 100, 300 and 1000) and normalized to the maximal response (1000 µM) for each cell. EC50 values were: 93 ± 3 µM for the WT and 109 ± 6 µM for the G47R, respectively. The predicted dose-response curves, calculated from the ratio of the mutant vs. WT response to the application of 1 mM GABA (D) are shown as dotted line.

whole GABA concentration range (Fig. 19 D, E). Additionally the GABA sensitivity was increased with an EC$_{50}$ value of 38 ± 4 µM for T336M in comparison with the 93 ± 3 µM for the WT GABA induced currents. The G47R showed a significant reduced current response to 1 mM GABA application, but the effect was less pronounced than for the other variants. In addition, no difference was observed in GABA sensitivity when compared to the WT (Fig. 20 E).

4.2 Functional analysis of two *de novo* mutations identified in patients with EE in the *GABBR2* gene

Mutations causing epilepsy have been identified in $GABA_AR$ encoding genes, but only recently two *de novo* epilepsy-causing mutations were detected in a metabotropic $GABA_BR$ subtype, *GABBR2*. These mutations were found by the EuroEPINOMICS-RES (rare epileptic syndromes) and Epi4K Consortium by whole exome sequencing of a joint cohort of 356 proband/parent trios, in which the proband suffers from severe epileptic encephalopathy. More specifically, in this case, the patients were affected with infantile spasms or Lennox-Gastaut syndrome with early seizure onset in the first years of life (Appenzeller *et al.,* 2014). Both patients have experienced the first seizure at 1.5 and 2.5 months of age. Additionally, they are severely affected by intellectual disability (ID) and impaired language capabilities. The patient carrying the p.S695I mutation is affected with infantile spasms (IS), focal dyscognitive seizures (FDS) and generalized tonic-clonic seizures (GTCS), while the patient carrying the I705N mutation has experienced only IS as seizure type (Table 8). The severity of the mutations was analyzed using the prediction program PolyPhen 2. This program assigns a maximum value of "1" for the mutations that are predicted as damaging. The mutations analyzed here were predicted as "probably damaging" with a score of 0.997 for the S695I mutation and 0.991 for I705N mutation.

Table 8. Clinical features of affected individuals with de novo GABBR2 mutations from Appenzeller et al. (2014)

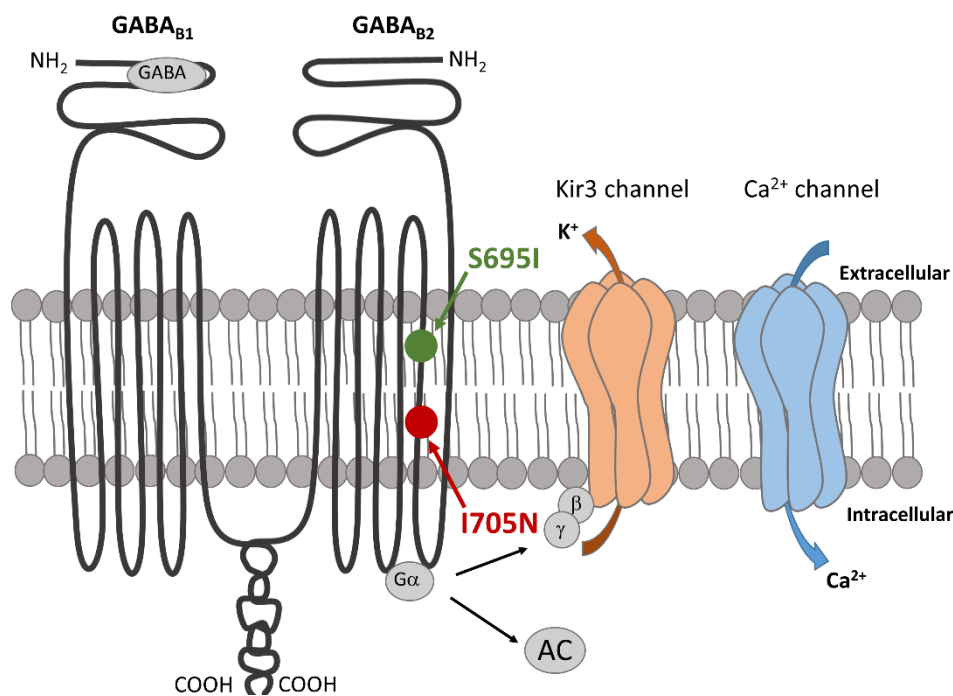| Mutation	Gender/Age	Seizure onset (Age)	Seizure type	Development
c.2084 G>T p.S695I	F/3y	1.5 m	Focal clonic, IS, FDS, GTCS	Profound ID. No head control, does not sit, no speech, reacts to music not to people
c.2114T>A p.I705A	M/18y	2.5 m	IS	Severe ID. Autism syndrome disorders. No speech, walks with support

Figure 21. Representation of the GABA$_B$R and localization of the identified mutations. Both mutations, S695I and I705N, are located in the GABA$_B$R subunit 2 in the sixth transmembrane domain.

Interestingly, both mutations are located in the sixth transmembrane domain of the GABA$_B$R subunit 2 and the changed amino acids are highly evolutionarily conserved (Fig. 21 and Fig. 23 C, 24 C). In this study, the mutations were analyzed using the *Xenopus laevis* oocyte expression system.

GABA$_B$ is a metabotropic receptor and mediates either the activation of the G-protein coupled inward rectifying potassium channels (*GIRK or* Kir) postsynaptically or the inhibition of the voltage-gated Ca^{2+} channels presynaptically. In this study, all electrophysiological experiments were performed using co-expressed *GIRK1* (Kir3.1) and *GIRK2* (Kir3.2) channels as reporter channels. Kir channels are heterotetrameric proteins and to be functional Kir 3.1 was combined with Kir 3.2. Oocytes were injected with cRNAs encoding the WT GABA$_B$ subunit 1 with WT or mutated GABA$_B$ subunit 2 to form a GABA$_B$ receptor dimers and Kir 3.1 and Kir 3.2 to be able to assess their function. After RNA injection and three days of incubation, GABA-mediated potassium currents were recorded using the fully automated Roboocyte2 system (MultiChannel Systems, Reutlingen).

To confirm that Kir 3.1/3.2 channels are functionally expressed in *Xenopus* oocytes and the current amplitudes are not affected by the mutations, only potassium currents mediated by Kir 3.1/3.2 channels were recorded. Currents were evoked using 500 ms lasting pulses to potentials ranging from -140 to 60 mV with a 10 mV increment from a holding potential of -10 mV. It is known that a high extracellular potassium solution is needed to enhance the magnitude of Kir 3.1/3.2 currents (Schwenk *et al.*, 2010). For this reason, the initial recordings were made using a low potassium solution (ND96 containing 2 mM KCl) as bath solution followed by an application of a bath solution containing a higher potassium concentration
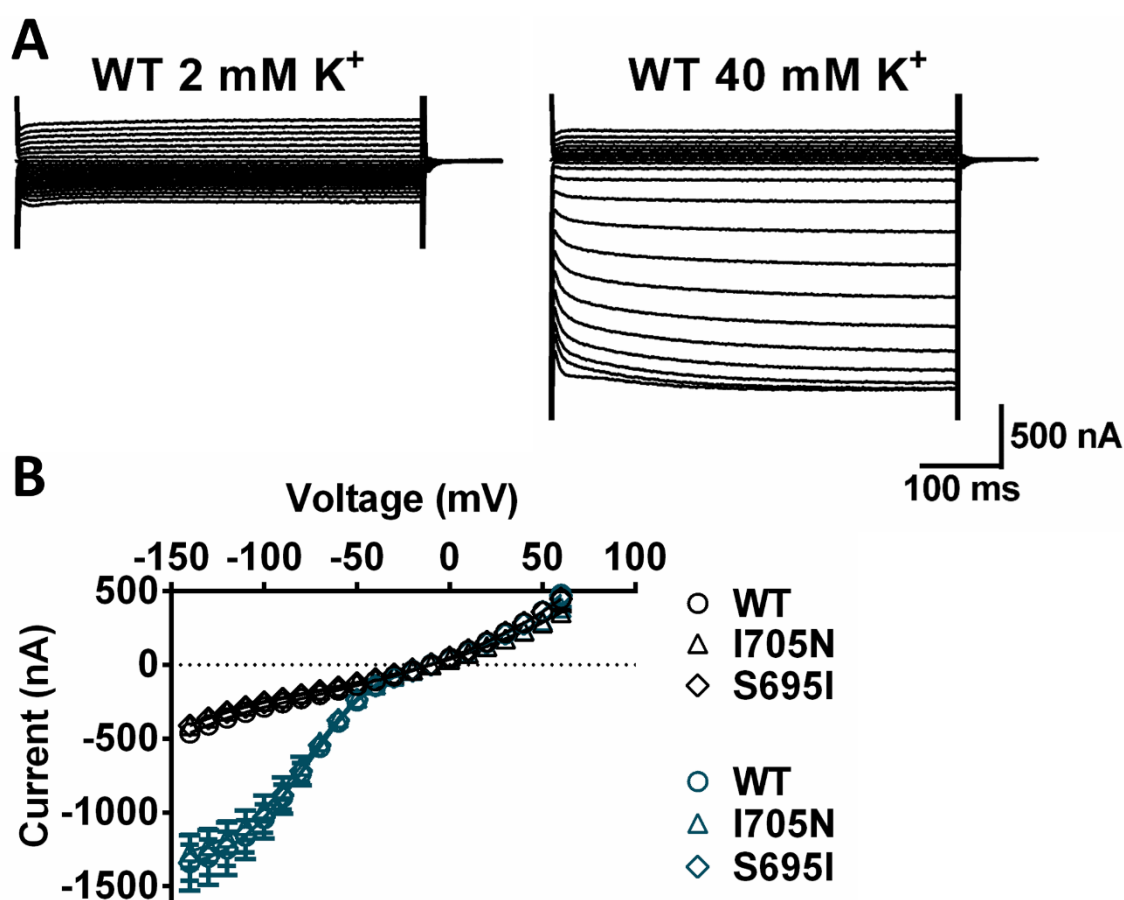

Figure 22. Kir 3.1/3.2 evoked currents. (A) Example of potassium currents mediated by Kir 3.1/3.2 channels recorded in ND96 solution (left), containing a low potassium concentration (2 mM K$^+$); to enhance Kir 3.1/3.2 currents, the oocytes were incubated with KD40 solution, which has a higher concentration of potassium (40 mM K$^+$; right). (B) Current-Voltage relations of Kir 3.1/3.2 currents recorded in oocytes injected either with the WT or with the mutated GABA$_{B2}$ subunit (WT n=23; I705N n=25; S695I n=24). In grey, IV curves are determined from Kir 3.1/3.2 channels recorded in ND 96 solution, or in blue in KD 40 solution.

(KD40 containing 40 mM of KCl). As shown in Figure 22, the potassium currents mediated by Kir 3.1/3.2 were significantly increased when exposed to solution containing a high in comparison with a low potassium concentration. No difference was observed in current amplitudes recorded from oocytes expressing the *GABBR2* mutations or the WT (Fig. 22 B). This result confirms that the effect seen in this study was only due to the mutations detected in the GABA$_B$R.

Once the functionality of Kir 3.1/3.2 channels was confirmed, the GABA-induced currents were recorded. To obtain a stable baseline of potassium currents activity mediated
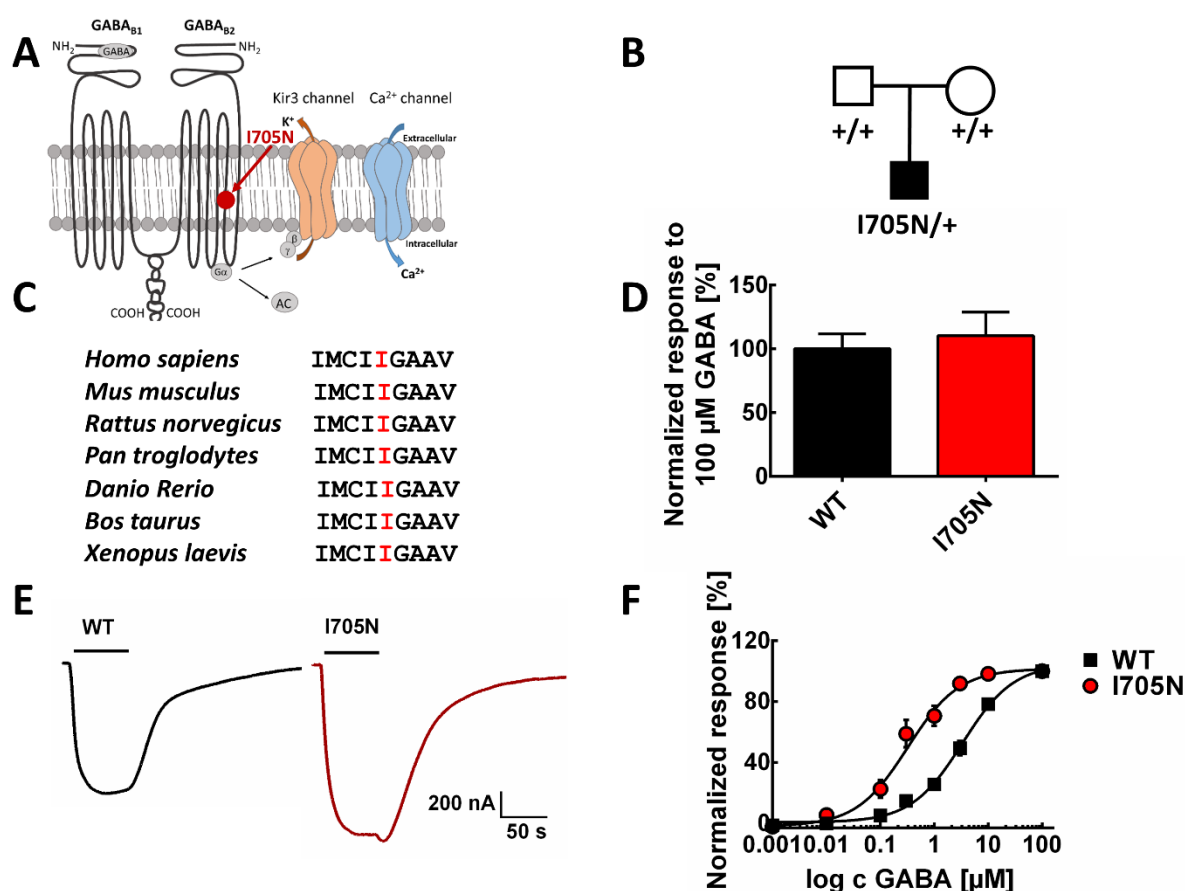

Figure 23. Functional analysis of I705N, a *de novo* mutation found in the *GABBR2* receptor. (A) Representation of the GABA$_B$R and localization of the I705N mutation on the sixth transmembrane domain of the GABA$_B$R subunit 2. (B) Trio showing the affected boy carrying the heterozygous mutation and the unaffected parents (C) Evolutionary conservation of the changed amino acid. (D) Normalized current response to 100 µM of GABA application for the WT (n=25) and I705N (n=20). (E) Example of a GABA-induced current for WT and I705N to 100 µM GABA concentration. Black line above the currents indicates the 60 s of GABA application. (F) Dose response curve for WT (n=14) and I705N (n=6) for different GABA concentrations (in µM: 0.001, 0.01, 0.1, 0.3, 1, 3, 10, 100) and calculated by normalizing each value to the maximum induced current (100 µM). The EC$_{50}$ value for the WT was 3.98 ± 0.68 µM while for the mutation it was significantly decreased with a value of 0.48 ± 0.16 µM; *$p<0.05$ t-test. Dashed line indicates the predicted dose-response curve for the mutation calculated from the ratio of the mutant *vs.* WT from the 100 µM application.

by Kir 3.1/3.2 channels and avoid the currents decline, which occurs in presence of high potassium solutions (Vorobiov *et al.*, 1998) and would make it difficult to perform repetitive dose-response recordings, oocytes were incubated at least 20 min prior the recordings with the high potassium solution. After this incubation period, oocytes were initially exposed to a high GABA concentration of 100 μM and GABA-induced potassium currents were recorded for WT or mutated channels. The I705N mutation shows no significant difference in comparison to the WT. In contrast, the second *de novo* mutation, S695I, manifests a 75.82 ± 2.8% reduction in the current amplitude when compared to the WT, indicating a loss of channel function (Fig. 23, 24 D and E).

To further functionally investigate these mutations, a dose-response experiment was performed by applying different GABA concentrations (from 1 nM to 100 μM). A significant difference in EC_{50} was found for the I705N mutation when compared to the WT. In fact, the EC_{50} value of the mutation was 0.48 ± 0.16 μM, thus significantly lower than for the WT (3.98 ± 0.68 μM; Fig. 23). This result, together with the fact that the current amplitude was at the same level as the WT, clearly indicates a gain of function for this mutation with an increased GABA sensitivity. The second mutation expressed in oocytes, S695I, was analyzed in a similar manner. First, after a 100 μM GABA application, the normalized current responses to the WT current response recorded in the same day showed a significant decrease in amplitude, which would imply a loss in channel function (Fig. 24 D). Second, the oocytes were exposed to different GABA concentrations and GABA-induced potassium currents were recorded. From these values, a dose-response curve was built for each cell by normalizing each current response to the maximum current induced by the highest GABA concentration (100 μM) and the GABA sensitivity was estimated through EC_{50} values. As for the previous mutation, the EC_{50} value of the S695I mutation was significantly decreased compared to the WT (0.31 ± 0.2 μM for S695I and 3.96 ± 0.85 μM for the WT respectively; Fig. 24, F), which indicates an increased GABA sensitivity. Moreover, for nanomolar GABA concentrations (100 nM), the current response normalized to the mean of the maximal GABA-induced current of the WT recorded in the same day, the S695I shows a higher response when compared to the WT. This results indicates a gain of function effect at nanomolar GABA concentrations (Fig. 24 G). This circumstance is possible when $GABA_B$Rs are activated by ambient GABA concentrations at extrasynaptic sites. Additionally, the time course of GABA deactivation was derived from a single-exponential fit from the current traces after 100 μM GABA applications (Fig. 25). This
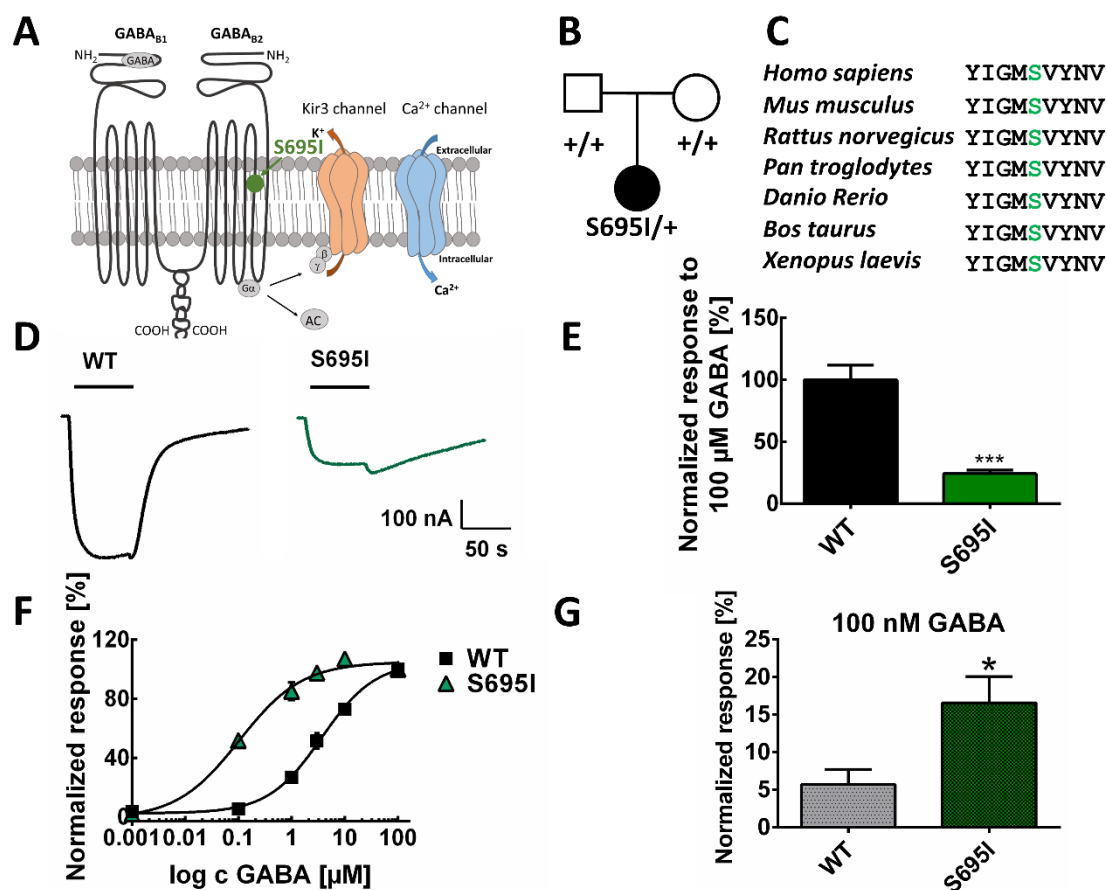
Figure 24. Functional analysis of S695I, a *de novo* mutation found in the *GABBR2* receptor. (A) Representation of the GABA$_B$R and localization of the S695I mutation on the sixth transmembrane domain of the GABA$_B$R subunit 2. (B) Trio showing the affected girl carrying the heterozygous mutation and the unaffected parents. (C) Evolutionary conservation of the changed amino acid. (D) Example of a GABA induced current for WT and S695I to 100 µM GABA concentration. Black line above the currents indicates the 60 s of GABA application. (E) Normalized current response to 100 µM of GABA application for the WT (n=12) and S695I (n=13); ***p<0.001 t-test. (F) Dose-response curve for WT (n=11) and S695I (n=9) for different GABA concentrations (in µM: 0.001, 0.01, 0.1, 1, 3, 10, 100) and calculated by normalizing each value to the maximum induced current (100 µM). The EC$_{50}$ value for the WT was 3.96 ± 0.85 µM while for the mutation was significantly decreased with a value of 0.31 ± 0.2 µM; ***p<0.001 Mann-Whitney test. Dashed line indicates the predicted dose-response curve for the mutation calculated from the ratio of the mutant *vs.* WT from the 100 µM application. (G) Average response of 100 nM GABA application normalized to the mean of the maximal GABA-induced current of the WT, measured in the same day; *p<0.05 t-test.

results shows a significantly increased time constant of deactivation for S695I in comparison with the WT, indicating that the channels will stay in an open state for a longer time, which would be a further evidence for the gain of function effect of this mutation.

Summarizing, two *de novo* mutations in the *GABBR2* gene, found in patients presenting severe epileptic encephalopathy with early seizure onset and critical intellectual disability affect two amino acids on the sixth transmembrane domain that are strongly evolutionarily

conserved (Fig. 23 A, C; Fig. 24 A, C). The results of the functional analysis performed here point out to a gain of function effect for both mutations. The I705N mutations shows an increased GABA sensitivity and no change in current amplitude, whereas the S695I shows a gain of function effect mainly at lower GABA concentrations, which could influence the GABA$_B$Rs expressed at extrasynaptic sites, if the receptor trafficking is not affected.
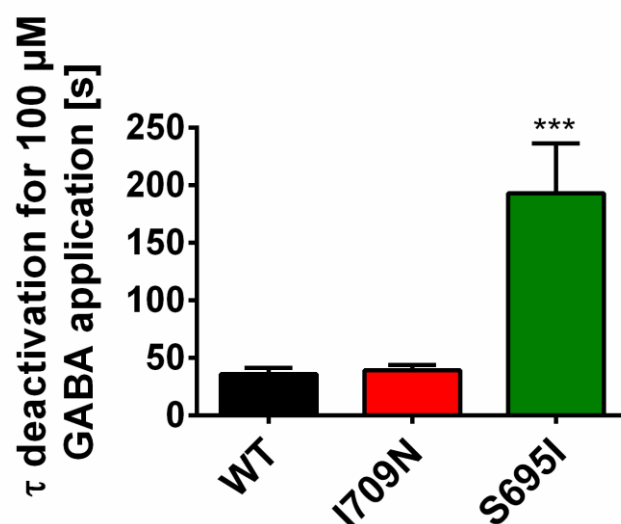

Figure 25. Time constant of deactivation for 100 µM GABA application. S695I shows an increased time constant of deactivation in comparison with the WT. *** p<0.001 One-way ANOVA, Dunn´s test; WT (n = 23), I709N (n = 5), S695I (n = 6).

4.3 ClC-2 channel and its role in neuronal excitability

It is known that the inhibition mediated by $GABA_A$ or $GABA_B$ receptors is essential for a correct function of neuronal networks in the brain as shown by dramatic diseases caused by mutations in these proteins (see 4.1 and 4.2).

In the next part of my thesis, I was interested to understand how inhibition might be modulated in a more complex system such as a mouse model, in which the chloride homeostasis could be impaired due to the absence of a chloride channel, specifically the ClC-2 channel. It is believed that this channel can play either a role in assisting $GABA_A$Rs inhibition by Cl^- extrusion (Staley, 1994; Staley *et al.*, 1996) or it could drive Cl^- ions into the cell, therefore being involved directly in neuronal excitability (Ratté & Prescott, 2011). To investigate how the ClC-2 channel influences Cl^- homeostasis, I have performed electrophysiological experiments in thalamocortical brain slices of WT, heterozygous and knockout (KO) ClC-2 mice. This type of brain slices was used for several reasons. First, the thalamocortical network plays an important role in generation of generalized seizures. Second, the thalamocortical system contains the *nucleus reticularis thalami* (NRT), a thin layer of GABAergic inhibitory neurons, in which the expression of the main Cl^- extruder in neurons, KCC2, is absent. Therefore, the NRT presents an interesting area to study the involvement of ClC-2 channels in the oscillatory activity of this network as well as the role of ClC-2 channels in neuronal excitability.

To achieve this goal, I performed patch-clamp experiments to study Cl^- currents carried by ClC-2 channels in three different areas of the thalamocortical slice: NRT, VB and cortex. Also, the excitability of NRT neurons was analyzed by measuring the number of APs generated in neurons of KO mice in comparison to those of WT mice. To further understand if the ClC-2 channel contributes to the function of the thalamocortical network and to investigate if the presence of proepileptic drugs may additionally perturb it, extracellular field potential recordings were performed and the spontaneous or drug-induced synchronous activity of neurons recorded in the three different areas simultaneously. Moreover, to investigate a different area of the brain and because ClC-2 channels are highly expressed in the hippocampus (Sık *et al.*, 2000), the network activity of ClC-2 hippocampal cultured neurons was analyzed *in vitro* at different time points in presence or absence of blockers of $GABA_A$ receptor using the microelectrode array (MEA) system.

4.3.1 Cl⁻ currents mediated by ClC-2 channels in acute thalamocortical slices

Cl⁻ currents mediated by ClC-2 channels were recorded from NRT, VB or layer V pyramidal neurons of the cortex from P10 to P18 mice. Some of the recordings were obtained together with Nele Dammeier (Dept. of Neurology and Epileptology, Tübingen). The currents were isolated by blocking sodium, potassium and for some experiments the hyperpolarization activated inward currents (I_h). However, the I_h current blocker had no effect on the inward recorded currents, confirming that these currents are not I_h mediated, result already shown by Rinke and colleagues (2010). Additionally, it was shown that the presence of extracellular cesium blocks the I_h activated current (Thoby-Brisson *et al.*, 2000). Moreover, it is known that Cl⁻ currents mediated by ClC-2 activate upon hyperpolarization and by a rise in intracellular Cl⁻, therefore a high concentration of intracellular Cl⁻ was used (Staley, 1994; Rinke *et al.*, 2010). Another characteristic of these currents is that they are slowly activating, reaching the steady state only after several seconds. Therefore the currents were elicited by 4 s long pulses from +40 mV to -120 mV. As shown in Figure 26 (A, B), the Cl⁻ mediated ClC-2 currents show inward
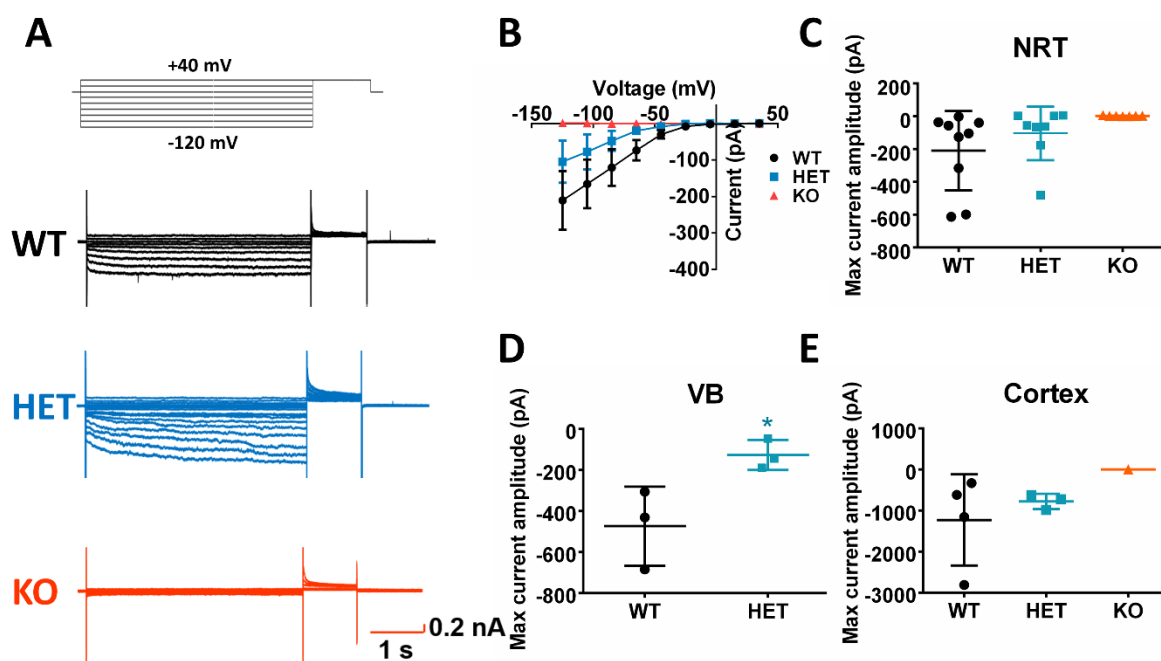
Figure 26. ClC-2 currents recordings in thalamus and cortex. (A) Top: Voltage step protocol used to elicit Cl⁻ mediated ClC-2 currents; Bottom: current examples from neurons of WT, HET or KO mice, recorded in the NRT; (B) current-voltage plots for the currents recorded in the NRT showing inward rectification. (C) The maximal current amplitude of WT, HET and KO cells measured in NRT, (D) VB or (E) layer V of the cortex. Data presented as mean ± SD of the maximum current amplitude for each recorded neuron (NRT: WT n = 9, HET n = 8, KO n = 7; VB: WT n = 3, HET n = 3; Cortex: WT n = 4, HET n = 3, KO n = 1), *p<0.05 unpaired t-test.

rectification, allowing the Cl⁻ ions to move out of the cell at potentials more negative than the equilibrium potential for Cl⁻, which in this case was 0 mV, because of equimolar Cl⁻ concentrations in the extracellular and intracellular solutions. The current amplitudes were assessed from the steady state currents recorded at the most negative potential (Fig. 26). As shown in Figure 26, it was possible to record Cl⁻ currents mediated by ClC-2 channels in all considered areas (NRT, VB and cortex) in neurons from WT and HET mice, meaning that all three areas express the ClC-2 channels. However, no difference could be detected between currents recorded in the NRT and the cortex of WT and HET animals, while recorded cells from the VB from HET animals had slightly reduced current amplitude. As expected, ClC-2 did not show any ClC-2 currents in the KO animals. This was verified in the NRT, and the cortex (Fig. 26 B, C, E).

4.3.2 Firing properties of inhibitory neurons in the NRT

After confirming that inhibitory neurons in the NRT express the ClC-2 channel, the aim of this study was to characterize the properties of these neurons in ClC-2 KO mice. This thin
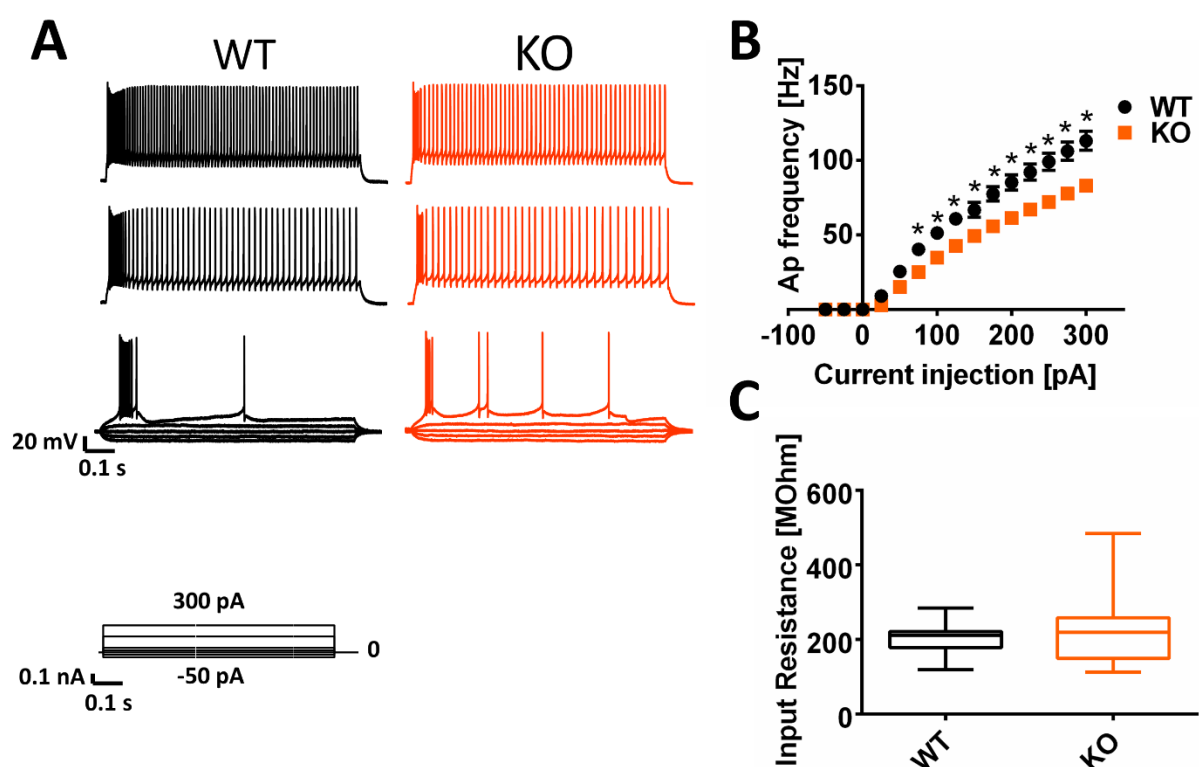

Figure 27. Firing properties of NRT inhibitory neurons. (A) Top: Representative trains of APs recorded in neurons of WT (black) or KO (red) animals; bottom: current step protocol used to induce the AP trains. (B) AP frequency plot against the current injection. WT (n=13), KO (n=11) *p<0.05 unpaired t-test; (C) input resistance; WT (n = 13), KO (n = 11).

layer of inhibitory neurons is important to maintain the rhythmic activity in the thalamocortical system and any alteration of their normal behavior could perturb the function of the whole system. In the past years, it was hypothesized that ClC-2 could act in a similar way as the KCC2 transporter, assisting Cl⁻ extrusion. Therefore, the absence of KCC2 from the NRT would help to isolate the ClC-2 contribution to the excitability of NRT neurons and consequently the whole network. For this reason, my first step was to analyze the neuronal firing properties in this area. Three different types of inhibitory neurons are found in the NRT: (1) typical bursting neurons, which show a fast bursting discharge at the beginning of the AP train, (2) atypical bursting neurons, which show a smaller amplitude of burst discharge, and (3) tonic firing neurons, which do not show any bursting behavior (Lee *et al.*, 2007). In this study, I have functionally analyzed typical bursting neurons, since they are the most abundant neurons expressed in the NRT. To this aim, I have used ClC-2 KO mice at post-natal day 14-18
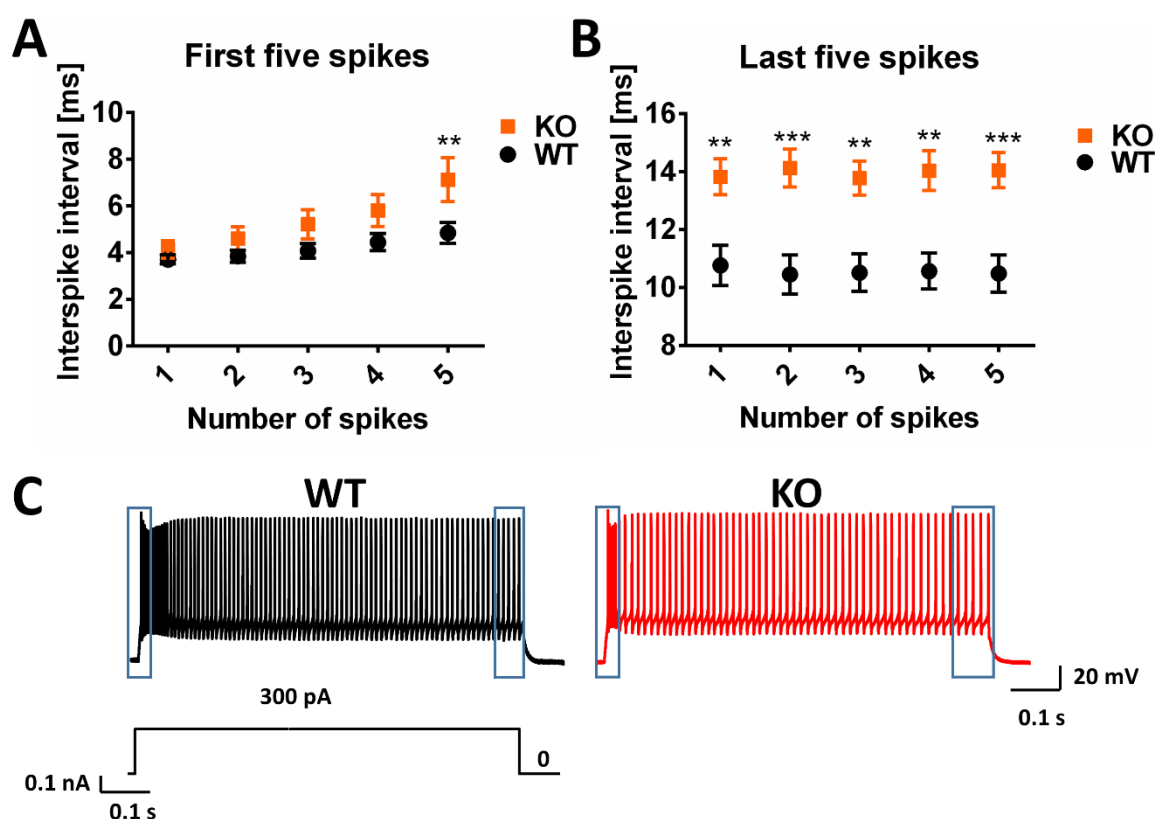
Figure 28. Interspike interval for 300 pA induced AP train recorded in the NRT neurons. (A) Interspike interval for the first five spikes in the train, WT (n = 13), KO (n = 11) **p<0.01 two-way ANOVA, Sidak´s multiple comparison test. (B) Interspike interval for the last five spikes in the train WT (n = 13), KO (n = 11) **p<0.01, ***p<0.001 two-way ANOVA, Sidak´s multiple comparison test. (C) Example of an AP train for WT and KO and protocol used to induce the AP train. Blue squares indicate the first and last spikes that were analyzed in the AP train.

(P14-P18) and analyzed the AP frequency for different current injection steps. Inhibitory neurons from ClC-2 KO animals showed a lower number of APs in comparison with those from WT mice, indicating a reduced inhibition in the thalamocortical network (Fig. 27 A, B). No difference was found in the input resistance (Fig 27 C).

To confirm the decreased firing rate in NRT inhibitory neurons, the interspike interval was analyzed. For this purpose, the AP train induced by a 300 pA current injection was investigated and the first five spikes within the burst and the last five spikes within the tonic firing period analyzed. The interspike interval was significantly increased in neurons from KO mice for all five last spikes, while within the burst only the fifth spike showed a longer interspike interval (Fig. 28). This result confirms the decrease in inhibition in the NRT inhibitory neurons derived from ClC-2 KO mice.

Additionally, the first AP in the train was analyzed. In Figure 29 A, an example of an AP and its first derivative is shown. The AP threshold was calculated as the corresponding voltage in the AP, at which the first derivative was reaching 50 mV/ms. The AP width was the
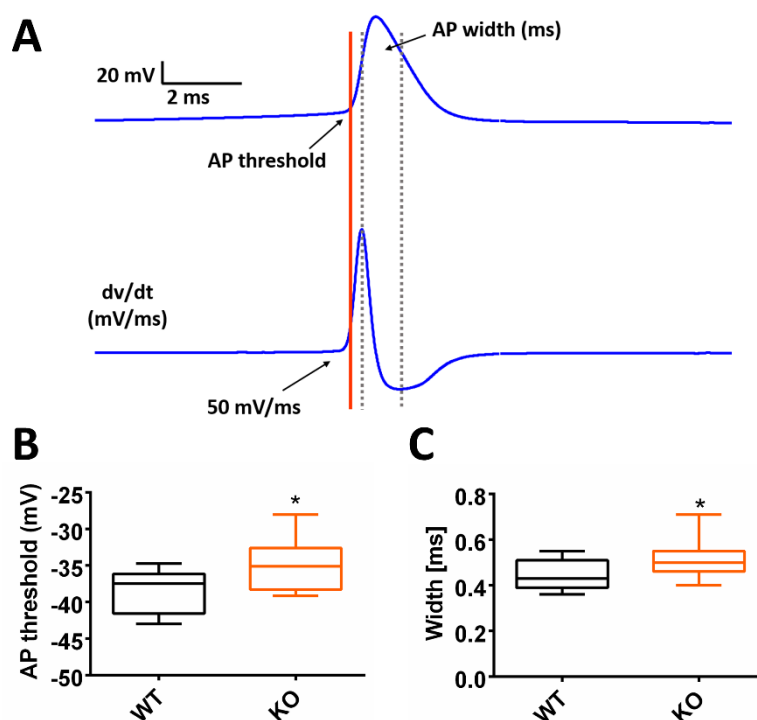

Figure 29. **Action potential properties.** (A) Example of the first AP in the train and its first derivative. (B) The AP threshold recorded in ClC-2 neurons of KO mice is significantly increased compared to the WT. *$p < 0.05$, unpaired t-test. (C) The width of the AP from KO mice was significantly broader than the WT. *$p < 0.05$ unpaired t-test.

corresponding time needed in the first derivative to go from peak to peak (Bean, 2007). A significant decrease in AP threshold was found in the ClC-2 inhibitory neurons derived from KO mice in comparison to the WT ones, meaning that additional current was needed for reaching a more depolarized threshold value. Furthermore, the width of the AP measured in neurons of ClC-2 KO mice was broader than the one measured in the WT (Fig. 29, B, C).

4.3.3 Extracellular recordings

To verify if the reduced activity of inhibitory NRT neurons has any effect on the whole thalamocortical network, I have performed extracellular recordings in acute thalamocortical brain slices, in which the connections between thalamus and cortex where kept intact. Spontaneous activity and synchrony were recorded simultaneously, using three different extracellular electrodes, one in the cortex, one in the VB and one in the NRT (Fig. 30 A). The thalamocortical slice was exposed to aCSF and the recorded spontaneous synchronous activity was not different between genotypes. I then induced synchronous spontaneous activity by applying 10 µM picrotoxin, a GABA$_A$ receptor blocker. Picrotoxin application induced synchronized bursting activities in all three areas with an increased frequency of synchronized bursting activity in brain slices derived from ClC-2 KO mice when compared to the WT (Fig. 30
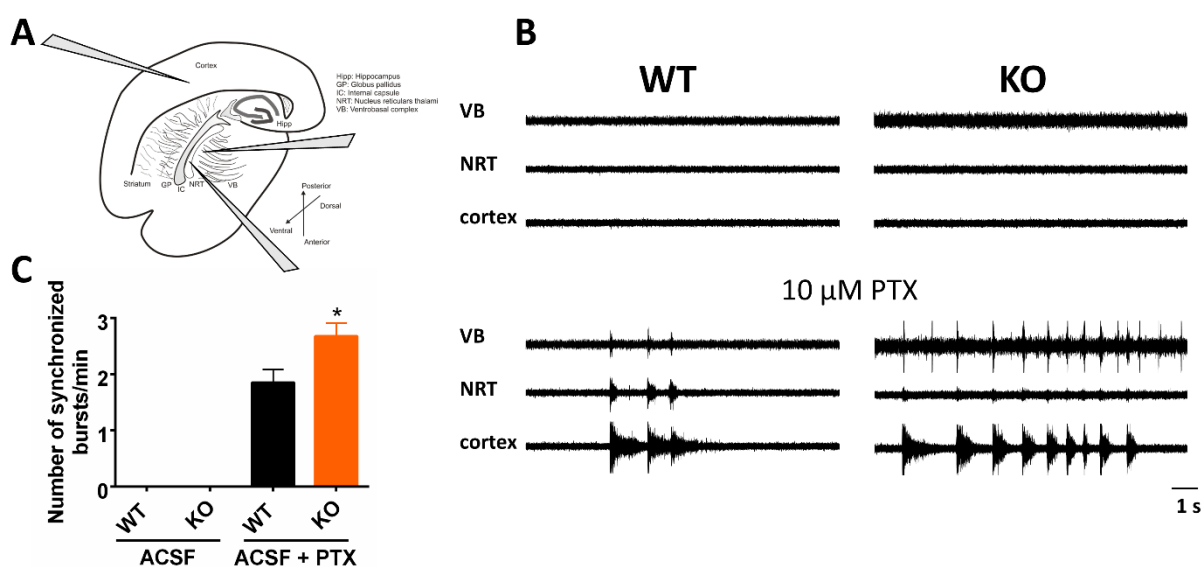
Figure 30. Extracellular recordings in thalamocortical slices of ClC-2 KO mice. (A) Position of the recording electrodes in cortex, NRT and VB. (B) Representative traces of recordings from WT and KO and synchronized burst activity across the three areas after application of 10 µM PTX. (C) Number of synchronized bursts per minute in WT and KO before and after application of PTX. The ClC-2 slices from KO mice showed an increased synchronized activity after PTX application when compared with the WT. *p<0.05 unpaired t-test, WT n=7; KO n=9.

B, C). This results implies that the absence of ClC-2 channel is not sufficient to induce increased spontaneous activity of the analyzed network, but can be considered as susceptibility factor for the increased excitability in this model.

4.3.4 Network analysis using the Microelectrode array (MEA) system

To further understand how ClC-2 affects the hippocampal neuronal network behavior, *in vitro* experiments were performed using a 60 electrodes MEA system, enabling extracellular recordings of spontaneous neuronal activity across all electrodes (Fig. 31).

The primary hippocampal neuronal cultures were used for several reasons. First, these type of neuronal cultures are an established system for the MEA recordings (Hedrich *et al.*, 2014). Second, it was shown that ClC-2 channel regulates neuronal excitability in the hippocampus (Rinke *et al.*, 2010), therefore it would be interesting to analyze more in detail its role at network level. For this purpose, primary hippocampal neuronal cultures derived from ClC-2
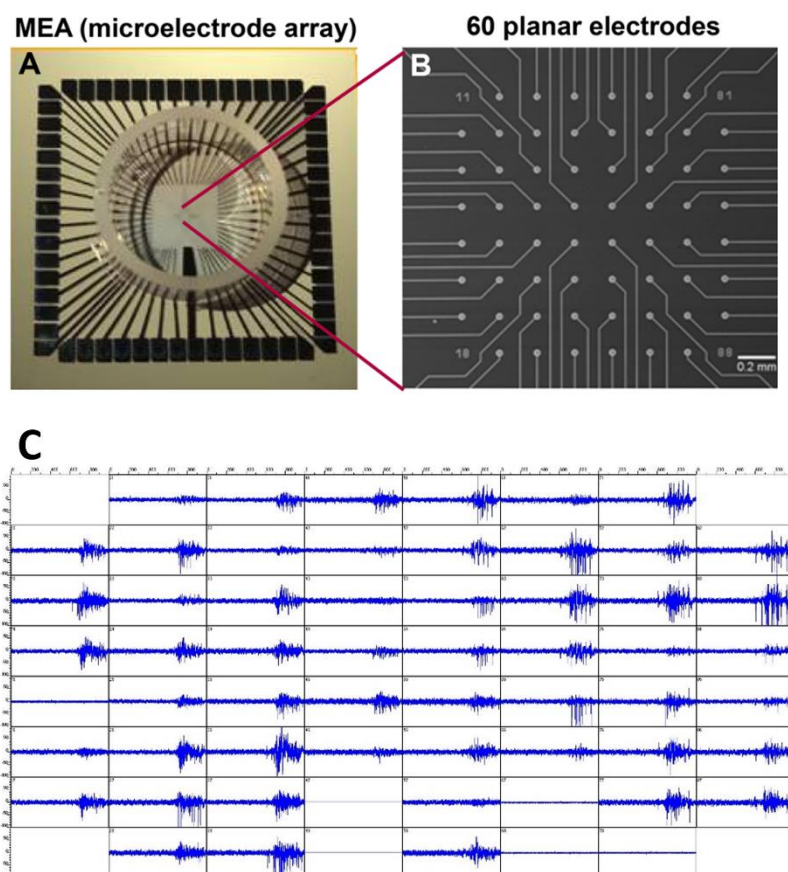

Figure 31. Microelectrode array features. (A) Mea dish containing in the center the 60 planar electrodes. (B) Enlarged representation of the electrodes. (C) Spontaneous neuronal activity across the electrodes. Each grid has a 1 second duration and 100 µV amplitude.

KO or WT mice were recorded at different time points: day in vitro (DIV) 11, DIV 18 and DIV 25. The neuronal network activity could be visualized through spike raster plots (SRPs), in which the spikes recorded from each electrode were plotted over time (Fig. 33 B). MEA recordings revealed active neurons and partly synchronized already at DIV 11. The population burst activity was indicated by spikes occurring at the same time on many electrodes. First, it was investigated how the neuronal cultures derived from WT or KO ClC-2 mice change during development and if there were any differences between the two genotypes during this period. The first developmental difference that could be observed is that the number of population bursts of neurons from WT mice decreased significantly after 25 days *in vitro,* whereas the burst duration did not change during this period (Fig. 32). In contrast, neurons from KO mice showed a tendency in reducing the number of population bursts already after 18 days *in vitro*, reaching a significant difference after 25 DIV. Furthermore, burst duration in neuronal cultures from KO mice significantly increased after DIV 18 and remained constant with further neuronal maturation (Fig. 32 B). Another parameter that indicates a higher synchrony when increased is the inter-burst interval. As indicated in Figure 32 C, the inter-population burst interval was significantly increasing in neuronal networks derived from WT and KO mice by DIV 25.
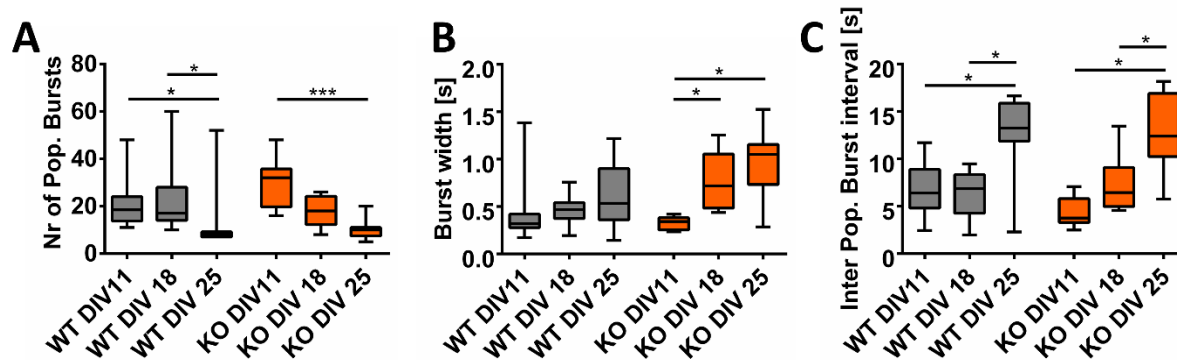
Figure 32. Developmental differences between WT and KO ClC-2 hippocampal neurons recorded on MEA. (A) Number of population bursts is significantly lower for WT DIV 25 in comparison with WT DIV 11 and 18 (n = 10); KO DIV 25 is significantly lower than KO DIV 11 (n =8); *p<0.05, ***p<0.001 one-way ANOVA, Dunn´s post-hoc test. (B) The burst width is significantly increasing for the KO DIV 18 and 25 in comparison with DIV 11; *p<0.05 One-way ANOVA, Tukey´s post-hoc test. (C) Inter population burst interval is significantly increasing after 25 DIV for WT and for KO neurons. *p<0.05 One-way ANOVA with Dunn´s or Tukey´s post-hoc test.
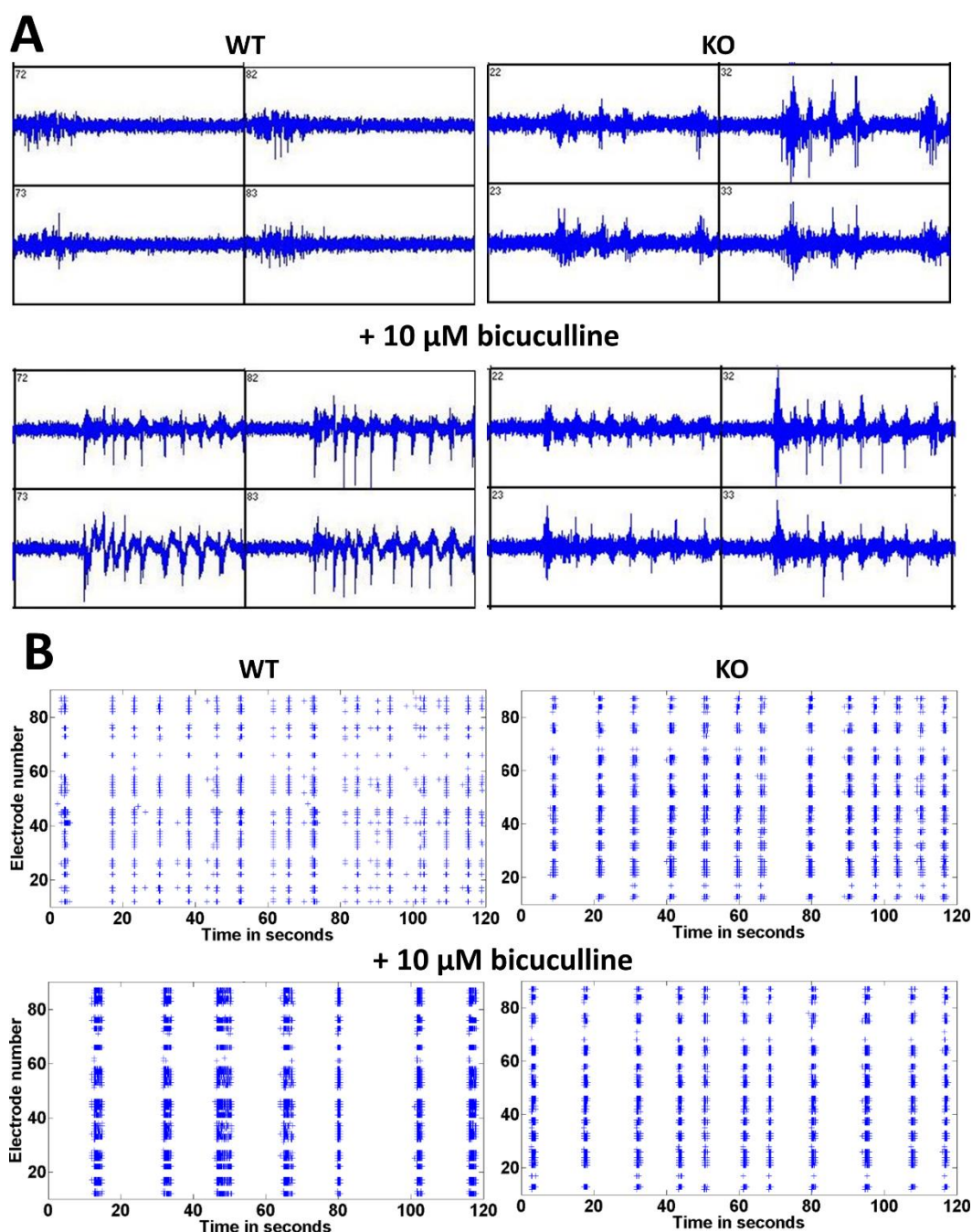
Figure 33. Network activities recorded with MEAs from ClC-2 hippocampal neurons derived from WT and KO mice. (A) Representative extracellular traces recorded from four channels before and after application of bicuculline. Each grid has a duration of one second and an amplitude of 100 µV. (B) SRPs from neurons derived from WT and KO mice before and after bicuculline application.

In the next step, network differences between cultures derived from WT and KO were compared more in detail. For this purpose, the network activity was analyzed at DIV 18, the time when the most striking differences were detected. Indeed, looking at the raw recordings and the SRPs, it was obvious that neuronal cultures derived from KO mice were more

synchronized than those from WT. This could be observed by the duration of the bursts, which were significantly longer in cultures derived from KO animals compared to WT (Fig. 33 A, B and Fig. 34 C).

Since it was hypothesized that there could be a tight connection between GABA$_A$R and ClC-2 channels, the recordings were also performed in the presence of bicuculline, a competitive antagonist of GABA$_A$Rs. It is known that application of bicuculline is inducing a more synchronized activity of neuronal networks, which may be visible by the organization of single spikes in population bursts, an increase in burst duration and increase of inter population burst interval (Baltz *et al.*, 2010; Hedrich *et al.*, 2014) (Fig. 33, 34). Spontaneous network activity was recorded for two minutes in the control condition followed by two minutes in the presence of 10 µM of bicuculline. In figure 33, recordings and spike raster plots (SRPs) of network activities of hippocampal neurons from WT and KO ClC-2 animals are shown. As expected, bicuculline was inducing an increase in synchronicity, changing all the parameters cited above in the WT cultures. However, SRPs and the quantification of the recorded bursts (Fig. 33, 34) revealed that in the hippocampal cultures derived from KO mice, the application of bicuculline did not lead to further statistically significant changes in the burst duration or in any of the parameters mentioned before.
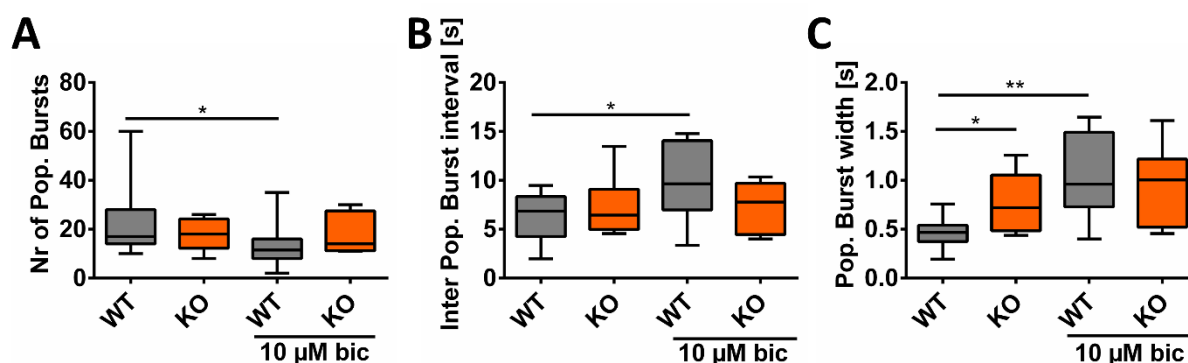
Figure 34. Quantitative analysis of the network activities from hippocampal neurons derived from KO and WT ClC-2 mice, recorded after 18 DIV. (A) The application of bicuculline was decreasing the number of population burst in neuronal cultures derived from WT mice. *p<0.05 Wilcoxon paired test. (B) Box plots showing an increase in inter-population-burst-interval after the application of bicuculline in neuronal cultures derived from WT mice; *p<0.05 paired t-test. (C) Increase in population burst width in neurons derived from KO mice in comparison with the WT. Bicuculline was inducing a significant increase in population burst width in neurons derived from WT mice. *p<0.05 unpaired t-test; **p<0.01 paired t-test. WT n=10; KO n=8.

5 Discussion

5.1 Novel *GABRA3* mutations as a cause of X-linked EE

In this thesis, I have investigated four novel mutations identified by our collaborators in the α3 subunit of the GABA$_A$R (gene *GABRA3*). Two of them were found in two families with severe epileptic encephalopathy and dysmorphic features. One additional mutation was identified in a proband of a family with a milder phenotype, idiopathic/genetic generalized epilepsy. A fourth mutation was found in a patient with autism spectrum disorder. Functional analysis of the first three mutations revealed a severe loss of channel function (> 75% reduction in current amplitudes), whereas for the last mutation, an only 46% in the reduction of current amplitude was observed. These results strongly suggest that *GABRA3* is a novel epilepsy gene, mutations of which cause different phenotypic outcomes from more severe X-linked EE to milder ones, probably due to incomplete penetrance in some of the families, as discussed in further detail below.

GABA$_A$ receptors are ligand-gated anion channels mediating fast synaptic inhibition at postsynaptic sites or tonic inhibition at extrasynaptic sites. So far, mutations in four different genes (*GABRA1, GABRB3, GABRG2* and *GABRD*) encoding the α1, γ2, β3 and δ subunits of GABA$_A$ receptors have been associated with different idiopathic epilepsy syndromes including childhood absence epilepsy (CAE), juvenile myoclonic epilepsy (JME), and febrile seizures (FS) with or without epilepsy including generalized/genetic epilepsy with febrile seizures plus (GEFS+). However, it is possible that mutations in *GABRA* genes can be the cause of more severe forms of epilepsy, such as Dravet syndrome (*GABRA1*, (Carvill *et al.*, 2014)), or Lennox–Gastaut syndrome (*GABRB3*, (Allen *et al.*, 2013)). Interestingly, genetic studies have shown that many of the most severe EEs are caused by *de novo* mutations (Claes *et al.*, 2001; Weckhuysen *et al.*, 2012; Allen *et al.*, 2013; Suls *et al.*, 2013; Carvill *et al.*, 2014; Lemke *et al.*, 2014; Nava *et al.*, 2014; Schubert *et al.*, 2014; Weckhuysen & Korff, 2014; Syrbe *et al.*, 2015). In contrast, our results implicate the possibility to transfer severe mutations by mildly affected female carriers to their severely affected sons.

5.1.1 Loss of function mutations in *GABRA3* gene and functional consequences

The *GABRA3* gene is located on the X chromosome and encodes for the α3 subunit of the GABA$_A$R. The first identified mutation, Q242L, was found in an Israeli family, in which females carriers are mildly affected, whereas males are severely affected. This transmission goes in line with an X-linked mode of inheritance. The two affected boys suffer from severe epileptic encephalopathy with early seizure onset, profound intellectual disability, and dysmorphic features. The type of seizure ranges from infantile spasms with Lennox-Gastaut syndrome for the first patient to epileptic spasms and tonic seizures for the other one.

Four males have been identified by our collaborators as carriers of the second *GABRA3* mutation, T166M. Two of them show an epileptic phenotype with intellectual disability, whereas of the other two, only one has a mild intellectual disability, and the other one is unaffected. Although we would have expected that all males were severely affected, the incomplete co-segregation of the mutation with the disease in this family could be explained by incomplete penetrance of the mutation.

An interesting feature in the families described above is the presence of dysmorphic features, which are partially overlapping between the two families, strongly suggesting that mutations in *GABRA3* gene may be responsible for epilepsy, intellectual disability and dysmorphic features. It is not clear how a subunit of GABA$_A$ receptors may be linked to changes in morphology, but it has been reported that homozygous *Gabrb3* knock-out mice exhibit a cleft-palate in about half of the cases, and the other half have feeding difficulties as neonates (DeLorey *et al.*, 1998). Since α3 subunits can combine with β3 subunits in the brain (Studer *et al.*, 2006) loss of function of α3 could affect β3 subunit containing GABA$_A$ receptors. In line with this study, it has been demonstrated that blockers of GABA$_A$Rs, such as picrotoxin, can induce partial or complete cleft palate in mice, indicating that GABA$_A$Rs and functional GABA signaling are required for palatogenesis (Ding *et al.*, 2004).

As described above, loss of function mutations in GABA$_A$Rs have been often observed as a cause of epilepsy, but so far no mutation was identified in the *GABRA3* gene. It has been observed that the α3-subunit of the GABA$_A$ receptor has a broad distribution in the rodent brain and is specifically expressed in thalamus, being the only alpha subunit expressed in the nucleus reticularis thalami (NRT) (Hortnagl *et al.*, 2013). Knock-out mice lacking this subunit do not show spontaneous seizures. On the contrary, they show an enhanced intra-NRT

inhibition and a reduced susceptibility to pharmacologically induced seizures, probably due to a strong compensatory mechanism increasing the expression of a different α-subunit (Schofield *et al.*, 2009). However, another mouse study has shown that GABAergic synapses are altered in a null mouse of *GABRA3* due to the absence of gephyrin clustering of post-synaptic receptors. This could have consequences in the thalamocortical circuit in the absence of compensatory mechanisms (Studer *et al.*, 2006). On the other hand, in epileptic rats, immunoreactivity experiments have demonstrated a loss of $\alpha 3$ subunit at the inhibitory synapses of NRT neurons, which may indicate a role for $\alpha 3$ in idiopathic generalized epilepsy (Liu *et al.*, 2007). Furthermore, an increase in spike and wave discharges, a typical feature of absence seizures, was identified in a mouse model in which the benzodiazepine binding site of the α3-subunit is disrupted (Christian *et al.*, 2013). This implies that an impaired function of the α3-subunit may lead to epileptic seizures, which are not observed in knock-out animals because of a possible compensatory mechanism (Schofield *et al.*, 2009).

IGE/GGE is more common than EE and presumed to have a polygenic background. The T336M mutation analyzed in this thesis shows a loss of function effect. However, this mutation was only detected in two females whithin the IGE family, the unaffected mother and one of the affected daughters, but not in the affected father or sister. The incomplete cosegregation of this family, no additional male carrying the mutation, togheter with the fact that the other females patients in the other families do not present IGE/GGE syndromes, suggests that other genetic variants probably contribute to the patient´s and her relatives´phenotypes.

The Q242L and T166M associated with more severe phenotype are both located on the N-terminal domain of the $\alpha 3$ subunit. Several other mutations identified in the GABA$_A$R are located in the N-terminal domain, thus indicating that this domain plays an important role for GABA$_A$R function (Macdonald *et al.*, 2010; Hirose, 2014). Indeed, it is known that this part is important for the ligand binding to the receptor (Jacob *et al.*, 2008). However, one of the potential mechanisms through which these mutations could act, might be a trafficking defect or impaired assembly of the subunits, which would lead to reduced number of receptors expressed on the membrane surface. This process may lead to increased excitability and may explain the seizure activity in the patients.

Other features, such as the observed nystagmus in the patients carrying Q242L or T166M mutations, may be attributed to a specific inhibitory function of GABA$_A$ receptor α3-

subunits in the brainstem or cerebellum. Expression of *GABRA3* in these structures has been shown using specific antibodies against this subunit (Pirker *et al.*, 2000).

Functional data for the G47R mutation associated with autistic spectrum disorder does not show a severe loss of channel function as for the other characterized mutations. This goes in line with the phenotype of the patients, which is not as severe as for the other patients in this study. Additionally, the brother of the proband presents the same phenotype without carrying the mutation. Probably in this family, the mutation in *GABRA3* has only a little contribution to the phenotype and other factors have a major contribution to their pathological phenotype.

5.2 *GABBR2 de novo* mutations as a cause of EE

Besides GABA$_A$Rs, GABA$_B$Rs are the main responsible receptors for inhibition in neurons. These metabotropic receptors mediate inhibition in the brain in two ways. First, they can interfere with the release of neurotransmitter by blocking Ca^{2+} channels, with a consequence drop in the Ca2$^+$ concentration at presynaptic sites; second they can activate the G-protein coupled inward rectifying potassium (GIRK) channels at postsynaptic sites, which results in hyperpolarization (Benarroch, 2012). Another consequence of GABA$_B$R signaling takes place at dendritic sites, where spillover of GABA by adjacent terminals, may activate GABA$_B$Rs and therefore hyperpolarize the neurons through activation of potassium channels resulting in inhibition of the backpropagation of the APs, which may influence synaptic plasticity and AP generation at axon initial segments (Hua A. Han, 2012).

Although many epilepsy-causing mutations have been detected in different subunits of GABA$_A$R, no mutations were found in GABA$_B$Rs until 2014, when the first two *de novo* mutations were identified in the *GABBR2* gene, in two patients suffering from severe EE and, more specifically, Infantile Spasms and Lennox-Gastaut Syndrome (Appenzeller *et al.*, 2014).

Interestingly, both mutated amino acids are highly evolutionarily conserved and located on the sixth transmembrane domain, only 10 amino acids from each other. Additionally, both patients share a similar severe phenotype with intellectual disability, no speech ability and severe seizures that go from infantile spasms to focal dyscognitive and generalized tonic-clonic seizures. The functional analysis of the two mutations performed in this study showed a gain of function effect for both of them.

5.2.1 Gain of function mechanism of *de novo* I705N and S695I mutations

The I705N and S695I mutations have a higher GABA sensitivity with significantly lower EC_{50} values in comparison to the WT. Additionally, both mutations have a higher current response in the nanomolar GABA concentrations range, which are proposed to be actual concentrations for ambient GABA in the brain (Farrant & Nusser, 2005). Furthermore, the S695I mutation has a slowing in current deactivation in comparison with the WT, which additionally suggests a gain of function effect for this mutation. However at higher GABA concentrations, the I705N has no difference in current amplitude when compared with the WT, while the current response for S695I is significantly lower than the WT. This would imply that these mutations may have a gain of function effect at extrasynaptic sites, where $GABA_B R$ may mediate the tonic inhibition by decreasing the release probability of GABA via autoreceptors or glutamate via heteroreceptors (Mapelli *et al.*, 2009). Such an effect would only be plausible if the underlining reason for the overall reduction of current amplitudes caused by S695I would not be a trafficking defect. Since these results were obtained exclusively in oocytes these study did not focus on the trafficking mechanisms.

A gain of function of postsynaptic $GABA_B Rs$ can enhance directly the activity of extrasynaptic $GABA_A Rs$. In dentate gyrus granule cells of the hippocampus it was shown that baclofen, an agonist of $GABA_B Rs$, can induce an increase in tonic $GABA_A$-mediated current at extrasynaptic sites in δ subunit containing $GABA_A Rs$ (Tao *et al.*, 2013). This effect is usually inhibitory, but in some areas of the brain, for instance the thalamocortical circuit, may develop in excitatory. The increase in inhibition in thalamocortical cells can trigger post inhibitory rebound bursts of APs, which may turn the whole circuit in a hyperactive and pathological state, being therefore a cause of seizure activity (Cope *et al.*, 2010). In line with these studies, it was demonstrated that stimulation of $GABA_B Rs$ either by baclofen or by γ-hydroxybutyrate, an endogenous ligand, are able to induce an increase in spike and wave discharges, a typical electroencephalogram pattern of absence seizures (Bortolato *et al.*, 2010). Moreover, in the hippocampus, baclofen seems to act in a dose-dependent manner. While at high dosage it can activate pre- and post-synaptic receptors, at a lower dosage, it acts only on the presynaptic transmission. Thus a gain of function via increased GABA sensitivity, observed for both mutations, would produce enhanced feedback in the low dosage range via reduced presynaptic Ca^{2+} signalling and thus a disinhibitory effect with suppression of the synaptic

output of some inhibitory neurons, which could promote high frequency oscillatory activity in the hippocampus (Dugladze *et al.*, 2013).

Furthermore, the gain of function effect of the GABA$_B$R mutations could be responsible for the medical condition observed in the patients. Several studies revealed that activation of GABA$_B$Rs by administration of baclofen to patients resulted in memory loss (Sandyk & Gillman, 1985). Likewise, in animal models, baclofen has been responsible for augmenting the amnesic effect produced by scopolamine in memory-related behavioral tests (Sidel *et al.*, 1988).

Although the experimental data for S695I indicate a higher sensitivity for lower GABA concentrations in the dose-response logarithmic curve, the maximal current amplitude induced by the highest GABA concentration has a significantly reduced response when compared with the WT. This might indicate a loss of function effect for higher GABA concentrations, not found at extrasynaptic sites where these receptors mostly exert their function.

The loss of function of GABA$_B$Rs has several functional consequences in the brain´s physiology. Confirmation of this mechanism emerges from the use of mouse models of GABA$_B$Rs. GABA$_B$ KO mice of both GABA$_{B1}$ and GABA$_{B2}$ displayed similar phenotypes. GABA$_{B2}$ subunit KO mice show spontaneous seizures, hyperalgesia, hyperlocomotor activity and severe memory impairment (Gassmann et al., 2004), whereas loss of pre- and post-synaptic GABA$_B$ responses, epilepsy, hyperalgesia and memory impairment were shown for GABA$_{B1}$ KO mice (Schuler et al., 2001).

Some years ago, it was demonstrated that GABA$_B$Rs associate in vivo with a subfamily of the KCTD (potassium channel tetramerization domain containing) proteins. These proteins interact with the C-terminal domain probably at the GABA$_{B2}$ subunit. The interaction changes the receptor´s kinetics by increasing agonist binding potency and by altering G-protein transmission (Schwenk *et al.*, 2010). Since both mutations analyzed in this thesis are located on the GABA$_{B2}$ subunit, they may act through a change in the conformation of the receptor, thus affecting the interaction with KCTD proteins. This could potentially represent another mechanism relevant for the epileptic phenotype observed in the patients, and further functional investigations would be necessary to verify such a hypothesis.

5.3 ClC-2 channels and their contribution to neuronal excitability

In the third part of this thesis, I aimed to investigate the mechanisms of chloride homeostasis in a more complex system, such as a mouse model. To this purpose, I used a KO mouse model of ClC-2 chloride channel. Several partially controversial studies pointed at the potential involvement of the ClC-2 in epilepsy (Niemeyer *et al.*, 2004; Kleefuss-Lie *et al.*, 2009; Saint-Martin *et al.*, 2009; Niemeyer *et al.*, 2010; Stolting *et al.*, 2013). However, a recent study showed that patients carrying mutations that disrupt the function of the ClC-2 channel are affected with leukoencephalopathy, but not epilepsy (Depienne *et al.*, 2013). Nevertheless, the function of this channel is not deeply understood, and different studies suggest that ClC-2 could have distinct, potentially opposite roles in neurons. On the one hand, it would help to maintain the hyperpolarized GABA response, by extruding Cl^- ions from the cell at potentials more negative that its equilibrium potential (Staley, 1994; Staley *et al.*, 1996). On the other hand, it was demonstrated that under physiological conditions, ClC-2 may directly contribute to neuronal excitability by conducting Cl^- into the cell, following the driving force (Ratté & Prescott, 2011).

5.3.1 ClC-2 channel and its expression in the thalamocortical system

Chloride homeostasis is essential for effective inhibition in the brain. Intracellular chloride accumulation in neurons can lead to an excitatory GABAergic response, emphasizing the importance of effective chloride extrusion mechanisms. The potassium chloride co-transporter 2 (KCC2) provides the major chloride extrusion pathway and a similar role has been proposed for the chloride channel ClC-2 (Staley, 1994; Ben-Ari, 2002; Rinke *et al.*, 2010). Interestingly, the nucleus reticularis of the thalamus (NRT) has a very low expression of the KCC2 transporter (Bartho *et al.*, 2004; Sun *et al.*, 2012), indicating the thalamocortical system as an ideal area to investigate the ClC-2 contribution to neuronal excitability. Smith *et al.* (1995) have deeply investigated the ClC-2 expression in different areas of the CNS and, in addition to the cortex and hippocampus, they identified high expression of the channel in the thalamus. Focusing on these results, I aimed to verify whether neurons of the thalamocortical system show ClC-2 mediated currents. As expected, ClC-2 currents have been detected in the NRT, VB and in the fifth layer of the cortex in neurons derived from WT and heterozygous mice, but no currents were detected in neurons derived from KO mice.

As demonstrated in other studies (Staley, 1994; Rinke *et al.*, 2010), using a high Cl^- concentration in the pipette, will result in currents showing inward rectification, thus indicating that they are suitable to conduct Cl^- ions inward rather than outward when voltages are more negative than the Cl^- equilibrium potentials. These conditions are sufficient to ensure Cl^- efflux rather than influx through the ClC-2 channel. Additional support for the importance of ClC-2 as a Cl^- extruder is derived from an analysis of synaptic connections of fast-spiking basket cells in the hippocampus. It was shown that these interneurons are regulated by ClC-2 channel and during high neuronal activity at specific inhibitory synapses, the voltage-gated Cl^- channel ClC-2 results to be vital for allowing efflux of accumulated internal Cl^- (Földy *et al.*, 2010).

5.3.2 Less inhibition in the thalamocortical system

The thalamocortical system is an important generator of rhythmic activity, such as sleep spindles during non-REM sleep, which may become pathologic with 3 Hz spike and wave discharges during absence seizures (Huntsman *et al.*, 1999; Avanzini *et al.*, 2000). Because of these properties and the lack of expression of KCC2 in these neurons (Bartho *et al.*, 2004; Sun *et al.*, 2012), I decided to focus on analyzing the change in excitability of NRT neurons in the ClC-2 KO mouse. Moreover, my observations point out that NRT neurons express ClC-2 channels, by showing ClC-2 currents.

In addition, the main result of this thesis is that NRT inhibitory neurons, derived from KO mice, show a lower firing rate in comparison with the neurons derived from WT mice, therefore suggesting a reduction of inhibition in the whole thalamocortical system. This finding was unexpected since hitherto the absence of ClC-2 was associated with an increase in excitability. In ClC-2 KO pyramidal neurons of the hippocampus, Rinke and colleagues (2010) demonstrated that the same current injection elicited more action potentials. Additionally, the loss of ClC-2 channel increased the input resistance, confirming the higher excitability of the pyramidal neurons. Similarly, loss of ClC-2 resulted in a higher excitability of inhibitory neurons of the hippocampus and, therefore, increased inhibition, which might compensate for the hyperexcitability of the network and prevent the development of seizures.

Although many ClC-2 studies were performed on hippocampal cells (Madison *et al.*, 1986; Földy *et al.*, 2010; Rinke *et al.*, 2010), no investigation was carried out on thalamic

neurons. Therefore, it is not clear what a decrease in firing rates in NRT inhibitory neurons could represent in the ClC-2 KO mouse and how this would affect the whole network activity. Perforated-patch recordings of NRT neurons demonstrated a higher concentration of intracellular Cl$^-$ than the one usually observed in adult neurons. This results in a much more depolarized Cl$^-$ reversal potential, which leads GABA$_A$Rs to behave in a depolarizing manner, triggering APs. Responsible of this behavior are the low levels of KCC2 transporter, which entails the absence of the main extrusion mechanism of Cl$^-$ from neurons (Sun *et al.*, 2012). This is an unusual circumstance because GABAergic transmission in the adult brain acts through hyperpolarization, due to higher expression of KCC2 (Rivera *et al.*, 1999). A depolarized GABAergic activity is usually described in immature cells or in epileptic tissue, where depolarizing GABA can trigger APs (Ben-Ari, 2002; Cossart *et al.*, 2005). This raises the question about the mechanisms that could be responsible for the lower excitability in NRT inhibitory neurons derived from ClC-2 KO mice. In conditions of low KCC2 expression, if ClC-2 would regulate intracellular Cl$^-$ concentration by extrusion mechanisms, an increase ClC-2 activity would compensate for the absence of KCC2, reducing the disinhibition. On the contrary, if ClC-2 would directly regulate the neuronal excitability by leaking Cl$^-$ into the neurons as previously proposed (Ratté & Prescott, 2011), then ClC-2 would further increase the Cl$^-$ accumulation in the absence of KCC2. According to the latter hypothesis, if in addition to KCC2 also ClC-2 is absent, then the intracellular Cl$^-$ would be lower and the E$_{Cl-}$ more hyperpolarized, resulting in less firing activity in the NRT neurons derived from ClC-2 KO mice, which would explain the obtained result in this thesis.

5.3.3 Contribution of neurons derived from ClC-2 KO mice to the network activities

I further aimed to verify if reduced activity of the NRT inhibitory neurons derived from ClC-2 KO mice has any influence on network activity of the thalamocortical circuit. Less intra-NRT inhibition should lead to higher excitability in the network and possibly to seizures (Crunelli & Leresche, 2002; Beenhakker & Huguenard, 2009). However, simultaneous recordings of synchronous activity in the thalamocortical brain slices, and more specifically in NRT, VB and V layer of the cortex, didn´t show any differences in the synchronized bursting behavior of thalamocortical slices from ClC-2 KO mice in comparison with the WT. Indeed, studies of ClC-2 deficient mice didn´t identify any spontaneous seizure activity (Bösl *et al.*,

2001), which may have resulted from excitatory effects of GABA as proposed in the past (Smith *et al.*, 1995; Staley *et al.*, 1996). This observation was later confirmed by Blanz and colleagues (2007), who determined the seizure susceptibility of ClC-2 KO mice by exposing them to pro convulsants and finding no differences between genotypes. On the other hand, electrocorticographic recordings of older ClC-2 KO mice (more than 6 months), revealed spontaneous slow spike and wave discharges, and blockage of $GABA_A$Rs increased even further the seizure activity (Cortez *et al.*, 2010). In line with this finding, incubation with picrotoxin induced a higher spontaneous and synchronous activity in the thalamocortical brain slice even in slices derived from younger ClC-2 KO mice when compared to WT. These experiments performed in the thalamocortical system point out that the absence of ClC-2 has an effect on the network excitability only in the presence of other perturbating factors, as it was found here by blocking $GABA_A$Rs. This confirms the finding that variations in the ClC-2 gene alone are not sufficient to produce an epileptic phenotype (Depienne *et al.*, 2013). Increasing evidence is suggesting that epilepsy is not only due to the occurrence of single mutations, but rather to a co-expression of variants affecting different genes, which may contribute to the epileptic phenotype (Kleefuss-Lie *et al.*, 2009; Saint-Martin *et al.*, 2009; Klassen *et al.*, 2011). In this picture, ClC-2 would rather act as a susceptibility factor of the disease and would have an effect on the neuronal excitability only when expressed in combination with mutations in other genes causing the disease or additional stressing factors.

Whilst no effect could be detected in the extracellular recording of thalamocortical slices derived from ClC-2 KO mice, spontaneous network activities of cultured hippocampal neurons from these mice, recorded using the microelectrode array (MEA) technique, revealed an increase in synchronized activity compared to the WT. The observed changes in some parameters, such as an increased burst duration, correspond well to the increase in excitation found in pyramidal neurons of the hippocampus in ClC-2 KO mice, although field potentials recordings in the same study showed a loss in excitation possibly due to increase of feedforward inhibition of a subset of inhibitory interneurons (Rinke *et al.*, 2010). The increased excitation in ClC-2 KO MEA recording is possibly due to an impairment in the GABAergic transmission, which is not further affected by the block of $GABA_A$Rs.

6 References

Agmon, A. & Connors, B. (1991) Thalamocortical responses of mouse somatosensory (barrel) cortex in vitro. *Neuroscience*, **41**, 365-379.

Alldred, M.J., Mulder-Rosi, J., Lingenfelter, S.E., Chen, G. & Luscher, B. (2005) Distinct gamma2 subunit domains mediate clustering and synaptic function of postsynaptic GABAA receptors and gephyrin. *The Journal of neuroscience : the official journal of the Society for Neuroscience*, **25**, 594-603.

Allen, A.S., Berkovic, S.F., Cossette, P., Delanty, N., Dlugos, D., Eichler, E.E., Epstein, M.P., Glauser, T., Goldstein, D.B., Han, Y., Heinzen, E.L., Hitomi, Y., Howell, K.B., Johnson, M.R., Kuzniecky, R., Lowenstein, D.H., Lu, Y.-F., Madou, M.R.Z., Marson, A.G., Mefford, H.C., Nieh, S.E., O'Brien, T.J., Ottman, R., Petrovski, S., Poduri, A., Ruzzo, E.K., Scheffer, I.E., Sherr, E.H., Yuskaitis, C.J. & Project, E.P.G. (2013) De novo mutations in epileptic encephalopathies. *Nature*, **501**, 217-221.

Appenzeller, S., Balling, R., Barisic, N., Baulac, S., Caglayan, H., Craiu, D., De Jonghe, P., Depienne, C., Dimova, P., Djémié, T., Gormley, P., Guerrini, R., Helbig, I., Hjalgrim, H., Hoffman-Zacharska, D., Jähn, J., Klein, K.M., Koeleman, B., Komarek, V., Krause, R., Kuhlenbäumer, G., Leguern, E., Lehesjoki, A.-E., Lemke, J.R., Lerche, H., Linnankivi, T., Marini, C., May, P., Møller, R.S., Muhle, H., Pal, D., Palotie, A., Pendziwiat, M., Robbiano, A., Roelens, F., Rosenow, F., Selmer, K., Serratosa, J., Sisodiya, S., Stephani, U., Sterbova, K., Striano, P., Suls, A., Talvik, T., von Spiczak, S., Weber, Y., Weckhuysen, S., Zara, F., Project, E.P.G. & Consortium, E.K. (2014) De Novo Mutations in Synaptic Transmission Genes Including DNM1 Cause Epileptic Encephalopathies. *American journal of human genetics*, **95**, 360.

Aridon, P., Marini, C., Di Resta, C., Brilli, E., De Fusco, M., Politi, F., Parrini, E., Manfredi, I., Pisano, T., Pruna, D., Curia, G., Cianchetti, C., Pasqualetti, M., Becchetti, A., Guerrini, R. & Casari, G. (2006) Increased sensitivity of the neuronal nicotinic receptor alpha 2 subunit causes familial epilepsy with nocturnal wandering and ictal fear. *American journal of human genetics*, **79**, 342-350.

Avanzini, G., Panzica, F. & De Curtis, M. (2000) The role of the thalamus in vigilance and epileptogenic mechanisms. *Clinical Neurophysiology*, **111**, S19-S26.

Baltz, T., De Lima, A.D. & Voigt, T. (2010) Contribution of GABAergic interneurons to the development of spontaneous activity patterns in cultured neocortical networks. *Frontiers in cellular neuroscience*, **4**.

Bartho, P., Payne, J., Freund, T. & Acsady, L. (2004) Differential distribution of the KCl cotransporter KCC2 in thalamic relay and reticular nuclei. *European Journal of Neuroscience*, **20**, 965-975.

Bean, B.P. (2007) The action potential in mammalian central neurons. *Nature Reviews Neuroscience*, **8**, 451-465.

Beenhakker, M.P. & Huguenard, J.R. (2009) Neurons that fire together also conspire together: is normal sleep circuitry hijacked to generate epilepsy? *Neuron*, **62**, 612-632.

Ben-Ari, Y. (2002) Excitatory actions of GABA during development: the nature of the nurture. *Nature Reviews Neuroscience*, **3**, 728-739.

Benarroch, E.E. (2007) GABAA receptor heterogeneity, function, and implications for epilepsy. *Neurology*, **68**, 612-614.

Benarroch, E.E. (2012) GABAB receptors: structure, functions, and clinical implications. *Neurology*, **78**, 578-584.

Berg, A.T., Berkovic, S.F., Brodie, M.J., Buchhalter, J., Cross, J.H., Van Emde Boas, W., Engel, J., French, J., Glauser, T.A. & Mathern, G.W. (2010) Revised terminology and concepts for organization of seizures and epilepsies: report of the ILAE Commission on Classification and Terminology, 2005–2009. *Epilepsia*, **51**, 676-685.

Biervert, C., Schroeder, B.C., Kubisch, C., Berkovic, S.F., Propping, P., Jentsch, T.J. & Steinlein, O.K. (1998) A potassium channel mutation in neonatal human epilepsy. *Science*, **279**, 403-406.

Blanz, J., Schweizer, M., Auberson, M., Maier, H., Muenscher, A., Hübner, C.A. & Jentsch, T.J. (2007) Leukoencephalopathy upon disruption of the chloride channel ClC-2. *The Journal of neuroscience*, **27**, 6581-6589.

Bortolato, M., Frau, R., Orrù, M., Fà, M., Dessì, C., Puligheddu, M., Barberini, L., Pillolla, G., Polizzi, L. & Santoni, F. (2010) GABA B receptor activation exacerbates spontaneous spike-and-wave discharges in DBA/2J mice. *Seizure*, **19**, 226-231.

Bösl, M.R., Stein, V., Hübner, C., Zdebik, A.A., Jordt, S.E., Mukhopadhyay, A.K., Davidoff, M.S., Holstein, A.F. & Jentsch, T.J. (2001) Male germ cells and photoreceptors, both dependent on close cell–cell interactions, degenerate upon ClC-2 Cl– channel disruption. *The EMBO journal*, **20**, 1289-1299.

Carvill, G.L., McMahon, J.M., Schneider, A., Zemel, M., Myers, C.T., Saykally, J., Nguyen, J., Robbiano, A., Zara, F., Specchio, N., Mecarelli, O., Smith, R.L., Leventer, R.J., Moller, R.S., Nikanorova, M., Dimova, P., Jordanova, A., Petrou, S., Euro, E.R.E.S.M.-A.E., Dravet working, g., Helbig, I., Striano, P., Weckhuysen, S., Berkovic, S.F., Scheffer, I.E. & Mefford, H.C. (2015) Mutations in the GABA Transporter SLC6A1 Cause Epilepsy with Myoclonic-Atonic Seizures. *American journal of human genetics*, **96**, 808-815.

Carvill, G.L., Weckhuysen, S., McMahon, J.M., Hartmann, C., Moller, R.S., Hjalgrim, H., Cook, J., Geraghty, E., O'Roak, B.J., Petrou, S., Clarke, A., Gill, D., Sadleir, L.G., Muhle, H., von Spiczak, S., Nikanorova, M., Hodgson, B.L., Gazina, E.V., Suls, A., Shendure, J., Dibbens, L.M., De Jonghe, P., Helbig, I., Berkovic, S.F., Scheffer, I.E. & Mefford, H.C. (2014) GABRA1 and STXBP1: novel genetic causes of Dravet syndrome. *Neurology*, **82**, 1245-1253.

Chang, B.S. & Lowenstein, D.H. (2003) Epilepsy. *The New England journal of medicine*, **349**, 1257-1266.

Christian, C.A., Herbert, A.G., Holt, R.L., Peng, K., Sherwood, K.D., Pangratz-Fuehrer, S., Rudolph, U. & Huguenard, J.R. (2013) Endogenous positive allosteric modulation of GABA(A) receptors by diazepam binding inhibitor. *Neuron*, **78**, 1063-1074.

Claes, L., Del-Favero, J., Ceulemans, B., Lagae, L., Van Broeckhoven, C. & De Jonghe, P. (2001) De novo mutations in the sodium-channel gene SCN1A cause severe myoclonic epilepsy of infancy. *American journal of human genetics*, **68**, 1327-1332.

Cope, J.L., Chung, E., Ohgami, Y. & Quock, R.M. (2010) Antagonism of the antinociceptive effect of nitrous oxide by inhibition of enzyme activity or expression of neuronal nitric oxide synthase in the mouse brain and spinal cord. *European journal of pharmacology*, **626**, 234-238.

Cortez, M., Li, C., Whitehead, S., Dhani, S., D'Antonio, C., Huan, L., Bennett, S., Snead, O. & Bear, C. (2010) Disruption of ClC-2 expression is associated with progressive neurodegeneration in aging mice. *Neuroscience*, **167**, 154-162.

Cortez, M.A. & Snead, O. (2006) Pharmacologic models of generalized absence seizures in rodents *Models of seizures and epilepsy*. Elsevier Ac Press San Diego, CA, pp. 114.

Cossart, R., Bernard, C. & Ben-Ari, Y. (2005) Multiple facets of GABAergic neurons and synapses: multiple fates of GABA signalling in epilepsies. *Trends in neurosciences*, **28**, 108-115.

Cossette, P., Liu, L., Brisebois, K., Dong, H., Lortie, A., Vanasse, M., Saint-Hilaire, J.M., Carmant, L., Verner, A., Lu, W.Y., Wang, Y.T. & Rouleau, G.A. (2002) Mutation of GABRA1 in an autosomal dominant form of juvenile myoclonic epilepsy. *Nature genetics*, **31**, 184-189.

Crunelli, V. & Leresche, N. (2002) Childhood absence epilepsy: genes, channels, neurons and networks. *Nature reviews. Neuroscience*, **3**, 371-382.

D'Arcangelo, G., D'Antuono, M., Biagini, G., Warren, R., Tancredi, V. & Avoli, M. (2002) Thalamocortical oscillations in a genetic model of absence seizures. *European Journal of Neuroscience*, **16**, 2383-2393.

D'Agostino, D., Bertelli, M., Gallo, S., Cecchin, S., Albiero, E., Garofalo, P.G., Gambardella, A., Hilaire, J.-M.S., Kwiecinski, H. & Andermann, E. (2004) Mutations and polymorphisms of the CLCN2 gene in idiopathic epilepsy. *Neurology*, **63**, 1500-1502.

De Fusco, M., Becchetti, A., Patrignani, A., Annesi, G., Gambardella, A., Quattrone, A., Ballabio, A., Wanke, E. & Casari, G. (2000) The nicotinic receptor beta 2 subunit is mutant in nocturnal frontal lobe epilepsy. *Nature genetics*, **26**, 275-276.

de Kovel, C.G., Trucks, H., Helbig, I., Mefford, H.C., Baker, C., Leu, C., Kluck, C., Muhle, H., von Spiczak, S. & Ostertag, P. (2010) Recurrent microdeletions at 15q11. 2 and 16p13. 11 predispose to idiopathic generalized epilepsies. *Brain : a journal of neurology*, **133**, 23-32.

DeLorey, T.M., Handforth, A., Anagnostaras, S.G., Homanics, G.E., Minassian, B.A., Asatourian, A., Fanselow, M.S., Delgado-Escueta, A., Ellison, G.D. & Olsen, R.W. (1998) Mice lacking the beta3 subunit of the GABAA receptor have the epilepsy phenotype and many of the behavioral characteristics of Angelman syndrome. *The Journal of neuroscience : the official journal of the Society for Neuroscience*, **18**, 8505-8514.

Depienne, C., Bugiani, M., Dupuits, C., Galanaud, D., Touitou, V., Postma, N., Van Berkel, C., Polder, E., Tollard, E. & Darios, F. (2013) Brain white matter oedema due to ClC-2 chloride channel deficiency: an observational analytical study. *The Lancet Neurology*, **12**, 659-668.

Dibbens, L.M., Feng, H.-J., Richards, M.C., Harkin, L.A., Hodgson, B.L., Scott, D., Jenkins, M., Petrou, S., Sutherland, G.R. & Scheffer, I.E. (2004) GABRD encoding a protein for extra-or peri-synaptic GABAA receptors is a susceptibility locus for generalized epilepsies. *Human molecular genetics*, **13**, 1315-1319.

Dibbens, L.M., Heron, S.E. & Mulley, J.C. (2007) A polygenic heterogeneity model for common epilepsies with complex genetics. *Genes, brain, and behavior*, **6**, 593-597.

Ding, R., Tsunekawa, N. & Obata, K. (2004) Cleft palate by picrotoxin or 3-MP and palatal shelf elevation in GABA-deficient mice. *Neurotoxicology and teratology*, **26**, 587-592.

Dugladze, T., Maziashvili, N., Börgers, C., Gurgenidze, S., Häussler, U., Winkelmann, A., Haas, C.A., Meier, J.C., Vida, I. & Kopell, N.J. (2013) GABAB autoreceptor-mediated cell type-specific reduction of inhibition in epileptic mice. *Proceedings of the National Academy of Sciences*, **110**, 15073-15078.

Duszyc, K., Terczynska, I. & Hoffman-Zacharska, D. (2015) Epilepsy and mental retardation restricted to females: X-linked epileptic infantile encephalopathy of unusual inheritance. *Journal of applied genetics*, **56**, 49-56.

Dutzler, R., Campbell, E.B., Cadene, M., Chait, B.T. & MacKinnon, R. (2002) X-ray structure of a ClC chloride channel at 3.0 Å reveals the molecular basis of anion selectivity. *Nature*, **415**, 287-294.

Epilepsy, I.L.A. (1989) Proposal for revised classification of epilepsies and epileptic syndromes. Commission on Classification and Terminology of the International League Against Epilepsy. *Epilepsia*, **30**, 389-399.

Escayg, A., MacDonald, B.T., Meisler, M.H., Baulac, S., Huberfeld, G., An-Gourfinkel, I., Brice, A., LeGuern, E., Moulard, B., Chaigne, D., Buresi, C. & Malafosse, A. (2000) Mutations of SCN1A, encoding a neuronal sodium channel, in two families with GEFS+2. *Nature genetics*, **24**, 343-345.

Farrant, M. & Nusser, Z. (2005) Variations on an inhibitory theme: phasic and tonic activation of GABAA receptors. *Nature Reviews Neuroscience*, **6**, 215-229.

Fisher, R.S., Acevedo, C., Arzimanoglou, A., Bogacz, A., Cross, J.H., Elger, C.E., Engel, J., Jr., Forsgren, L., French, J.A., Glynn, M., Hesdorffer, D.C., Lee, B.I., Mathern, G.W., Moshe, S.L., Perucca, E., Scheffer, I.E., Tomson, T., Watanabe, M. & Wiebe, S. (2014) ILAE official report: a practical clinical definition of epilepsy. *Epilepsia*, **55**, 475-482.

Földy, C., Lee, S.-H., Morgan, R.J. & Soltesz, I. (2010) Regulation of fast-spiking basket cell synapses by the chloride channel ClC-2. *Nature neuroscience*, **13**, 1047-1049.

Fritschy, J.M., Meskenaite, V., Weinmann, O., Honer, M., Benke, D. & Mohler, H. (1999) GABAB-receptor splice variants GB1a and GB1b in rat brain: Developmental regulation, cellular distribution and extrasynaptic localization. *European Journal of Neuroscience*, **11**, 761-768.

Garcia-Olivares, J., Alekov, A., Boroumand, M.R., Begemann, B., Hidalgo, P. & Fahlke, C. (2008) Gating of human ClC-2 chloride channels and regulation by carboxy-terminal domains. *The Journal of physiology*, **586**, 5325-5336.

Harkin, L.A., Bowser, D.N., Dibbens, L.M., Singh, R., Phillips, F., Wallace, R.H., Richards, M.C., Williams, D.A., Mulley, J.C. & Berkovic, S.F. (2002) Truncation of the GABA A-receptor γ2 subunit in a family with generalized epilepsy with febrile seizures plus. *The American Journal of Human Genetics*, **70**, 530-536.

Hedrich, U.B., Liautard, C., Kirschenbaum, D., Pofahl, M., Lavigne, J., Liu, Y., Theiss, S., Slotta, J., Escayg, A., Dihne, M., Beck, H., Mantegazza, M. & Lerche, H. (2014) Impaired action potential initiation in GABAergic interneurons causes hyperexcitable networks in an epileptic mouse model carrying a human Na(V)1.1 mutation. *The Journal of neuroscience : the official journal of the Society for Neuroscience*, **34**, 14874-14889.

Herlenius, E., Heron, S.E., Grinton, B.E., Keay, D., Scheffer, I.E., Mulley, J.C. & Berkovic, S.F. (2007) SCN2A mutations and benign familial neonatal-infantile seizures: the phenotypic spectrum. *Epilepsia*, **48**, 1138-1142.

Hirose, S. (2014) Mutant GABA(A) receptor subunits in genetic (idiopathic) epilepsy. *Progress in brain research*, **213**, 55-85.

Hoegg-Beiler, M.B., Sirisi, S., Orozco, I.J., Ferrer, I., Hohensee, S., Auberson, M., Gödde, K., Vilches, C., de Heredia, M.L. & Nunes, V. (2014) Disrupting MLC1 and GlialCAM and ClC-2 interactions in leukodystrophy entails glial chloride channel dysfunction. *Nature communications*, **5**.

Hortnagl, H., Tasan, R.O., Wieselthaler, A., Kirchmair, E., Sieghart, W. & Sperk, G. (2013) Patterns of mRNA and protein expression for 12 GABAA receptor subunits in the mouse brain. *Neuroscience*, **236**, 345-372.

Hua A. Han, M.A.C., O. Carter Snead III (2012) GABAB Receptor and Absence Epilepsy. *Jasper's Basic Mechanisms of the Epilepsies*, **80**, 242.

Huntsman, M.M., Porcello, D.M., Homanics, G.E., DeLorey, T.M. & Huguenard, J.R. (1999) Reciprocal inhibitory connections and network synchrony in the mammalian thalamus. *Science*, **283**, 541-543.

Illes, S., Theiss, S., Hartung, H.P., Siebler, M. & Dihne, M. (2009) Niche-dependent development of functional neuronal networks from embryonic stem cell-derived neural populations. *BMC neuroscience*, **10**, 93.

Ishii, A., Kanaumi, T., Sohda, M., Misumi, Y., Zhang, B., Kakinuma, N., Haga, Y., Watanabe, K., Takeda, S., Okada, M., Ueno, S., Kaneko, S., Takashima, S. & Hirose, S. (2014) Association of nonsense mutation in GABRG2 with abnormal trafficking of GABAA receptors in severe epilepsy. *Epilepsy research*, **108**, 420-432.

Jacob, T.C., Moss, S.J. & Jurd, R. (2008) GABA(A) receptor trafficking and its role in the dynamic modulation of neuronal inhibition. *Nature reviews. Neuroscience*, **9**, 331-343.

Jentsch, T.J., Steinmeyer, K. & Schwarz, G. (1990) Primary structure of Torpedo marmorata chloride channel isolated by expression cloning in Xenopus oocytes. *Nature*, **348**, 510-514.

Jeworutzki, E., López-Hernández, T., Capdevila-Nortes, X., Sirisi, S., Bengtsson, L., Montolio, M., Zifarelli, G., Arnedo, T., Müller, C.S. & Schulte, U. (2012) GlialCAM, a protein defective in a leukodystrophy, serves as a ClC-2 Cl– channel auxiliary subunit. *Neuron*, **73**, 951-961.

Jouvenceau, A., Eunson, L.H., Spauschus, A., Ramesh, V., Zuberi, S.M., Kullmann, D.M. & Hanna, M.G. (2001) Human epilepsy associated with dysfunction of the brain P/Q-type calcium channel. *Lancet*, **358**, 801-807.

Kaila, K., Price, T.J., Payne, J.A., Puskarjov, M. & Voipio, J. (2014) Cation-chloride cotransporters in neuronal development, plasticity and disease. *Nature Reviews Neuroscience*, **15**, 637-654.

Kananura, C., Haug, K., Sander, T., Runge, U., Gu, W., Hallmann, K., Rebstock, J., Heils, A. & Steinlein, O.K. (2002) A splice-site mutation in GABRG2 associated with childhood absence epilepsy and febrile convulsions. *Archives of neurology*, **59**, 1137-1141.

Klassen, T., Davis, C., Goldman, A., Burgess, D., Chen, T., Wheeler, D., McPherson, J., Bourquin, T., Lewis, L. & Villasana, D. (2011) Exome sequencing of ion channel genes reveals complex profiles confounding personal risk assessment in epilepsy. *Cell*, **145**, 1036-1048.

Kleefuss-Lie, A., Friedl, W., Cichon, S., Haug, K., Warnstedt, M., Alekov, A., Sander, T., Ramirez, A., Poser, B., Maljevic, S., Hebeisen, S., Kubisch, C., Rebstock, J., Horvath, S., Hallmann, K., Dullinger, J.S., Rau, B., Haverkamp, F., Beyenburg, S., Schulz, H., Janz, D., Giese, B., Muller-Newen, G., Propping, P., Elger, C.E., Fahlke, C. & Lerche, H. (2009) CLCN2 variants in idiopathic generalized epilepsy. *Nature genetics*, **41**, 954-955.

Kole, M.H. & Stuart, G.J. (2008) Is action potential threshold lowest in the axon? *Nature neuroscience*, **11**, 1253-1255.

Kralic, J., Korpi, E., O'Buckley, T., Homanics, G. & Morrow, A. (2002) Molecular and pharmacological characterization of GABAA receptor α1 subunit knockout mice. *Journal of Pharmacology and Experimental Therapeutics*, **302**, 1037-1045.

Krampfl, K., Maljevic, S., Cossette, P., Ziegler, E., Rouleau, G.A., Lerche, H. & Bufler, J. (2005) Molecular analysis of the A322D mutation in the GABAA receptor α1-subunit causing juvenile myoclonic epilepsy. *European Journal of Neuroscience*, **22**, 10-20.

Landisman, C.E., Long, M.A., Beierlein, M., Deans, M.R., Paul, D.L. & Connors, B.W. (2002) Electrical synapses in the thalamic reticular nucleus. *The Journal of neuroscience*, **22**, 1002-1009.

Lee, S.E., Lee, J., Latchoumane, C., Lee, B., Oh, S.-J., Saud, Z.A., Park, C., Sun, N., Cheong, E. & Chen, C.-C. (2014) Rebound burst firing in the reticular thalamus is not essential for pharmacological absence seizures in mice. *Proceedings of the National Academy of Sciences*, **111**, 11828-11833.

Lee, S.H., Govindaiah, G. & Cox, C.L. (2007) Heterogeneity of firing properties among rat thalamic reticular nucleus neurons. *The Journal of physiology*, **582**, 195-208.

Lemke, J.R., Hendrickx, R., Geider, K., Laube, B., Schwake, M., Harvey, R.J., James, V.M., Pepler, A., Steiner, I., Hortnagel, K., Neidhardt, J., Ruf, S., Wolff, M., Bartholdi, D., Caraballo, R., Platzer, K., Suls, A., De Jonghe, P., Biskup, S. & Weckhuysen, S. (2014) GRIN2B mutations in West syndrome and intellectual disability with focal epilepsy. *Annals of neurology*, **75**, 147-154.

Lerche, H., Shah, M., Beck, H., Noebels, J., Johnston, D. & Vincent, A. (2013) Ion channels in genetic and acquired forms of epilepsy. *The Journal of physiology*, **591**, 753-764.

Liu, X.-B., Coble, J., van Luijtelaar, G. & Jones, E.G. (2007) Reticular nucleus-specific changes in α3 subunit protein at GABA synapses in genetically epilepsy-prone rats. *Proceedings of the National Academy of Sciences*, **104**, 12512-12517.

Lujan, R. & Ciruela, F. (2012) GABAB receptors-associated proteins: potential drug targets in neurological disorders? *Current drug targets*, **13**, 129-144.

Macdonald, R.L., Kang, J.Q. & Gallagher, M.J. (2010) Mutations in GABAA receptor subunits associated with genetic epilepsies. *The Journal of physiology*, **588**, 1861-1869.

Madison, D.V., Malenka, R.C. & Nicoll, R.A. (1986) Phorbol esters block a voltage-sensitive chloride current in hippocampal pyramidal cells.

Maljevic, S., Krampfl, K., Cobilanschi, J., Tilgen, N., Beyer, S., Weber, Y.G., Schlesinger, F., Ursu, D., Melzer, W., Cossette, P., Bufler, J., Lerche, H. & Heils, A. (2006) A mutation in the GABA(A)

receptor alpha(1)-subunit is associated with absence epilepsy. *Annals of neurology*, **59**, 983-987.

Mapelli, L., Rossi, P., Nieus, T. & D'Angelo, E. (2009) Tonic activation of GABAB receptors reduces release probability at inhibitory connections in the cerebellar glomerulus. *Journal of neurophysiology*, **101**, 3089-3099.

Mihalek, R.M., Bowers, B.J., Wehner, J.M., Kralic, J.E., VanDoren, M.J., Morrow, A.L. & Homanics, G.E. (2001) GABAA-receptor δ subunit knockout mice have multiple defects in behavioral responses to ethanol. *Alcoholism: Clinical AND Experimental Research*, **25**, 1708-1718.

Mohler, H. (2006) GABA(A) receptor diversity and pharmacology. *Cell and tissue research*, **326**, 505-516.

Molleman, A. (2003) *Patch clamping: an introductory guide to patch clamp electrophysiology*. John Wiley & Sons.

Myers, C.T. & Mefford, H.C. (2015) Advancing epilepsy genetics in the genomic era. *Genome medicine*, **7**, 1-11.

Nava, C., Dalle, C., Rastetter, A., Striano, P., de Kovel, C.G., Nabbout, R., Cances, C., Ville, D., Brilstra, E.H., Gobbi, G., Raffo, E., Bouteiller, D., Marie, Y., Trouillard, O., Robbiano, A., Keren, B., Agher, D., Roze, E., Lesage, S., Nicolas, A., Brice, A., Baulac, M., Vogt, C., El Hajj, N., Schneider, E., Suls, A., Weckhuysen, S., Gormley, P., Lehesjoki, A.E., De Jonghe, P., Helbig, I., Baulac, S., Zara, F., Koeleman, B.P., Euro, E.R.E.S.C., Haaf, T., LeGuern, E. & Depienne, C. (2014) De novo mutations in HCN1 cause early infantile epileptic encephalopathy. *Nature genetics*, **46**, 640-645.

Neher, E. & Sakmann, B. (1976) Single-channel currents recorded from membrane of denervated frog muscle fibres. *Nature*, **260**, 799-802.

Ng, G.Y., Clark, J., Coulombe, N., Ethier, N., Hebert, T.E., Sullivan, R., Kargman, S., Chateauneuf, A., Tsukamoto, N., McDonald, T., Whiting, P., Mezey, E., Johnson, M.P., Liu, Q., Kolakowski, L.F., Jr., Evans, J.F., Bonner, T.I. & O'Neill, G.P. (1999) Identification of a GABAB receptor subunit, gb2, required for functional GABAB receptor activity. *The Journal of biological chemistry*, **274**, 7607-7610.

Nieh, S.E. & Sherr, E.H. (2014) Epileptic encephalopathies: new genes and new pathways. *Neurotherapeutics : the journal of the American Society for Experimental NeuroTherapeutics*, **11**, 796-806.

Niemeyer, M.I., Cid, L.P., Sepulveda, F.V., Blanz, J., Auberson, M. & Jentsch, T.J. (2010) No evidence for a role of CLCN2 variants in idiopathic generalized epilepsy. *Nature genetics*, **42**, 3.

Niemeyer, M.I., Yusef, Y.R., Cornejo, I., Flores, C.A., Sepúlveda, F.V. & Cid, L.P. (2004) Functional evaluation of human ClC-2 chloride channel mutations associated with idiopathic generalized epilepsies. *Physiological genomics*, **19**, 74-83.

Otto, F., Illes, S., Opatz, J., Laryea, M., Theiss, S., Hartung, H.P., Schnitzler, A., Siebler, M. & Dihne, M. (2009) Cerebrospinal fluid of brain trauma patients inhibits in vitro neuronal network function via NMDA receptors. *Annals of neurology*, **66**, 546-555.

Pin, J. (2007) Recommendation for the recognition and nomenclature of G protein-coupled receptor heteromultimers. *Pharmacol. Rev*, **59**, 5-13.

Pin, J.P., Kniazeff, J., Binet, V., Liu, J., Maurel, D., Galvez, T., Duthey, B., Havlickova, M., Blahos, J., Prezeau, L. & Rondard, P. (2004) Activation mechanism of the heterodimeric GABA(B) receptor. *Biochemical pharmacology*, **68**, 1565-1572.

Pirker, S., Schwarzer, C., Wieselthaler, A., Sieghart, W. & Sperk, G. (2000) GABA(A) receptors: immunocytochemical distribution of 13 subunits in the adult rat brain. *Neuroscience*, **101**, 815-850.

Purves, D., Augustine, G.J., Fitzpatrick, D., Hall, W.C., Lamantia, A.-S., McNamara, J.O. & Williams, S.M. (2004) Neuroscience, chapter 13. Sinauer Associates Inc.

Ratté, S. & Prescott, S.A. (2011) ClC-2 channels regulate neuronal excitability, not intracellular chloride levels. *The Journal of Neuroscience*, **31**, 15838-15843.

Reid, C.A., Kim, T., Phillips, A.M., Low, J., Berkovic, S.F., Luscher, B. & Petrou, S. (2013) Multiple molecular mechanisms for a single GABAA mutation in epilepsy. *Neurology*, **80**, 1003-1008.

Rinke, I., Artmann, J. & Stein, V. (2010) ClC-2 voltage-gated channels constitute part of the background conductance and assist chloride extrusion. *The Journal of Neuroscience*, **30**, 4776-4786.

Rivera, C., Voipio, J., Payne, J.A., Ruusuvuori, E., Lahtinen, H., Lamsa, K., Pirvola, U., Saarma, M. & Kaila, K. (1999) The K+/Cl− co-transporter KCC2 renders GABA hyperpolarizing during neuronal maturation. *Nature*, **397**, 251-255.

Rudolph, U. & Mohler, H. (2004) Analysis of GABAA receptor function and dissection of the pharmacology of benzodiazepines and general anesthetics through mouse genetics. *Annual review of pharmacology and toxicology*, **44**, 475-498.

Saint-Martin, C., Gauvain, G., Teodorescu, G., Gourfinkel-An, I., Fedirko, E., Weber, Y.G., Maljevic, S., Ernst, J.-P., Garcia-Olivares, J. & Fahlke, C. (2009) Two novel CLCN2 mutations accelerating chloride channel deactivation are associated with idiopathic generalized epilepsy. *Human mutation*, **30**, 397-405.

Sandyk, R. & Gillman, M. (1985) Baclofen-induced memory impairment. *Clinical neuropharmacology*, **8**, 294-295.

Scheel, O., Zdebik, A.A., Lourdel, S. & Jentsch, T.J. (2005) Voltage-dependent electrogenic chloride/proton exchange by endosomal CLC proteins. *Nature*, **436**, 424-427.

Schofield, C.M., Kleiman-Weiner, M., Rudolph, U. & Huguenard, J.R. (2009) A gain in GABAA receptor synaptic strength in thalamus reduces oscillatory activity and absence seizures. *Proceedings of the National Academy of Sciences of the United States of America*, **106**, 7630-7635.

Schubert, J., Paravidino, R., Becker, F., Berger, A., Bebek, N., Bianchi, A., Brockmann, K., Capovilla, G., Dalla Bernardina, B. & Fukuyama, Y. (2012) PRRT2 mutations are the major cause of benign familial infantile seizures. *Human mutation*, **33**, 1439-1443.

Schubert, J., Siekierska, A., Langlois, M., May, P., Huneau, C., Becker, F., Muhle, H., Suls, A., Lemke, J.R., de Kovel, C.G., Thiele, H., Konrad, K., Kawalia, A., Toliat, M.R., Sander, T., Ruschendorf, F., Caliebe, A., Nagel, I., Kohl, B., Kecskes, A., Jacmin, M., Hardies, K., Weckhuysen, S., Riesch, E., Dorn, T., Brilstra, E.H., Baulac, S., Moller, R.S., Hjalgrim, H., Koeleman, B.P., Euro, E.R.E.S.C., Jurkat-Rott, K., Lehman-Horn, F., Roach, J.C., Glusman, G., Hood, L., Galas, D.J., Martin, B., de Witte, P.A., Biskup, S., De Jonghe, P., Helbig, I., Balling, R., Nurnberg, P., Crawford, A.D., Esguerra, C.V., Weber, Y.G. & Lerche, H. (2014) Mutations in STX1B, encoding a presynaptic protein, cause fever-associated epilepsy syndromes. *Nature genetics*, **46**, 1327-1332.

Schuler, V., Lüscher, C., Blanchet, C., Klix, N., Sansig, G., Klebs, K., Schmutz, M., Heid, J., Gentry, C. & Urban, L. (2001) Epilepsy, hyperalgesia, impaired memory, and loss of pre-and postsynaptic GABA B responses in mice lacking GABA B (1). *Neuron*, **31**, 47-58.

Schwenk, J., Metz, M., Zolles, G., Turecek, R., Fritzius, T., Bildl, W., Tarusawa, E., Kulik, A., Unger, A. & Ivankova, K. (2010) Native GABAB receptors are heteromultimers with a family of auxiliary subunits. *Nature*, **465**, 231-235.

Sidel, E.S., Tilson, H.A., McLamb, R.L., Wilson, W.A. & Swartzwelder, H.S. (1988) Potential interactions between GABAb and cholinergic systems: baclofen augments scopolamine-induced performance deficits in the eight-arm radial maze. *Psychopharmacology*, **96**, 116-120.

Sık, A., Smith, R. & Freund, T. (2000) Distribution of chloride channel-2-immunoreactive neuronal and astrocytic processes in the hippocampus. *Neuroscience*, **101**, 51-65.

Smith, R., Clayton, G., Wilcox, C., Escudero, K. & Staley, K. (1995) Differential expression of an inwardly rectifying chloride conductance in rat brain neurons: a potential mechanism for cell-specific modulation of postsynaptic inhibition. *The Journal of neuroscience*, **15**, 4057-4067.

Staley, K. (1994) The role of an inwardly rectifying chloride conductance in postsynaptic inhibition. *Journal of neurophysiology*, **72**, 273-284.

Staley, K., Smith, R., Schaack, J., Wilcox, C. & Jentsch, T.J. (1996) Alteration of GABA A receptor function following gene transfer of the CLC-2 chloride channel. *Neuron*, **17**, 543-551.

Steinlein, O. (1995) Detection of a CfoI polymorphism within exon 5 of the human neuronal nicotinic acetylcholine receptor alpha 4 subunit gene (CHRNA4). *Human genetics*, **96**, 130.

Steriade, M., McCormick, D.A. & Sejnowski, T.J. (1993) Thalamocortical oscillations in the sleeping and aroused brain. *Science*, **262**, 679-685.

Stölting, G., Fischer, M. & Fahlke, C. (2014) CLC channel function and dysfunction in health and disease. *Frontiers in physiology*, **5**.

Stolting, G., Teodorescu, G., Begemann, B., Schubert, J., Nabbout, R., Toliat, M.R., Sander, T., Nurnberg, P., Lerche, H. & Fahlke, C. (2013) Regulation of ClC-2 gating by intracellular ATP. *Pflugers Archiv : European journal of physiology*, **465**, 1423-1437.

Studer, R., von Boehmer, L., Haenggi, T., Schweizer, C., Benke, D., Rudolph, U. & Fritschy, J.M. (2006) Alteration of GABAergic synapses and gephyrin clusters in the thalamic reticular nucleus of GABAA receptor alpha3 subunit-null mice. *The European journal of neuroscience*, **24**, 1307-1315.

Suls, A., Jaehn, J.A., Kecskes, A., Weber, Y., Weckhuysen, S., Craiu, D.C., Siekierska, A., Djemie, T., Afrikanova, T., Gormley, P., von Spiczak, S., Kluger, G., Iliescu, C.M., Talvik, T., Talvik, I., Meral, C., Caglayan, H.S., Giraldez, B.G., Serratosa, J., Lemke, J.R., Hoffman-Zacharska, D., Szczepanik, E., Barisic, N., Komarek, V., Hjalgrim, H., Moller, R.S., Linnankivi, T., Dimova, P., Striano, P., Zara, F., Marini, C., Guerrini, R., Depienne, C., Baulac, S., Kuhlenbaumer, G., Crawford, A.D., Lehesjoki, A.E., de Witte, P.A., Palotie, A., Lerche, H., Esguerra, C.V., De Jonghe, P., Helbig, I. & Euro, E.R.E.S.C. (2013) De novo loss-of-function mutations in CHD2 cause a fever-sensitive myoclonic epileptic encephalopathy sharing features with Dravet syndrome. *American journal of human genetics*, **93**, 967-975.

Sun, Y.-G., Wu, C.-S., Renger, J.J., Uebele, V.N., Lu, H.-C. & Beierlein, M. (2012) GABAergic synaptic transmission triggers action potentials in thalamic reticular nucleus neurons. *The Journal of Neuroscience*, **32**, 7782-7790.

Syrbe, S., Hedrich, U.B., Riesch, E., Djemie, T., Muller, S., Moller, R.S., Maher, B., Hernandez-Hernandez, L., Synofzik, M., Caglayan, H.S., Arslan, M., Serratosa, J.M., Nothnagel, M., May, P., Krause, R., Loffler, H., Detert, K., Dorn, T., Vogt, H., Kramer, G., Schols, L., Mullis, P.E., Linnankivi, T., Lehesjoki, A.E., Sterbova, K., Craiu, D.C., Hoffman-Zacharska, D., Korff, C.M., Weber, Y.G., Steinlin, M., Gallati, S., Bertsche, A., Bernhard, M.K., Merkenschlager, A., Kiess, W., Euro, E.R., Gonzalez, M., Zuchner, S., Palotie, A., Suls, A., De Jonghe, P., Helbig, I., Biskup, S., Wolff, M., Maljevic, S., Schule, R., Sisodiya, S.M., Weckhuysen, S., Lerche, H. & Lemke, J.R. (2015) De novo loss- or gain-of-function mutations in KCNA2 cause epileptic encephalopathy. *Nature genetics*, **47**, 393-399.

Tao, W., Higgs, M.H., Spain, W.J. & Ransom, C.B. (2013) Postsynaptic GABAB receptors enhance extrasynaptic GABAA receptor function in dentate gyrus granule cells. *The Journal of Neuroscience*, **33**, 3738-3743.

Thiemann, A., Gründer, S., Pusch, M. & Jentsch, T.J. (1992) A chloride channel widely expressed in epithelial and non-epithelial cells. *Nature*, **356**, 57-60.

Thoby-Brisson, M., Telgkamp, P. & Ramirez, J.M. (2000) The role of the hyperpolarization-activated current in modulating rhythmic activity in the isolated respiratory network of mice. *The Journal of neuroscience : the official journal of the Society for Neuroscience*, **20**, 2994-3005.

Ulrich, D. & Bettler, B. (2007) GABA B receptors: synaptic functions and mechanisms of diversity. *Current opinion in neurobiology*, **17**, 298-303.

Vorobiov, D., Levin, G., Lotan, I. & Dascal, N. (1998) Agonist-independent inactivation and agonist-induced desensitization of the G protein-activated K+ channel (GIRK) in Xenopus oocytes. *Pflugers Archiv : European journal of physiology*, **436**, 56-68.

Wallace, R.H., Marini, C., Petrou, S., Harkin, L.A., Bowser, D.N., Panchal, R.G., Williams, D.A., Sutherland, G.R., Mulley, J.C., Scheffer, I.E. & Berkovic, S.F. (2001) Mutant GABA(A) receptor gamma2-subunit in childhood absence epilepsy and febrile seizures. *Nature genetics*, **28**, 49-52.

Weber, Y.G. & Lerche, H. (2008) Genetic mechanisms in idiopathic epilepsies. *Developmental medicine and child neurology*, **50**, 648-654.

Weckhuysen, S. & Korff, C.M. (2014) Epilepsy: old syndromes, new genes. *Current neurology and neuroscience reports*, **14**, 447.

Weckhuysen, S., Mandelstam, S., Suls, A., Audenaert, D., Deconinck, T., Claes, L.R., Deprez, L., Smets, K., Hristova, D., Yordanova, I., Jordanova, A., Ceulemans, B., Jansen, A., Hasaerts, D., Roelens, F., Lagae, L., Yendle, S., Stanley, T., Heron, S.E., Mulley, J.C., Berkovic, S.F., Scheffer, I.E. & de Jonghe, P. (2012) KCNQ2 encephalopathy: emerging phenotype of a neonatal epileptic encephalopathy. *Annals of neurology*, **71**, 15-25.

Woolson, R.F. & Clarke, W.R. (2011) *Statistical methods for the analysis of biomedical data*. John Wiley & Sons.

Wu, Y., Chan, K.F., Eubanks, J.H., Guin Ting Wong, C., Cortez, M.A., Shen, L., Che Liu, C., Perez Velazquez, J., Tian Wang, Y., Jia, Z. & Carter Snead, O., 3rd (2007) Transgenic mice over-expressing GABA(B)R1a receptors acquire an atypical absence epilepsy-like phenotype. *Neurobiology of disease*, **26**, 439-451.

7 Acknowledgments

First of all, I would like to thank Prof. Holger Lerche for having allowed me to accomplish my PhD studies in the Dept. of Neurology and Epileptology. His observations, constructive comments and empathy for some "problematic" aspects of my research played a fundamental role in the development of this thesis.

Snezana Maljevic, thank you so much for your support. You were essential for the development of some of my projects and I really appreciate all the help and precious advises you gave me over the years. I regret that I could not manage to discuss this thesis before your departure. I hope to meet you again (hopefully on a sunny beach in Australia or Bali).

Additionally, I would like to thank my dear colleague and friend Uli (Hedrich-Klimosch). Thank you for your help, tips and assistance during several experimental procedures. It has been a pleasure for me to have you as my desk colleague, and to have shared with you great moments.

A special thank goes to Nele Dammeier, who was my first guide and supervisor concerning the electrophysiological part of my thesis. I´ve really appreciated her help, suggestions and patience.

I would like to thank Yvonne, with whom I spent plenty of time in the "experimental room". I have improved my knowledge of German more through her lessons, than through many official courses. Many thanks to Merle, for all her support during these years. I enojoyed making experiments together and think we are a great team. A special thank goes to my PhD brothers Julian, Filip, Stephan and Niklas.

I would like to thank all the people that are currently no longer in the lab, but with whom I had a special connection: Aura, Julia, Kübra, Katja.

Yuanyuan, Heidi, Nicole, thank you for all the advises and help you gave me during these years. My dear friend Gina, I should visit you and you shoud visit me. I would like to thank Henner (my nightmare, I´m joking, ok?) and all the people I met during this years, we shared special moments together.

Special thanks goes to my friends and family. It was hard to be so far away from you, but you were always there for me, thank you for your support!

Last, but not least I would like to thank Duilio, for sharing this path together. When we first came to Germany we didn´t know what goals we would have reached and now we are here sharing this important stage of our life together. I hope this is just the begininng and many special moments are going to come. Thank you with all my heart!